# Biopolymer Foams from Novatein Thermoplastic Protein and Poly(lactic acid)

A thesis submitted in fulfilment

of the requirements for the degree

of

**Master of Philosophy with Publication in Materials and Processing**

at

**The University of Waikato**

by

**Anuradha Walallavita**


THE UNIVERSITY OF
WAIKATO
*Te Whare Wānanga o Waikato*
School of Engineering

2018

# Abstract

Novatein is the only commercial thermoplastic protein made from bloodmeal, a highly denatured protein and a readily available by-product of the meat processing industry. One of the major limitations of Novatein is its hydrophilic nature and loss of plasticizer during processing which leads to poor mechanical properties. To address these issues, Novatein has been blended with another biodegradable polymer with good mechanical properties, polylactic acid (PLA).

Blending two components can lead to poor mechanical properties of the blend due to weak interfacial adhesion and thermodynamic incompatibility. These problems can be overcome with the use of a compatibilizer which helps to stabilize the interface by coalescence suppression of the dispersed domains. In this work, itaconic anhydride grafted PLA (PLA-g-IA) was chosen as a compatibilizer for Novatein-PLA blends because IA is extremely stable when reacted with proteins and less harmful compared to maleic anhydride.

Reactive extrusion was used to blend different proportions of Novatein and PLA and the compatibilizing effects of itaconic anhydride was examined. Results showed that fewer agglomerated Novatein particles and less phase separation was visible in the presence of compatibilizer. At 50-50 Novatein/PLA, the absence of compatibilizer produced a dispersed morphology which caused the material to disintegrate in chloroform. Upon the addition of itaconic anhydride, the 50-50 blend stayed intact which was thought to be a result of co-continuous morphology. Incorporating 50 wt.% of PLA-g-IA improved the tensile strength of Novatein by 42% and impact strength by 36%. The effect of compatibilizer was evident in wide-angle x-ray scattering. Three phases were detected in the absence of compatibilizer: crystalline Novatein, amorphous Novatein, and amorphous PLA phases. With compatibilizer, the blend was moving toward two phases: crystalline Novatein, and an amorphous blend of Novatein and PLA. Itaconic anhydride grafted PLA improved miscibility between Novatein and PLA, which lead to the fabrication of Novatein-PLA foams.

Foaming Novatein is a new area of study which has never been investigated before. The foamability of a material depends on the ability of the material to withstand the stretching forces during bubble growth and hold the newly formed cellular structure. The low melt strength of Novatein, however, make it difficult to induce a cellular structure in the proteinous bioplastic. Therefore, the foaming ability of Novatein can be improved by blending with PLA, which can successfully be foamed using a batch process with carbon dioxide as the blowing agent.

Various compositions of Novatein/PLA were batch foamed with and without compatibilizer. Results showed that pure Novatein cannot form a cellular structure at a foaming temperature of 80°C, however, in a blend with 50 wt.% PLA, micro cells formed with a higher cell density ($8.44x10^{21}$ cells $cm^{-3}$) and smaller cell sizes (3.36 µm) compared to pure PLA and blends with higher amounts of PLA. A further reduction in cell size and increase in cell density was observed upon the addition of compatibilizer due to the higher crystallinity of grafted PLA. The co-continuous morphology obtained upon the addition of compatibilizer led to the development of foams with more uniform cell sizes, which was stable for cell nucleation even at high temperatures.

# Acknowledgements

There are many people I would like to warmly thank who have made my research a possibility. First and foremost, I would like to thank my chief supervisor, Assoc. Prof. Johan Verbeek. Thank you for your encouragement, understanding, patience, and excellent guidance throughout this journey. I have learned a lot from you and thank you for always pushing me to dig a little deeper. You have provided me with support in more ways than one and for that I will always be grateful. Thank you to Dr Mark Lay for sharing your technical expertise, you have taught me a lot and we have had good laughs on the way.

I would like to thank the Polymers and Composites Research group in C.G.11 for our chats, coffee breaks, help whenever needed, bouncing ideas, and friendship. There have been too many to name, however, I acknowledge all the members, international students, fourth years, Masters and PhD students, for supporting me in many ways. In particular, I am eternally grateful for the support of my dear friends Safiya, Maria, Sandra, Herman, and Kavwa. You have always been there for me and your faith in me was motivation for me to always push through. When times were hard, I could always rely on you. You made this experience enjoyable, and one that I will never forget.

I kindly appreciate the support of all the staff members and lab technicians at the University of Waikato. Thank you to Mary for her warm smile, open nature, and excellent secretarial skills. I can always rely on you for anything. Thank you to Helen Turner, for making the SEM my favourite equipment to use, your chats and warm sense of humour always made my day. Thank you to Chris, Yuanji, and Lisa for teaching me many laboratory equipment and always providing support whenever needed. Thanks to David Nicholls for IT support and assistance. Thank you to Liz and Tony, for your friendship and warm smiles which always brightened up my day. Thank you to Rob Torrens, James Carson, and Michael Walmsley, for providing me the opportunity to be involved with fourth year courses. I dearly appreciate the support of Cheryl Ward, you have always been a phone call away whenever I had an emergency with my journal articles and overall thesis. You are extremely kind and a wonderful person. Thank you to Michael Mucalo, Kay

Weaver, and the Graduate Research Team at the University of Waikato. You have always worked hard behind the scenes and provided me with the necessary support to make my thesis completion a possibility.

I really appreciate the wonderful support of the Biopolymer Network for allowing me to carry out experiments at Scion. Thank you to Kate, Dawn, Samir, and Stephanie for their excellent guidance and expertise. Thank you to Saad and Gildas for being kind friends. Thank you to Toni for your friendship and I am grateful to the Sinisa family for being a home away from home. I am also thankful for the Ministry of Business, Innovation and Employment for funding my research.

Last and most importantly, I would like to thank my family for the role you have played in my life. My dear parents, and my brother, you have provided me with unconditional love and support, and have always encouraged my dreams, even if I had not realized these yet. You believed in me at times when I did not and you never failed to see my potential. Everything I am today, I am because of you, you are my happiness. Thank you to Shehan for being there for me in a time when I needed you the most. You are my light and your unconditional love and support gave me the final push I needed to see this through to the end. I love you all.

# Table of Contents

# List of Figures

# List of Tables

# 1

# Introduction

# Introduction

The meat industry is New Zealand's largest manufacturing industry and second largest goods exporter, generating $7 billion in export revenue in June 2017. Over one million tonnes of red meat and co-products are exported to over 120 countries around the world [1]. Co-products play a crucial role in the industry's business initiative of utilising and valorising all parts of a carcass in the best returning market. Exports of co-products accounted for NZ$1.46 billion in 2016/17, of which 26% are hides and skins, 16% are edible offals and 11% are other products such as blood. Approximately 80,000 tonnes of blood is collected annually from New Zealand slaughterhouses [2] and processed into bloodmeal which is sold as low-value animal feed and fertilizer, or discarded as effluent. However, discarding directly into the environment causes animal blood to be a problematic by-product of the meat industry especially when produced at high volumes.

Bloodmeal consists of at least 85% proteins and less than 10% moisture, this high source of protein and relatively low cost makes bloodmeal a good starting material for conversion to thermoplastics. The development of bio-based alternatives using proteins have arisen from environmental concerns regarding conventional plastics. Bioplastics have been produced from plant and animal proteins, including casein, whey, keratin, gelatine, corn, gluten, sunflower, soy and bloodmeal [3]. Bloodmeal and water alone is incapable of forming an extrudable melt due to protein crosslinking induced by heat treatment, and therefore require additives such as sodium sulfite (SS), sodium dodecyl sulfite (SDS) and urea [4]. SS disrupts chemical crosslinking by reducing disulfide bonds, and SDS disrupts hydrophobic interactions. Urea acts as a protein denaturant and interrupts the secondary structure such as beta sheets. These additives can be combined with triethylene glycol (TEG) as plasticizer to produce Novatein Thermoplastic Protein [5], an effective thermoplastic which can be extruded and injection moulded. Novatein finds use in agricultural applications such as plant pots, weasand clips, and weed mat pegs [6].

Novatein, however, has some limitations such as loss of water during processing and storage which leads to embrittlement and loss of functionality [7]. A solution to these problems is blending Novatein with other polymers, which can improve the properties of Novatein for use in wider applications such as biopolymer foams. The

vast majority of commercial polymeric foams involves mainly polystyrene, polypropylene, polyvinylchloride (PVC), high-density and low-density polyethylene (HDPE, LDPE) and, to a more limited extent, polyethylene terephthalate (PET). The production of biodegradable foams to be used as compostable packaging systems is challenging. However, due to intense political and environmental pressures, the need for biodegradable foam materials is being realized. Biodegradable polymers, such as polylactic acid (PLA), poly(ε-caprolactone) (PCL), and thermoplastic starch [8] have recently been successfully processed into foams. PLA has enhanced mechanical properties comparable to petroleum-based polymers and good biocompatibility which makes PLA a popular candidate for biopolymer blends. Furthermore, PLA can be batch foamed using environmentally benign carbon dioxide and has mechanical and thermal properties similar to expanded polystyrene [9; 10].

The advantage of batch processing when compared to continuous extrusion processing, is the possibility to prepare foams under free expansion conditions. During free expansion, the material does not experience extensional and/or shear stresses and the analysis of cell nucleation and growth is more rigorous. The batch foaming system consists of a pressure vessel, where the temperature is kept constant by means of an oil bath or an electrical resistance. A blowing agent is introduced to the chamber at certain pressure conditions and, after complete solubilisation in the polymeric melt, the pressure is released at a controlled rate, producing a foamed material [11].

This thesis is a Master of Philosophy (MPhil) with publication submitted as a fulfilment of the requirements set out at the University of Waikato. This thesis comprises of an introduction, which provides a contextual overview of the thesis, a literature review, two peer-reviewed journal articles, and a concluding discussion highlighting the overall contribution of the research. The journal publications are preceded by a summary page containing a short overview of how the chapter contributes to the overall thesis. All other publications which I have co-authored are listed in the appendices, including a copy of each contribution. These consist of a published book chapter, a full conference paper, and a list of conference participations.

The two peer-reviewed journal articles can be divided into two objectives, to assess the properties of a compatible blend between Novatein and PLA, and to produce a biopolymer foam under batch processing conditions, more specifically:

**Objective 1**

Compatibilization effects of Novatein/PLA blends

- Grafting itaconic anhydride onto PLA using reactive extrusion for use as a compatibilizer with Novatein.
- To determine the blend morphology, mechanical and thermal properties, and crystallinity of a blend between Novatein and PLA.
- Conclusions as to whether itaconic anhydride was an effective compatibilizer for Novatein/PLA and its use in biopolymer foam blends.

This objective led to the following publication:

1. Walallavita, A. S., Verbeek, C. J. R. Lay, M. C. (2018). Morphology and Mechanical Properties of Itaconic Anhydride Grafted Poly(lactic acid) and Thermoplastic Protein Blends. *International Polymer Processing*. Accepted for publication, in press.

**Objective 2**

Batch foaming Novatein/PLA blends using subcritical carbon dioxide

- $CO_2$ sorption and desorption experiments to determine how well the blend could retain the blowing agent.
- To determine the effect of compatibilizer, foaming conditions, and crystallinity on Novatein/PLA foam cell structure and density.
- Conclusions as to whether the foamability of Novatein could be improved by blending with PLA.

This objective led to the following publication:

2. Walallavita, A. S., Verbeek, C. J. R. Lay, M. C. (2018). Biopolymer Foams from Novatein Thermoplastic Protein and Poly(lactic acid). *Applied Polymer Science.* Volume 134, Issue 48, December 20 2017, DOI: 10.1002/app.45561.

Laboratory scale experiments were carried out at the University of Waikato and Scion. This research was funded by the Ministry of Business, Innovation and Employment and the Biopolymer Network.

# References


[1] Meat Industry Association. (2017). *Annual Report.* Wellington, New Zealand. 35p. https://www.mia.co.nz/assets/Annual-Reports/MIA-Annual-report-2017-online.pdf.

[2] van den Berg, L. E. (2009). *Development of 2nd Generation Proteinous Bioplastics.* Masters thesis, University of Waikato, Hamilton, New Zealand.

[3] Verbeek, C. J. R., & van den Berg, L. E. (2010). Extrusion Processing and Properties of Protein-Based Thermoplastics. *Macromolecular Materials and Engineering, 295*(1), 10-21.

[4] Verbeek, C. R., & van den Berg, L. (2011). Development of Proteinous Bioplastics Using Bloodmeal. *Journal of Polymers and the Environment, 19*(1), 1-10.

[5] Pickering, K. L., Verbeek, C. J. R., Viljoen, C., & Van Den Berg, L. E. (2010). Plastics material.

[6] Aduro Biopolymers. (2016). *Novatein*. Retrieved November, 2017, from http://www.adurobiopolymers.com/Novatein.

[7] Ku‐Marsilla, K., & Verbeek, C. J. R. (2015). Compatibilization of Protein Thermoplastics and Polybutylene Succinate Blends. *Macromolecular Materials and Engineering, 300*(2), 161-171.

[8] Alavi, S. H., Rizvi, S. S. H., & Harriott, P. (2003). Process dynamics of starch-based microcellular foams produced by supercritical fluid extrusion. II: Numerical simulation and experimental evaluation. *Food Research International, 36*(4), 321-330.

[9] Parker, K., Garancher, J.-P., Shah, S., & Fernyhough, A. (2011). Expanded polylactic acid - an eco-friendly alternative to polystyrene foam. *Journal of Cellular Plastics, 47*(3), 233-243.

[10] Witt, M. R. J., & Shah, S. (2012). Methods of manufacture of polylactic acid foams.

[11] *Biodegradable Polymers and Plastics*. (2003). New York: Kluwer Academic/Plenum Publishers.

# 2

# Literature Review

# Literature Review

## 2.1 Biodegradable Polymers

Polymeric materials have been widely accepted because of their ease of processability and amenability to provide a large variety of cost effective items that help enhance the comfort and quality of life in the modern industrial society [1]. Despite the convenience of plastics and polymeric materials in daily human life, their widespread utilization and waste disposal have had a serious negative impact on the environment due to their high volume to weight ratio and resistance to degradation.

The current utilization of natural resources such as fossil fuel and oil are being subjected to prize fluctuations and will eventually be depleted. Furthermore, combustion of fossil fuels are causing a rise in atmospheric carbon dioxide levels which increase global temperature, and in turn, may cause droughts and crop losses. Fuel shortage and waste accumulation in the environment are generating a worldwide interest in alternative, renewable resources both as an energy source and as raw materials for the production of polymers and plastics.

Natural polymers, or biopolymers, are produced in nature by living organisms through biosynthetic processes that involve carbon dioxide consumption. Natural polymers are ultimately degraded and consumed in nature in a continuous recycling of resources. Other advantages of natural polymers include, biodegradability, renewability, recyclability, non-waste producing, neutrality on greenhouse effect and functionality. Biodegradability has been explored in agriculture to prevent the growth of weeds, excessive moisture loss and to alleviate recyclability problems, i.e. agricultural film should last as long as necessary and then disintegrate under UV irradiation and/or under the influence of microorganisms [2].

The sustainable supply and biodegradability of natural polymers such as starch, cellulose and proteins, have made them more favourable over synthetic plastics due to rising economic and environmental concerns. By-products or wastes from the agricultural and horticultural industries contain proteins. As a result, plant proteins

(corn, soy, sunflower, wheat gluten) and animal proteins (casein, gelatine, keratin and whey) have been manufactured into plastics [3-9].

### 2.1.1 Proteins

Proteins can contain up to 20 different amino acid monomers forming a polypeptide chain [11]. The repeating amino acid contains one nitrogen and two carbon atoms, differing only in their functional side groups. Figure 1 shows hydrophobic interactions and hydrogen bonding between amino acid functional groups stabilizing the protein and allowing it to fold into secondary, tertiary and quaternary structures. Once folded, the structure may be stabilized further with covalent cross-links [10]. The final properties of the polymer, such as hydrophobicity, cross-link density, rigidity and proportion of various secondary structures, is determined by the sequence of amino acids.

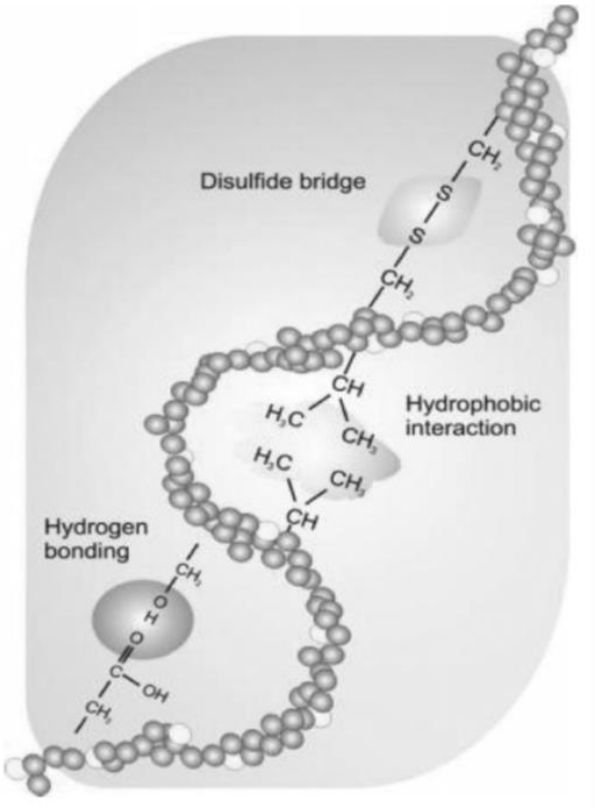


**Figure 1: Hydrophobic interactions and hydrogen bonding in protein chains (Reproduced with permission from Verbeek et al. 2010) [10].**

A protein-based material could be defined as a three-dimensional macromolecular network, stabilized and strengthened by hydrophobic interactions, disulfide bonds and hydrogen bonds [12]. Some proteins must unfold and realign before a new three-dimensional network can be formed and stabilized by new inter- and intra-molecular interactions [5; 13-15]. In order to produce protein-based bioplastics, denaturation induced by thermal or chemical means must be applied [13]. The denaturation temperature of proteins depends on the amino acid sequence, chemical additives used and processing

method employed [13]. A large variety of biodegradable materials with various functional properties can be produced from proteins due to their unique structure [16].

## 2.2 Bloodmeal-based Thermoplastic

The New Zealand red meat sector generates nearly NZ$8 billion annually in export earnings and is a principal driver of New Zealand's economy and identity [17]. Blood is a by-product of the meat industry and, for environmental and economic reasons, blood is dried to low-value blood meal and typically sold as animal feed or fertilizer [18; 19]. Blood-meal contains at least 86 wt. % protein and less than 10 wt. % moisture [20].

Bloodmeal bioplastics is an alternative to synthetic polymers and offer a sustainable option over raw material competing with food sources [21]. Chemical additives are required in order for bloodmeal to be processed via extrusion and injection moulding. These have the ability to break covalent cross-links, intermolecular and intramolecular forces such as hydrophobic and hydrogen bonding, as well as to plasticize the protein chains [19; 22]. A material's final properties is influenced by molecular organization and structural characteristics of polymers [5; 22]. Chain alignment and inter/intra-molecular interactions are affected by the combination of heat, pressure, shear and chemical additives.

### 2.2.1 Novatein Thermoplastic Protein

Protein processing is difficult using conventional equipment such as extruders and injection moulders without disrupting strong inter- and intra-molecular interactions. Sufficient amounts of water and plasticizers are required to ensure processability. Previous studies have shown that bloodmeal can be successfully converted into a bioplastic by mixing with sodium sulfite (SS), sodium dodecyl sulfite (SDS), urea, tri-ethylene glycol (TEG) and water [18; 19; 21-28]. This material is known as Novatein® Thermoplastic Protein [29]. Novatein is commonly used in agricultural and horticultural applications such as biodegradable plant pots, seedling trays, containers, pegs and vine clips [24], and more recently, Novatein has uses in abattoirs as weasand clips.

Prior to processing, bloodmeal must be treated with a combination of water, a protein denaturant (urea), a reducing agent (sodium sulfite, SS), and surfactant (sodium dodecyl sulfite, SDS) [19]. Without them, processing temperature will need to be raised which can lead to thermal degradation of the protein. In conjunction with these additives, water can be used to actively reduce the softening temperature to below the onset of thermal degradation, as well as acting as a plasticizer for protein [10; 19; 30; 31].

After conditioning, Novatein has mechanical properties ranging between 7 and 27.4 MPa, Young's modulus between 0.5 and 1.5 GPa, and elongation at break between 1.4 and 12.1% [25]. Novatein is plasticized with triethylene glycol (TEG). Amphiphilic plasticizers containing both polar and non-polar regions such as TEG have been shown to be more efficient plasticizers than polar molecules when compared to a molar or hydrogen bonding capability basis [30; 31]. Without TEG, Novatein has high tensile stress (15.6 MPa) and high Young's modulus (1.8 GPa) but these samples were very brittle and had low toughness (0.1 MPa) [30]. Higher plasticizer content reduced strength, but increased chain mobility which allowed for some chain rearrangements in response to the applied force. Other studies have shown that the mechanical properties of Novatein can be improved with the addition of core-shell particles [32], or by blending with other polymers [21; 33; 34].

## 2.3 Polymer Blends

Polymer blends constitute almost one third of the total polymer consumption and their global demand is continuing to grow. Polymer blends offers material and manufacturer benefits such as:

- Producing materials with a full set of desired properties at the lowest price
- Tailoring to improve specific properties, i.e. impact strength
- Product uniformity, improved processability, scrap reduction
- High productivity and quick formulation changes

The concept of physically blending two or more existing polymers to obtain new products or, to improve the properties of the starting materials, is attracting widespread

attention and commercial utilization. The successful implementation of this concept requires new techniques and understanding which can be used to develop novel polymers with enhanced properties.

Blending constituent existing polymers is always more cost effective than designing new polymers with special properties by chemical synthesis. A material blend with optimal properties for a specific application can be produced by careful selection and combination of polymeric components in a certain ratio. A remarkable broad spectrum of properties can be achieved by blending, mainly, processability, mechanical strength and stiffness, toughness, heat distortion temperature, elongation, permeability, chemical and weathering resistance, and thermal/dimensional stability. As a result, polymer blends find applications in numerous fields such as electrical, electronic, automotive industries, computer and business housings, and medical components. Annually, about 4,900 patents related to polymer blends are published worldwide [2]. The intensified technological interest in polymer blends over the past three decades has led to the study of processing-morphology-property relations to become a topic of major scientific interest.

### 2.3.1 Miscibility and Compatibility

A fundamental question, which firstly needs to be addressed about any blend system is of course, if the blend is miscible or not. Chemically dissimilar polymer mixtures can be divided on the basis of their components being miscible, partially miscible, or fully immiscible (Figure 2). Mixing two polymers usually results in coarse, easy to alter morphology with large domains and poor adhesion, this is known as an immiscible system. Mechanical properties such as strain at break, impact strength, and yield strength are also affected, and the blend morphology is unstable and irreproducible. Understanding the role of the interface, the region between the two phases, is important in order to control the degree of dispersion, adhesion between the phases, and stabilising the morphology.

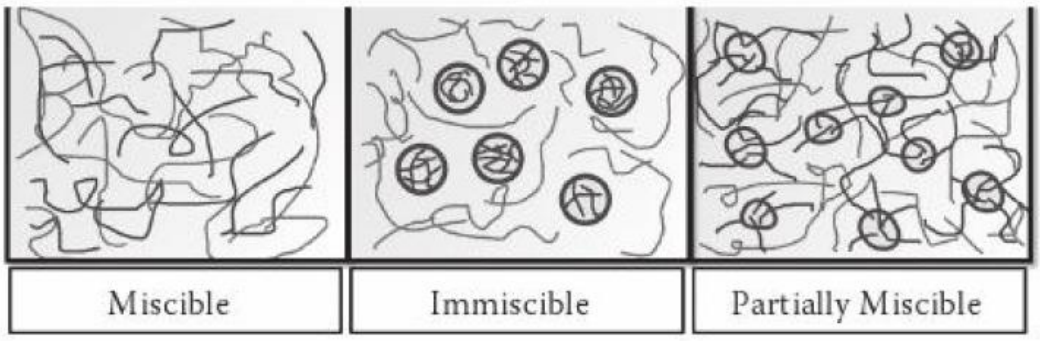


**Figure 2: Typical polymer blend classification [35].**

Surface tension is the reversible work required to create a unit surface area at constant pressure, *P*, temperature, *T*, and composition, *n*. The surface tension coefficient, $v_i$, of the substance, *i*, is given by the Equation 1 [2]:

$$v_i = \left(\frac{\partial G}{\delta A}\right)_{T,P,n} \quad [1]$$

where G is the Gibbs free energy and A is the surface area. In immiscible liquids, the physical boundary at the interface is where interactions between components takes place. The work of adhesion, *W*, is the energy required to reversibly separate the two liquids, given by Equation 2:

$$W = v_1 + v_2 + v_{12} \quad [2]$$

where $v_1$ and $v_2$ are surface tension coefficients of the neat components and $v_{12}$ is the interfacial tension coefficient between the liquids 1 and 2.

It is seldom possible to mix two or more polymers and create a blend with useful properties. When two immiscible polymers are blended without compatibilization, the mixture obtained generally has physical properties worse than those of the individual polymer. It is therefore necessary when preparing a new polymer from immiscible resins to devise a specific strategy for compatibilizing the mixture to obtain long term stability and optimum physical performance. Compatibilization has three aspects:

1. Reducing interfacial tension and thus allowing fine dispersion.

2. Stabilizing morphology against destructive processing techniques which require high stress and strain (i.e. during injection moulding).
3. Improving adhesion between phases which facilitates stress transfer and thereby improving mechanical properties.

Thermoplastics go through intensive mixing and melt extrusion, and if the blend is immiscible, the morphology on a microscopic scale would often consist of dispersed droplets of the more viscous polymer in a continuous matrix of the less viscous polymer. This is also dependent on the viscosities and relative amounts of the two polymers in the blend. Generally, the more viscous polymer will form the dispersed phase even at concentrations above 50 vol.%. Morphology stabilization is important otherwise the dispersed phase may coalescence during heat and/or stress treatment. Coalescence can result in delamination, brittleness and poor surface appearance in the moulded part.

Common compatibilization strategies include:

- Adding block, graft, or cross-linked copolymer of two or more separate polymers.
- Or to form copolymers through ionic or covalent bonds in-situ during a reactive compatibilization step.

The copolymer resides in the interface between the dispersed and matrix phases, acting as an emulsifying agent, preventing the dispersed particles from coalescing and providing interfacial adhesion. Morphology stabilization can be achieved with immiscible polymer blends with as little as 0.5 – 2.0 wt.% copolymer. However, more frequently, higher amounts such as 10 – 20 wt.% copolymer is necessary to obtain optimal physical properties such as impact strength.

### 2.3.2 Gibbs Free Energy of Mixing

To understand the thermodynamics of miscibility and discuss the phase diagram of polymer blends, the Flory-Huggins equation is widely used.

$$\frac{\Delta G_M}{RT(\frac{V}{V_r})} = \frac{\emptyset_1}{r_1} ln\emptyset_1 + \frac{\emptyset_2}{r_2} ln\emptyset_2 + \emptyset_1\emptyset_2\chi_{12} \quad [3]$$

where $\Delta G_M$ is the Gibbs free energy of mixing, $R$ is the gas constant, $V$ and $V_r$ are the total and reference volumes, respectively. The combinatorial entropy of mixing is given by the first two terms on the right side of the equation, where $\emptyset_i$ is the volume fraction and $r_i$ is the segment number of a polymer chain of component $i$. $\chi_{12}$ is the interaction parameter which takes into account all contributions to the free energy not denoted by the combinatorial entropy. In polymer blends, miscibility is improved if $\Delta G_M$ decreases as $\chi_{12}$ becomes smaller. Therefore, if there are favourable interactions between pairs of dissimilar polymers, a negative contribution for $\Delta G_M$ means the polymers are miscible [2].

There are several categories that can be used to classify miscible polymer blends. A blend that tends to phase separate at high temperatures is classified as a lower critical solution temperature (LCST), and one that separates at lower temperatures is termed an upper critical solution temperature (UCST). Some polymer pairs are completely miscible and they have both LCST and UCST characteristics. Figure 3 shows the phase diagrams of a binary blend having LCST- and UCST-type phase behaviour, respectively. The boundary between the one-phase and two-phase regions in the equilibrium state is denoted by the solid "binodal line". The dashed "spinodal line" is when the second derivative of the Gibbs free energy of mixing by compositions is equal to zero, i.e. $\frac{\partial^2 \Delta G}{\partial \emptyset^2} = 0$. The style of phase separation in a mixture can be divided into nucleation and growth (NG) type and spinodal decomposition (SG) type. The metastable region on the phase diagram between the spinodal and binodal lines is where phase separation by NG takes place. SD occurs in the unstable region framed by the spinodal lines, i.e. $\frac{\partial^2 \Delta G}{\partial \emptyset^2} < 0$.

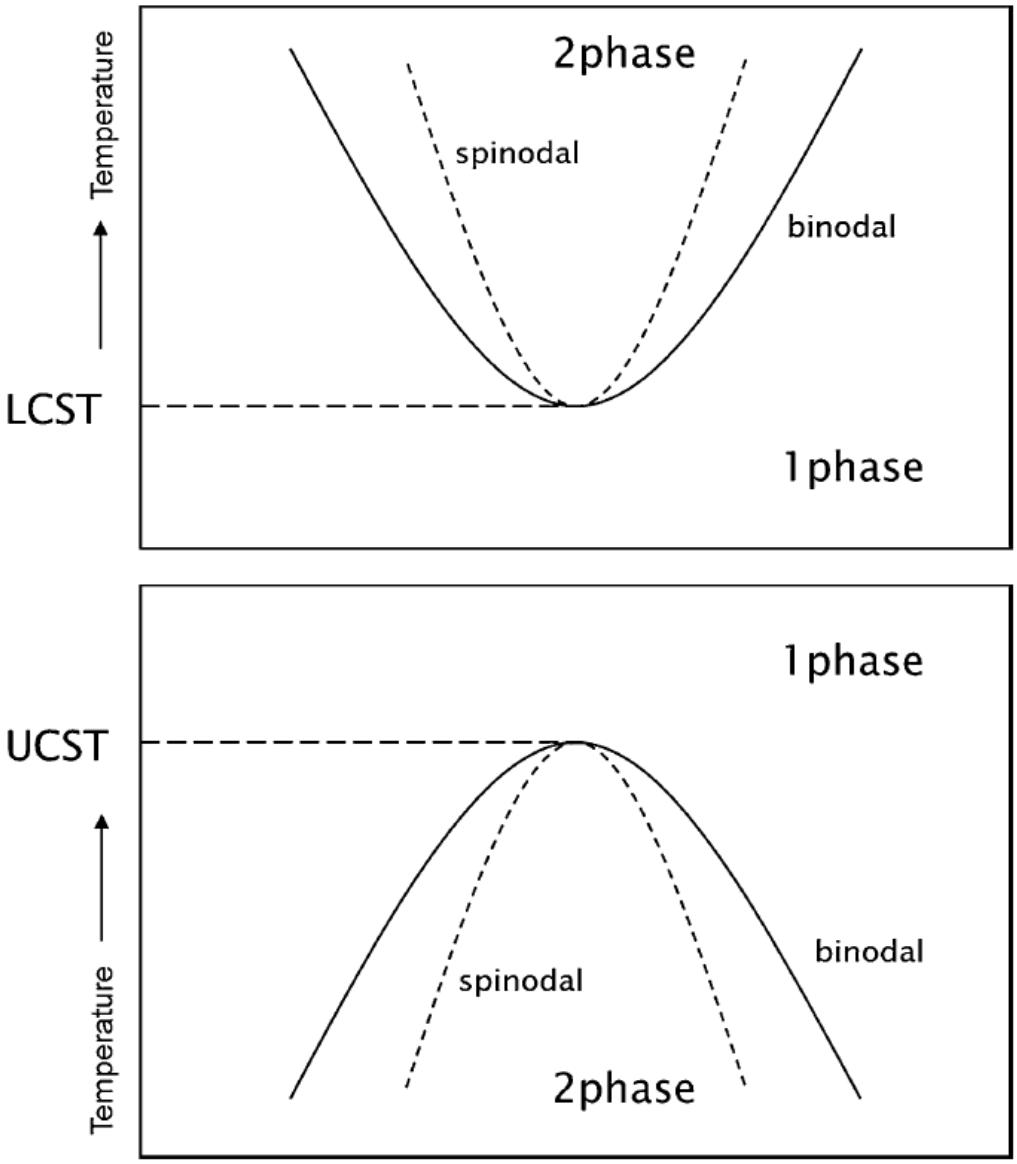


**Figure 3: LCST- and UCST-type phase diagrams [2].**

### 2.3.3 Protein-based Polymer Blends

Polymer blending is a cost-effective method for improving the properties of one or both of the components. Natural polymers such as starch and soy protein have been blended with other biodegradable polymers such as PLA for the purpose of cost reduction and improving degradation rate of the composites. However, PLA and soy protein for example are thermodynamically immiscible due to their large differences in hydrophilicities. Therefore, grafted copolymers or interfacial modifiers containing reactive functional groups which are able to generate in situ formed blocks are used to

improve compatibilization. Poly(2-ethyl-2-oxazoline) (PEOX) is considered to be a broadly compatible polymeric solvent or compatibilizing agent for many polymer blends. PEOX has good affinity with soy protein, resulting in fine phase morphology and substantially improved mechanical properties [36]. Polymeric methylene diphenyl diisocyanate (pMDI) is also a widely used compatibilizer in natural polymer and PLA blends [37]. MDI is highly reactive and can form urethane linkages with hydroxyl and carboxylic groups. Tensile strength of PLA/starch composites improved from 36.0 to 66.7 MPa when 0.5 wt.% pMDI was added [38]. Ku-marsilla et. al. [34] prepared blends of polybutylene succinate (PBS) with 50 wt.% Novatein thermoplastic protein using PEOX and pMDI as compatibilizers. Adding PEOX during Novatein production improved tensile strength and energy to break. This was due to PEOX improving dispersion of Novatein, and pMDI strengthening adhesion between PBS and Novatein. Resulting morphologies was fine and well dispersed, with virtually no phase separation.

However, pMDI does have some limitations especially in food packaging applications because of its environmentally hazardous nature. This has led to the discovery of a more promising interfacial modification route for binary immiscible blends. This route involves grafting a reactive moiety, such as maleic anhydride (MA), onto the polymer matrix, causing a reaction between the moiety and the polymer. Maleic anhydride has been used to graft onto polyethylene (PE-g-MAH) and blended with Novatein [21]. Compatibility between Novatein and PLA was improved when grafted with MA, and tensile strength never dropped below that of neat Novatein. MA has also been grafted onto PLA (PLA-g-MA) and blended with starch [39; 40], talc [41], silicate [42], and soy protein concentrate (SPC) [37]. Zhu et al. [37] found that when 4 phr compatibilizer was added to PLA/SPC blends, tensile strength increased by 19% due to good interfacial adhesion between the components. Addition of 5 phr PLA-g-MA to wheat-straw based composites resulted in a 20% increase in tensile strength and 14% increase in flexural strength [43].

Although MA grafted polymers have shown great importance as compatibilizers, their reaction with proteins can result in unstable amide bonds which can easily be hydrolysed. Grafting MA onto polyolefins is an established technique, however, MA

grafted onto PLA is not commercially available. Therefore, an alternative to MA is the chemically similar moiety, itaconic anhydride (IA). IA is less harmful compared to MA and a very reactive monomer in free radical grafting as it can produce tertiary radicals. IA is extremely stable when reacted with proteins as it can be used for acetylating lysine, cysteine, and tyrosine [44]. IA has been successfully grafted onto polyethylene with a high degree of grafting [45]. IA has been used as a renewable monomer for the synthesis of bio-based PLA-graft copolymers via conventional copolymerisation [46], and blending with proteins can lead to a 100% bio-derived blend.

## 2.4 Polymeric Foams

Polymeric foams have gained interest since World War II, and has become a very important part of our everyday life. The industry is growing rapidly due to the beneficial characteristics of polymeric foam, including light weight, sound absorption properties, and influence on material savings. Uses include seat cushioning, thermal insulation and protective packaging. The polymeric foam industry has become quite diversified due to the unique properties, processes and technologies that are constantly developed to explore new application opportunities. The manufacturing process involves scientific principles and engineering parameters which makes foaming itself a dynamic and complex phenomenon [47].

The material (foam) and the phenomenon (foaming) both involve the presence of a gas phase encapsulated by a dense, spherical shell phase. In nature, cork, wood and pumice are good examples of this type of product. In many ways, whether known or unknown, foam impacts almost every aspect of human life. For example, rice grains expand in water when heated and renders the grain edible; and gas is generated in flour through yeast. Both rice and flour possess a cellular structure that has been compatible with our digestive tissue as food for thousands of years. Another example is a sponge that has an open cell structure and is useful in absorbing and desorbing liquids.

The porous structures in foams can be perceived as gaseous voids surrounded by a dense gas-solid phase. Gases and solids have a drastic difference in nature which gives

a unique combination to foams with special properties for certain applications. For example, the presence of a cellular structure can regulate flow velocity, dissipate disturbance, and enlarge mass transfer area [47]. Polymeric foams can be viewed from different perspectives, as presented in Table 1 [48; 49].

**Table 1: Foaming perspectives.**

| Perspective | Terminology |
|---|---|
| Material | Thermoplastic and Thermoset |
| Mechanism | Soluble Foaming and Reactive Foaming |
| Nature | Flexible and Rigid |
| Structure | Closed Cell and Open Cell |
| Cell Size | Microcellular and Cellular |
| Density | High Density and Low Density |
| Dimension | Board and Thin Sheet |

### 2.4.1 Thermoset and Thermoplastic Foams

Since the 1940s and 1950s, two types of foams have been developed which are now solid drivers for the foam industry. One was thermoset foams such as polyurethane (PU); the other was thermoplastic foams such as polystyrene (PS), polyvinylchloride (PVC) and polyolefin. When multifunctional monomers were introduced for reaction, instead of a 2D linear structure, a 3D matrix was built up. This is known as a thermoset polymer and has different heat processing properties in comparison to thermoplastic polymers. Thermoplastics possess thermo-reversible morphology, whereas thermosets are no longer re-processible once set [50].

Design challenges are different in nature for thermoset foam in comparison with thermoplastic foam. The challenge in the former lay in the chemical reaction, and for the latter in physical mixing. Thermosets require high pressure from gas generation and thermoplastics also require high pressure to supress the gas in the polymer.

Thermoset foams can further be divided into two branches: soft foam and rigid foam. Two completely different products which arose from the same raw materials in different morphological structures. PU foam has become the dominant thermoset foam

in a wide range of markets including automotive, furniture, packaging, construction, recreation and transportation [50].

Thermoplastic foams took off after WWII due to their valuable use as floating docks. Thermoplastic polymers have a processing and material uniqueness characterised by their viscoelastic nature. Their expanded cellular structure shows interesting properties which allow them to be classified as foamable materials. However, not every polymer is a good candidate to foam. Lee and Ramesh [47] suggested the following must be taken into consideration in order for a polymeric material to foam:

i. Processing window
ii. Compatibility with gas
iii. Capability to hold dynamic foaming
iv. Stability during gas replacement by air

Polyolefin is a classic example of thermoplastic foams which can be extruded, injection moulded and cross-linked. Thermoplastic foams serve the public through mass production (e.g. cups, trays), as well as high quality products (e.g. cross-linked PE foam) with good insulation properties [50].

### 2.4.2 Foaming Technologies

A foam is produced when a plethora of bubbles join together in a polymer matrix to form a cellular structure. Gas molecules are able to dwell in the holes and micro-spaces that exist between polymer backbones. Foaming usually occurs when enough gas molecules are clustered to reach the thermodynamic instability threshold, which is then followed by unstable bubble nucleation and growth. The threshold is known as the critical bubble radius. Once the critical bubble radius is reached, energy is dissipated with bubble growth until another equilibrium is reached, or until there is enough resistance to stop the growth [50]. A summary of foaming technology is given in Table 2 [47].

**Table 2: General technologies used to make polymeric foams.**

| Technology | Polymers | Applications |
|---|---|---|
| Reactive foaming | PU, Phenolics | Construction, automotive, sports, toy, furniture, packaging |
| Extrusion | PS, PVC, PE, PP, PET | Food, construction, decoration, packaging, medical |
| Injection moulding | PS, PE, PP | Automotive |
| Mould bead | PS, PP, X-PE | Food, packaging, thermoforming |
| Cross-linked PE | PE | Sports, thermoforming |
| Batch Foaming | PS, PLA, PCL | Scaffolds in tissue engineering |

Once foamed, the polymer's structure, morphology and properties are altered. The gaseous voids dispersed in the polymer matrix makes it appealing and valuable to many aspects of industry. Its lighter density has lent itself to commercial floatation since the 1940s. Its cellular structure is ideal for insulation, which is a substantial business. When the cell wall possesses enough elasticity, it can be used in the athletic and furniture industries. Not to mention the various other industries, automotive, medical, packaging, that are also enhanced by the use of polymeric foams [47].

### 2.4.3 Foaming Methodologies

There are two major foaming methodologies in the polymeric foam industry:

1. Physical foaming, also known as soluble foaming
2. Chemical foaming, also known as reactive foaming

The former involves physical variation in polymer states, and the latter is solely dependent on chemical reaction. In other words, physical foaming involves the mixing of a blowing agent with the polymer in a chamber to promote gas vaporization while reducing pressure, and chemical foaming involves blending reactants in reactive conditions leading to gas evolution within a dense medium. Both methods share the common foundation of gas implementation, gas evolution, and foam stabilization [47].

Solubility, in soluble foaming, is usually dictated by the surrounding pressure. A pressure that is too low may not generate enough superheat for proper foaming, and a pressure that is too high causes processor concerns. Polystyrene, polyvinylchloride, and polyolefin are common foam materials that correspond to soluble foaming

principles. Each has unique processing and product features, which are summarized in Table 3 [47].

**Table 3: Common thermoplastic foams with soluble foaming principles.**

| | **Polystyrene** | **Polyvinylchloride** | **Polyolefin** |
|---|---|---|---|
| Polymer | Amorphous | Amorphous | Semi-crystalline |
| Processing | Extrusion | Extrusion | Extrusion |
| | Injection Moulding | Injection Moulding | Injection Moulding |
| | Mould Bead | | Mould Bead |
| | | | Cross-linking |
| Product Properties | Rigid | Flexible and Rigid | Soft to Rigid |
| | Used in Insulation | Fire Retardancy | Chemical Resistance |
| | | Low Temp Stability | Low Temp Stability |

Reactive foaming, on the other hand, characterizes materials using reaction kinetics. Reactions that generate gases and form long chain polymers must occur at the right time otherwise transient bubbling or limited expansion will occur. In order to obtain the correct reaction time and desired foam property, appropriate functional groups and their ratios with catalysts and surfactants should be controlled. The exothermic nature can easily develop extra heat for additional expansion of the formed gas, but it also makes stability hard to control [51].

### 2.4.4 Foaming Mechanisms

Production of foamed polymers includes three stages that occur within the polymer: gas implementation, gas evolution, and polymer stabilization. Different mechanisms and parameters occur and sometimes overlap in different stages. Processing parameters and their effects in different stages of foaming is illustrated in Table 4 [47].

**Table 4: Effects of processing parameters in different stages of foaming.**

| | Implementation | Expansion | Stabilization |
|---|---|---|---|
| **Temperature** | Solubility ↑<br>Viscosity ↓<br>Reactivity ↑<br>Diffusivity ↑ | Volatility ↑<br>Surface Tension ↓<br>Viscosity ↓ | Solidification ↓<br>Permeability ↑ |
| **Pressure** | Solubility ↑<br>Viscosity −<br>Homogenization ↑ | Shear Heat ↑<br>Surface Tension −<br>Nucleation ↑ | Solidification − |
| **Shear** | Solubility −<br>Dissolution ↑<br>Dispersion ↑ | Nucleation ↑<br>Growth ↑<br>Cell Distribution ↑ | Solidification ↓ |

Where ↑ = increases ↓ = decreases − = remains constant

## 2.4.5 Fundamentals of Bubble Nucleation and Growth in Polymers

The need to develop better control of foaming operations is realized due to the banning of chlorofluorocarbons (CFCs) in the early 1980s, along with the need for health, safety and environmental considerations from the foam industry. In order to control the foaming process effectively, bubble nucleation and bubble growth during foam expansion must be understood [47].

### 2.4.5.1 Bubble Nucleation

In order for polymeric materials to foam, bubbles must first nucleate and grow within the molten or plasticized viscoelastic material. The initial nucleation is induced by a change in thermodynamic conditions, such as temperature and/or pressure. During this stage a second phase is generated from the metastable polymer/gas homogeneous mixture. Subsequently, the increase of viscosity during cooling and reduction of plasticization must cause the structure to set. Finally, solidification of the continuous phase occurs [1].

Foam nucleation is different for different systems and foaming mechanisms are quite complex. It is difficult to monitor the initial birth of cell formation in polymers and

liquids since the size of potential nuclei are very small, on the order of nanometres or angstroms in scale. Nucleation occurs in a fraction of a second, making it difficult for foam scientists to capture in real life [47]. Table 5 shows various nucleation types and mechanisms [52-62].

**Table 5: Nucleating types and mechanisms [47].**

| Nucleation Type | Nucleation Mechanism | Influencing Factors | Nucleating Systems |
|---|---|---|---|
| Homogeneous | Bubbles formed due to superheat and pressure reduction | Temperature and pressure | Boiling water and organic liquids |
| Heterogeneous | Bubbles formed with assistance from tiny particles | Geometry and nature of particle | Bubble nucleation using fillers such as talc in polymers |
| Mixed-mode | Supersaturation of gas in polymers containing solid particles | Gas concentration in polymer and its solubility limit | Polystyrene with zinc stearate, stearic acid, and carbon black |
| Cavity | Poor wetting of gas/liquid acts as a potential nucleating site | Geometry of cavity and pressure drop in the system | Boiling of water and organic liquids in a rough-surfaced vessel having microcavities. |
| Shear induced | Shear force induces birth of cells | Shear rate in foam extrusion | Polymeric foam extrusion |
| Microvoid | Presence of microvoids due to rapid polymer cooling and interface cavitations in polymer blends | Cooling rate of polymer melt | Bubble nucleation in High Impact Polystyrene or its blends with polystyrene |
| Devolatalization | Volatile diffusion of solvent within polymer melt | Vacuum level and diffusion rate | Devolatilization of styrene monomer from polystyrene |
| Chemical reaction | Liquid reaction and generation of gas assisted by mixing causes bubble formation | Temperature, reactant ratio and degree of mixing | Reaction of polyol and isocyanate to form polyurethane |
| Mechanical energy (mixing and ultrasonic) | Pressure change generated by ultrasonic wave propagation and mixing of chemicals in polyurethane making | Ultrasonic frequency, agitator speed, shear rate, temperature | LPPE/PE Wax blend and high speed mixing of polyol and isocyanate |

Various nucleation mechanisms depend on energy levels involved in the systems. In order to generate bubbles in a liquid or solid, the free energy of the system must increase. This increase is utilized to create new surfaces through the formation of tiny bubbles. A reversible thermodynamic process giving rise to the birth of a gas bubble in a polymer has an excess free energy associated with it, known as Gibbs free energy (ΔG). This can be expressed mathematically as shown in Equation 4.

$$\Delta G = -V_b \Delta G_v + A\sigma \qquad [4]$$

where

$V_b$ = Volume of bubble nucleus

$\Delta G_v$ = Difference between the gas and polymer phases of the standard Gibbs free energy per unit volume

$\sigma$ = Surface tension of the liquid or polymer

A = Interfacial area

V = Volume of the bubble

Subscript b = Bubble

Thus, using surfactants to lower the surface tension will assist in the formation of bubbles. Nucleating agents such as diatomaceous earth, talc, and silica are more effective because they offer voids at the interface [47].

Interestingly, in the 1930s it was Einstein [63] that proposed the probability of nucleation being directly proportional to an exponential function, $\exp\left(-\frac{W^*}{kT}\right)$, where $W^*$ is the minimum work required to make the system unstable and to generate a large number of bubbles in a continuous phase.

The steady and transient roles of nucleation are given as

$$J_s = Z\beta^* N exp\left(-\frac{\Delta G^*}{kT}\right) \quad [5]$$

$$J(t) = J_s\, exp\left(-\frac{t}{\tau}\right) \quad [6]$$

where

| | | |
|---|---|---|
| J | = | Nucleation rate (nuclei/cm-s) |
| Subscript s | = | Steady state |
| t | = | Transient state |
| Z | = | Zeldovich non-equilibrium factor ($\approx 10^{-2}$) |
| $\beta^*$ | = | Rate at which gas molecules are added to the critical nucleus |
| N | = | Number of nucleation sites per unit volume |
| $\Delta G^*$ | = | Gibbs free energy of forming a critical nucleus |
| k | = | Boltzmann's constant |
| T | = | Absolute temperature |
| $\tau$ | = | Induction period for establishing steady-state nucleation |

The type of nucleating systems and processing conditions can cause all of these variables to change, therefore, they must be carefully evaluated on an individual basis to fit real-life applications [47].

The Gibbs free energy of the system must exceed the mechanical work needed, in order for bubbles to nucleate. Mathematically, this is expressed as:

$$\Delta G > \frac{3 \cdot \sigma}{\rho \cdot r} \quad [7]$$

where

| | | |
|---|---|---|
| $\sigma$ | = | surface tension |
| r | = | bubble nucleation radius |
| $\rho$ | = | gas density |

Surface tension is regulated with the use of silicone surfactants which have the ability to control cell count or size. In the cases of low density foams, below 30 kg/m$^3$, surfactants are able to produce open cells to maintain dimensional stability upon cooling to ambient temperature [47].

#### 2.4.5.2 Bubble Growth

Following cell nucleation, bubbles grow due to the diffusion of excess gas in the polymer. The foam growth process is controlled by variables such as polymer viscosity, gas concentration, foaming temperature, amount of nucleating agent and its nature. Foaming is highly preferred in the molten state, or above its glass transition temperature, $T_g$. Temperature needs to be reduced to solid state to hold the gaseous bubbles, essentially eliminating surface tension. Under certain circumstances, the bubble grows to exceed the material limit causing cell rupture and leads to the formation of open cells [50]. The degree of gas supersaturation when pressure is suddenly reduced governs the formation of a gas bubble. Its growth is kinetically governed by the diffusion from the polymer/gas solution to the gas phase and by viscoelastic forces around the expanding bubble. This expansion dynamic of polymeric foam is complex and has been scrutinized by foam scientists and engineers for the past 90 years [47]. If bubble nucleation and growth rates are controlled, the foam morphology (number and size of cells) can be optimised, and as consequence, the performances of the cellular structure [1].

#### 2.4.5.3 Homogeneous Nucleation

When a second phase (e.g. gas bubble) forms in a primary phase (e.g. molten polymer) this is known as homogeneous nucleation. In order for homogeneous nucleation to occur, a sufficient number of gas molecules need to form clusters for a long enough

time to make a critical bubble radius to cross over the resistance path, as shown in Figure 4.

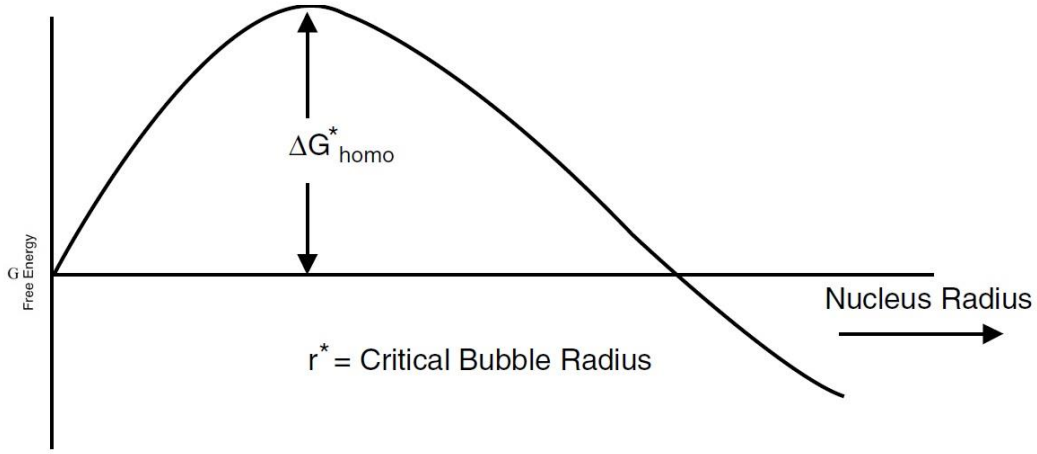


**Figure 4: Homogeneous bubble nucleation [47].**

Nucleation arises due to thermodynamic instability. Figure 5A shows a single phase containing a molten polymer saturated with gas at a certain pressure. Figure 5B shows the formation of a second gas phase when the pressure is reduced from $P_o$ to $P_s$ [47].

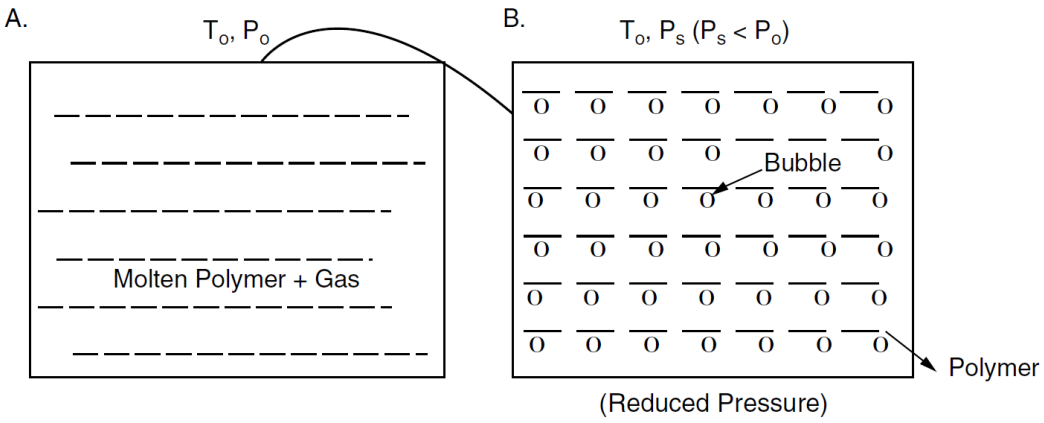


**Figure 5: Typical nucleation process. $T_o$ = temperature, $P_o$ = initial pressure (higher than surrounding pressure), $P_s$ = final pressure or surrounding atmospheric pressure [47].**

New surfaces with certain volumes must be created in order to form bubbles. Simple mathematical expressions can be derived from thermodynamic principles given the assumption that embryos are spherical in size. For homogeneous nucleation, Equation 2 can be rewritten to express Gibbs free energy as shown in Equation 8 [57].

$$\Delta G = -\frac{4}{3}\pi r^3 \cdot \Delta P + 4\pi r^2 \sigma \quad [8]$$

where

r = Bubble radius

ΔP = Pressure drop

σ = Surface tension of the polymer matrix

The maximum value of ΔG, denoted as $\Delta G^*$, occurs at a critical size, $r^*$, or when there are a critical number of gas molecules in the embryo, and represents the free energy of formation of the critical nucleus. Differentiating the free energy term and making it equal to zero gives

$$\frac{\partial \Delta G}{\partial r} = 0 \quad [9]$$

which gives an expression for critical radius, $r^*$:

$$r^* = \frac{2\sigma}{\Delta P} \quad [10]$$

A nucleus with a spherical shape is assumed because this represents minimum resistance to nucleation for a given volume. This assumption is reasonable but, in polymeric systems, non-spherical geometries might be encountered. The activation free energy for homogenous nucleation of a critical nucleus is derived as

$$\Delta G^*_{homo} = \frac{16\pi\sigma^3}{3\Delta P^2} \quad [11]$$

where

σ = surface tension of the polymer

ΔP = saturation pressure given by $P_{sat}$ - $P_s$

For a batch microcellular process system, $P_{sat}$ is the gas saturation pressure and $P_s$ is the surrounding pressure at which nucleation occurs. Usually $P_s$ is equal to atmospheric pressure [47].

It should be noted that gaseous foaming agents often soften the polymer, causing an increase or decrease in surface tension of the polymer based on the foaming agent dissolved in it. The nucleation rate expression can be calculated based on the classical

nucleation theory equation. According to Colton and Suh [57], homogeneous nucleation in a gas-polymer system is given by Equation 12.

$$N_{homo} = f_o C_o \exp\left(-\frac{\Delta G^*_{homo}}{kT}\right) \quad [12]$$

where

$f_o$ = frequency factor for the rate at which gas molecules join a critical nucleus

$C_o$ = concentration of gas molecules

Both critical radius and critical free energy decreases when the degree of supersaturation is increased. This means that bubble formation is easier when there is a greater amount of gas in the polymer. Similarly, the higher the pressure drop, the higher the nucleation rate of bubbles [47].

#### 2.4.5.4 Heterogeneous Nucleation

The most common type of nucleation in polymer systems containing additives is heterogeneous nucleation. There are several factors influencing the bubble producing efficiency, such as the type and shape of nucleating particles and interfacial tensions of solid and solid-gas interface. The interface acts as a catalyst for nucleation because the presence of tiny particles and cavities reduces the activation energy required to achieve a stable nucleus. Gibbs free energy is reduced during heterogeneous nucleation as shown in Figure 6 [47].

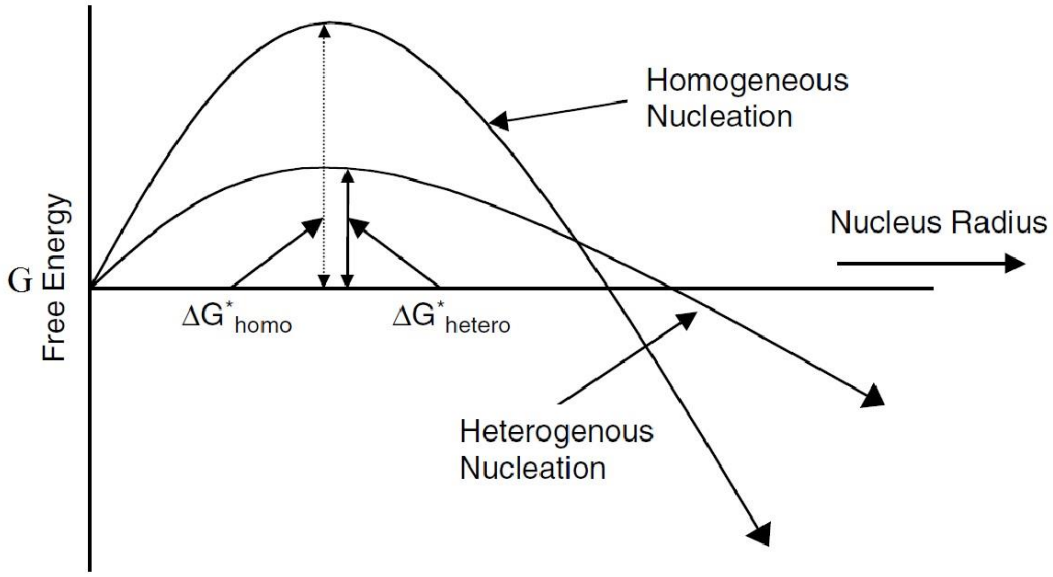


**Figure 6: Heterogeneous bubble nucleation. $\Delta G^*_{hetero} < \Delta G^*_{homo}$ [47]**

Uhlmann and Chalmers [64] describes the thermodynamics of heterogeneous nucleation and its mathematical analysis. The activation energy term can be corrected using the heterogeneity factor as shown in Equations 13 and 14:

$$\Delta G^*_{hetero} = \Delta G^*_{homo} f(\theta) \quad [13]$$

$$\Delta G^*_{hetero} = \frac{16\pi\sigma^3}{3\Delta P^2} f(\theta) \quad [14]$$

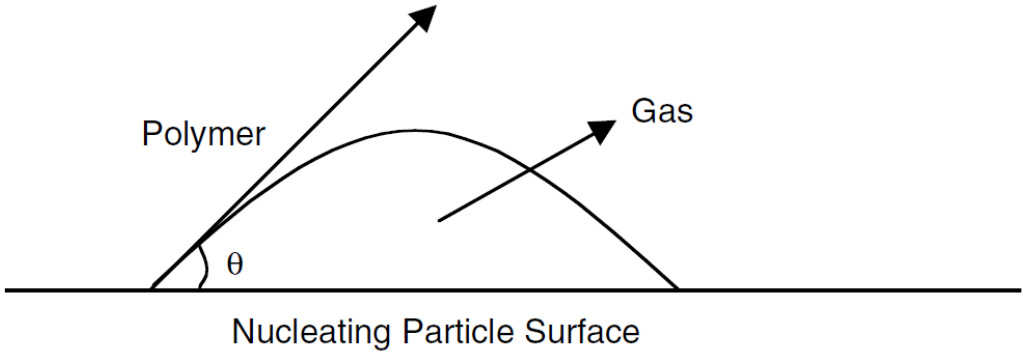


**Figure 7: Schematic of nucleating particle interaction with gas and polymer [47].**

Uhlmann and Chalmers [64] derived an expression for $f(\theta)$, Equation 15, using the configuration shown in Figure 7.

$$f(\theta) = \frac{(2+cos\theta)(1-cos\theta)^2}{4} \quad [15]$$

where

| | | |
|---|---|---|
| θ | = | wetting angle |
| $f(\theta)$ | = | heterogeneity factor |
| σ | = | interfacial tensions of a polymer-gas bubble |

Heterogeneous nucleation agents can improve the final mechanical properties of polymer foams by increasing the cell nucleation rate. The following examples show how natural fibres/additives aided the foaming behaviour of PLA degradable biocomposite foams. Kang et al. [65] investigated the effects of 1, 3, 5 and 7 wt.% of silk fibroin powder on $CO_2$ induced PLA batch foaming. They showed that the average cell size of neat PLA was 52 µm which dropped to 15 µm in PLA with 7 wt.% silk. Pilla et al. [66] reported on the foam injection moulding of PLA and flax fibre composites at 1, 10, and 20 wt.% using silane as the coupling agent. They found that foam crystallinity and cell density improved with flax fibre content, and average cell density was as low as 3 µm with 20 wt.% flax fibres.

#### 2.4.5.5 Nucleating and Blowing Agents

In polymeric foaming, nucleating agents play the role of providing even dispersion in the gaseous phase, and in turn, bubble nucleation. Common nucleating agents are porous materials, i.e. talc, whose surface becomes the residence for blowing agents and improves cell size distribution significantly. In some processes, addition of a nucleating agent is not necessary such as when foaming with volatile inorganic gas [50].

When nucleation and growth is completed, the polymeric foam is saturated with the blowing agent. The gas concentration gradient can induce counter-diffusion fluxes when exposed to the atmospheric environment, causing air to enter. After enough time, the concentration gradient diminishes to render a foam product filled with primarily air. In other words, the role of the blowing agent is like a catalyst. A simple illustration is given in Figure 8 [50].

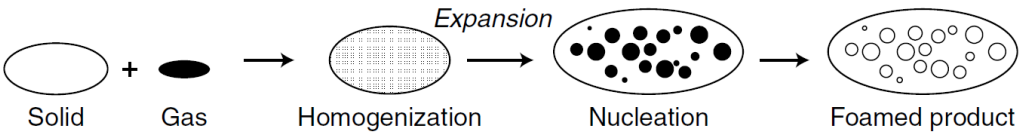


**Figure 8: Blowing agent as the catalyst [50].**

There are two major groups of blowing agents:

1. Chemical blowing agents (CBA); release gas by decomposition reaction.
2. Physical blowing agents (PBA); mainly gases or liquids.

CBA is highly favoured from an environmental and emission perspective because it can generate fine cell structures by liberating inorganic gases. CBA can be added as a nucleating agent in PBA foaming, which when compared with talc, leaves no residue, making reuse easier in nucleation control. In terms of expansion ratio and economics, PBA is favoured in conventional foam extrusion [50].

There are several useful chemical blowing agents available commercially [47]:

- Citric acid/sodium bicarbonate (endothermic)
- Azodicarbonate (exothermic)
- p-toluene sulfonyl hydrazide (exothermic)
- Sodium borohydride (endothermic)

An inert substance such as talc or a reactive ingredient such as a chemical foaming agent can be used to improve gas distribution in the foaming process. Endothermal systems such as fruit acids tend to have the best performance. The following criteria must be met in order for the acids to be suitable for endothermic foaming agents: efficiency, pricing, availability, process condition, decomposition products, reactivity and stability. Organic fruit/food, inorganic acids and carbonates are useful nucleating agents in physical foaming systems, and they can also be used as chemical blowing agents. Sodium bicarbonate ($NaHCO_3$) is a relevant carbonate used as CBA. When $NaHCO_3$ is reacted together with citric acid, the following reaction is endothermic and liberates carbon oxides. $NaHCO_3$ and citric acid together have a decomposition range

of 130-230 °C, an approximate gas evolution of 110-180 ml/g and the main gases produced are $CO_2$ and $H_2O$ [50].

## 2.4.6 Foam Properties

Polymers have an interesting organic long chain structure and exhibit unique properties compared with inorganic materials. As with foamed inorganic materials, foamed organic materials also extend the polymer material spectrum. Their morphology and foam structure are the main components for their properties. The four areas to be addressed are physical, mechanical, thermal and acoustical properties of foam [50].

### 2.4.6.1 Physical Properties

Polymers have unique physical properties. Amongst gaseous voids, gaseous cells are separated and supported by a polymeric skeleton. The physical properties of the polymeric skeleton such as melting, crystallization, decomposition and glass transition temperature remain basically unchanged. It is important to note that even though the thermodynamic properties remain similar, kinetics may change dramatically.

The volume-based physical property, however, changes significantly. The more gas, the lower the density since gases possess a large volume to weight ratio under normal circumstances. Solubility determines how much gas can be dissolved into a polymer and diffusivity determines how soon the dissolution is completed. When cells are dispersed within a polymer, a mass reduction per unit volume is anticipated. If the foam can meet the performance requirement with the minimum weight of material, or the highest expansion, then the product is economically ideal [50].

Cell size and distribution is another physical aspect that contribute to foam structure and thus, profoundly affects polymer properties [67; 68]. Quite a few applications are dependent on the internal surface area; for example, sound attenuation and diffusion-controlled phenomena such as devolatilization. A change in cell size leads to a considerable change in surface area at a given expansion ratio.

#### 2.4.6.2 Mechanical Properties

Polymer foam mechanical strength is important in almost all applications. Compressive or tensile modulus in terms of density can be expressed as:

$$\frac{E_f}{E_p} = X\left(\frac{\rho_f}{\rho_p}\right)^2 \quad [16]$$

for open cell foams, and:

$$\frac{E_f}{E_p} = (1 - X)\left(\frac{\rho_f}{\rho_p}\right) \quad [17]$$

for closed cell foams, where X denotes shape factor, and subscripts *f* and *p* denote foam and polymer, respectively. Closed cell foams are more effective in energy absorption because they have a smaller reduction in modulus than open cell foams at the same expansion [50].

Foam rigidity and flex modulus are determined by the type of polymer, the expansion ratio and sometimes, the cell structure of the foam. For packaging and filling types of applications, low mechanical strength is acceptable. For seating, mattresses and trays, medium mechanical strength is required. For high-end structural applications, engineered polymer foam is necessary for strength and insulation.

#### 2.4.6.3 Thermal Properties

Foams have favourable thermal properties which make them useful in many applications. The impressive insulation properties of foams were easily adapted for the purpose of heat retention in applications such as cups, cup sleeves, appliance doors/panels and thermal chamber insulation. Special foam packaging systems were designed to meet the needs of medical systems that are extremely sensitive to a thermal environment. The use of foams in building insulation boards was especially important in climates where energy loss is critical. The use of polymeric foam consumes less energy, reduces gas emissions and global warming overall [50].

#### 2.4.6.4 Acoustic Properties

The sound wave is considered to be an energy wave or pressure transfer. Foam, due to its cellular structure, is effective with two kinds of sound waves: airborne and contact.

Airborne refers to mid-frequency speech and high frequency engine room noise. Contact sound refers to, for example, walking on a hard floor. In present times, foams are incorporated into construction codes for residencies, warehouses, gyms, studious, and auditoriums. Sound absorption foams are desirable in populated areas where residencies are in close proximity and a reduction of noise is necessary [50].

### 2.4.7 Need for Biodegradable and Environmentally Friendly Foams

The dawn of the 21st century also brought about rising concerns in environmental climates which are dramatically changing. Global warming, energy security and sustainable sources have fuelled the need for degradable foams. Another factor is the petroleum price, which was stable for a quarter of a century. A sudden increase in 2004 from US$20 per barrel to over US$100 per barrel in 2007 also influenced the raw material price for polymers [50]. As a result, the pressures for alternative resources to polymers have also increased significantly.

The two halogenated gasses involved in degrading the ozone layer, CFCs and HCFCs, have been phased out due to the discovery of the depletion of the ozone layer in the late 1980s [69]. The emission of inorganic carbon dioxide is inevitable in any energy generation process. While technology facilitates our living, it also generates carbon dioxide which causes global warming.

In relation to polymer production: resin preparation, processing, converting, and even collecting a blowing agent to convert to atmospheric carbon, will all involve carbon dioxide emission. More and more communities are now focussing on polymers made from sustainable sources. For example, in the 1990s, Mitsui Toatsu Chemicals Inc. succeeded in making polylactide foam [70].

#### 2.4.7.1 Environmental Regulations

The wide consumption of polymeric foams and its use in daily life has raised environmental, health, and safety concerns. Material safety data sheets (MSDS)

became mandatory in the 1990s and a renewed safety and toxic list was published on the regular basis [50].

**Table 6: Common foams made from bioplastics.**

| Polymer | Source |
|---|---|
| Polylactic acid (PLA) | Corn |
| Starch | Corn, potato, wheat |
| Polyvinylalchohol (PVOH) | Vinyl acetate monomer |
| Poly caprolacton (PCL) | Crude oil |

Starch-based foams and polyvinylalchohol (PVOH) foams are water soluble and can disintegrate in water after disposal, provided that moisture is properly maintained in processing and usage. Table 6 shows common degradable foam. It is worth noting that when a foam is degraded or has disappeared from sight, it eliminates a basic unit operation but does not solve all the problems. When dissolved, it may generate global warming by-products. A summary of common disposal methods and their effects are given in Table 7 [50].

**Table 7: Advantages and disadvantages of common foam disposal methods.**

| Methods | Advantage | Disadvantage |
|---|---|---|
| Incineration | Generates energy | Produces global warming gas |
| Landfill | Low cost | Time consuming and space needed |
| Water soluble | Easy | Expensive |
| Biodegradable | Quick volume reduction | Negate recycle and reuse |

Foams play an important role in human civilization, making daily life much more convenient, yet the amount of unsolved problems is in abundance. Environmental conditions however, have a more serious impact on human living conditions. Issues in relation to the ozone layer, carbon concentration, earthquakes and climate-induced famine will not disappear. How foam plays a more active role in those pending topics, yet, continues to enrich human convenience, is a challenge to the global foam society.

## 2.5 Polymer Foaming Methods

### 2.5.1 Extrusion Foaming

The physical blowing agent is introduced to the polymer melt at elevated temperatures and pressures in the extruder [71]. The first three screw zones consist of melting, solubilisation, and pressurization stages. Further solubilisation occurs in the static mixer due to an increased residence time and contact between the two phases. Immediately following solubilisation, the polymer/gas solution is passed through a narrow capillary where a fast pressure drop provokes nucleation. The configuration of the capillary (length and diameter) impacts the cellular structure. A longer capillary (length = 30 mm) leads to finer cellular structure, whereas a shorter capillary (length = 10 mm) gives larger cell diameters [1].

In the extrusion process, bubbles nucleate and grow in non-isothermal conditions once the melt exits the die. The increase in viscosity during the cooling/crystallization of the polymer is necessary to stabilize the cellular structure and to avoid bubble collapse or coalescence. For this reason, the investigation of polymer crystallization behaviour is crucial in order to optimise the temperature profile in the extruder and the die [1].

Extrusion foaming of semi-crystalline polymers, such as PP, is difficult and restricted to a narrow temperature range, unlike high glass transition temperature amorphous polymers. This is due to the linearity of the chain structure associated with the lack of strain hardening usually observed for branched structures, as typically encountered in LDPE for instance. Crystallization kinetics is a relevant factor in foam processability. High quality, low-density foam can be attained at a slow crystallization rate at a processing temperature approaching the crystallization temperature ($T_c$) [71].

Extrusion foaming can be used to produce PLA foams especially if using a low shear screw technology such as the Turbo-Screws® technology developed by Plastic Engineering Associates [72]. Turbo-screw technology is able to achieve higher output and faster cooling due to rectangular holes through the screw flights at the root, which move the melt from the root to the barrel wall. Sheet densities of ~50 g/L with closed

cell counts of 90% and greater are achievable. These extrusion foams are used for thermoformed packages and easily trimmed into containers suitable for hot food contact.

### 2.5.2 Direct Gassed Foam Extrusion

Gases are introduced directly into the extruder via pressure in the melt, distributed and mixed before leaving the machine exit (i.e. die, nozzle, etc.) as a blend. The newly introduced gas acts like a temporary plasticizer and drastically reduces the melt viscosity, allowing for lower processing temperatures. Gases used in foam extrusion are from the atmosphere like nitrogen, carbon dioxide and air. Other gases from gasoline production such as alkanes or halogenated alkanes can also be used, but are heavily debated due to detrimental environmental impacts [50]. Reignier et al. have studied the extrusion foaming of PLA using $CO_2$ as blowing agent [71]. Foam densities of 20 – 25 g/L with 8 wt.% $CO_2$ concentration have been reported.

Nucleating agents come into use in direct gassed foam extrusion for improved distribution of the gas in substrates. These include fine minerals (talc, silica, calcium carbonates, pigments) used to chemically produce carbon dioxide, or blends of carbonates (magnesium, sodium, calcium) with organic acids (citric, tartaric) or inorganic acids (boric acid, acidic phosphates). Desired properties of gases used in foam extrusion are as follows [73; 74]:

- Non-flammable
- Non-toxic
- Low diffusion rate
- Environmentally friendly
- Low molecular weight
- Low vapour thermal conductivity
- Appropriate latent/specific heat
- Adequate solubility
- Non-reactive
- Low cost

### 2.5.3 Direct Gassed Injection Moulding

Foam injection moulding is also known as structural foam moulding due to the formation of an integral skin [75]. The classical concept of an injection moulding machine involves feeding with an extruder into an accumulator and shooting with a piston-operated system into the mould. A screw can also be used in place of the piston. Gases are introduced into the molten polymer through the barrel of the extruder to make foamed parts, as shown in Figure 9.

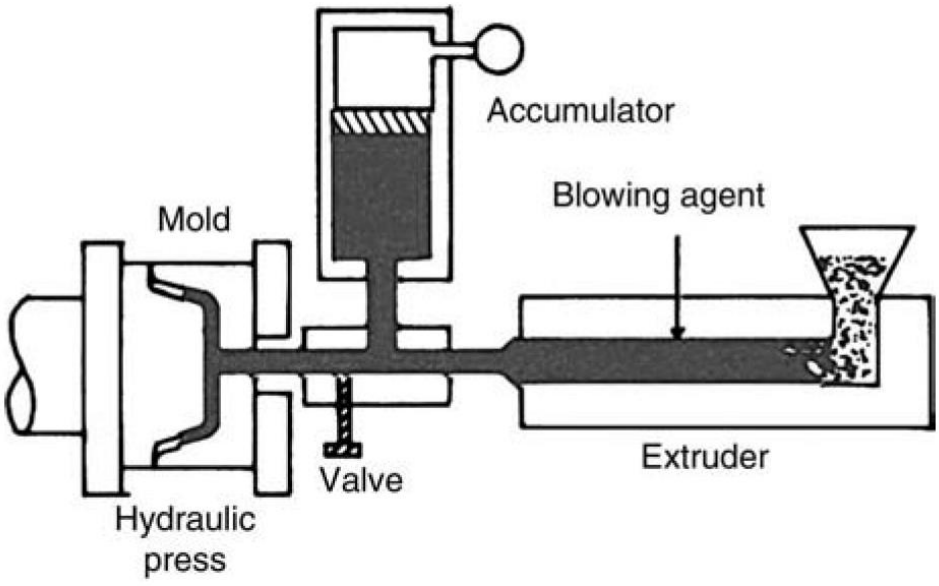


**Figure 9: Direct gassed injection moulding apparatus [50].**

### 2.5.4 Microwave Foaming

Microwave foaming is used in many food related industrial applications and is a quick way of adding heat. Sjöqvist, and Gatenholm [76] produced porous structures of potato amylopectin starch by pre-extruding and foaming using microwave. Water was the blowing agent and when starch extrudates were heated by microwaves, the moisture generated superheated steam creating a high internal pressure. Starch in the presence of water underwent a phase transition from a glassy to rubbery state upon heating. Moisture loss during heating and cooling after treatment caused the structure to return to the glassy state and the porous structure became permanent.

### 2.5.5 Batch Foaming

Two methods commonly reported for manufacturing thermoplastics are continuous extrusion foaming and batch foaming. This study will focus on the foaming of Novatein and PLA blends using the batch foaming method.

The batch processing method, also known as the autoclave method, is mainly utilized for small production of microcellular foams. The batch foaming process involves two stages:

1. The polymer sample is placed in a high-pressure gas environment which allows the gas to diffuse into the polymer matrix.
2. Nucleation and bubble growth are induced either by controlled depressurization in the autoclave (called the pressure-quench method) or from the temperature rise induced in a hot fluid bath (called the temperature soak process).

The physical mechanisms of extrusion foaming and the autoclave method may be similar, yet the dynamic is completely different. The batch process generally allows the control of foaming over the largest possible temperature range [71]. The blowing agents considered for use in this research is subcritical $CO_2$.

### 2.5.6 Absorption and Desorption of Blowing Agent

The effect of $CO_2$ on polymers is similar to those of organic solvents, including swelling [77-80] and depression of glass transition temperature, i.e. plasticization [81-83]. The mild critical conditions of $CO_2$ allow it to be handed as a liquid at room temperature under rather moderate pressures. The critical temperature is 31°C and saturated vapour pressure at 25°C is 64.6 atm (950 psi). As a result, near-critical $CO_2$ can be considered a highly volatile solvent, rather than a gas, in polymer interactions [84]. Compressed $CO_2$ is uniquely useful at promoting the impregnation of many polymers with a wide variety of additives due to its high diffusivity, solubility, and plasticizing effects.

The general experimental method involves sorption of $CO_2$ into polymer sheets in a simple pressure vessel, followed by rapid venting of pressure and transferring the samples to a balance for recording weight changes during desorption. The sample is placed in a pressure vessel fitted with a valve, pressure gauge and screw closure which can be opened quickly. The vessel is then evacuated and filled to the desired sorption pressure, $\boldsymbol{P_s}$, with liquid or gaseous $CO_2$ and held at this pressure for an appropriate sorption period, $\boldsymbol{t_s}$. There should be no change in pressure during this sorption period because of the relative sizes of sample and vessel. At the end of the sorption period, $CO_2$ pressure is rapidly released to atmosphere and the sample is removed and weighed. Sample weights during desorption is recorded as a function of desorption time, $\boldsymbol{t_d}$, at intervals as short as 5 seconds beginning within 10 – 20 seconds after venting the vessel [84].

A complete picture of sorption equilibria, including the kinetics of both absorption and desorption, can be obtained using only sample weights at time, $\boldsymbol{w_t}$, and dry weight, $\boldsymbol{w_o}$, recorded during desorption. The mass of the sample during certain desorption times can be calculated using Equation 18:

$$M_{t,d} = \frac{w_t - w_o}{w_o} \qquad [18]$$

Liquid $CO_2$ has a low solubility parameter, suggesting that it should behave like a non-polar hydrocarbon. However, Berens and Huvard [84] found that liquid $CO_2$ has an unexpectedly high solubility in polar polymers, possibly due to its H-bonding basicity, and its behaviour resembles a somewhat polar organic solvent. This behaviour seems to be a reasonable consequence of the high solubility and plasticizing action of $CO_2$ at high pressures.

#### 2.5.6.1 Effect of Pressure

The effect of pressure on final porous structures is studied at constant temperature and depressurization rate while changing the range of pressures. A typical behaviour of foaming polymers with $CO_2$ is that the average pore size decreases, while the cell density increases when pressure is increased [85-88]. The pressure increase enhances the solubility of $CO_2$ in the polymer matrix and decreases the energy barrier to nucleation

[85]. In other words, at higher pressures, nucleation and growth of pores occur because there is more dissolved fluid available in the polymer matrix.

#### 2.5.6.2 Effect of Temperature

The effect of temperature on final porous structure is studied at constant pressure and depressurization rate while changing the range of temperatures. A small increase in temperature leads to a slight decrease in bulk foam density and cell density [87; 88]. Nucleation theory predicts that at higher temperatures, the energy barrier to nucleation decreases [85]. Furthermore, viscosity of the polymer decreases as temperature increases which promotes the growth and coalescence of neighbouring pores, resulting in larger cell sizes [87; 88]. Cells also grow faster due to an increased diffusivity of the fluid.

#### 2.5.6.3 Effect of Saturation Time

The effect of saturation time on final porous structure is studied at constant pressure and temperature. An increase in average pore diameter and decrease in pore wall thickness is expected as saturation time increases. This is because a longer soaking time allows more blowing agent to diffuse into the polymer matrix and expand the pores within the structure. Furthermore, diffusivity increases with saturation time which leads to a more porous structure [86].

#### 2.5.6.4 Effect of Depressurization Rate

The effect of depressurization rate on final porous structure is studied at constant pressure, temperature, and saturation time. As depressurization rate increases, mean pore diameter decreases and cell population density increases [87]. This is possibly due to more gas being used for cell nucleation instead of cell growth, at higher pressure drop rates [89]. This means that more nuclei are generated but the hindrance to growth leads to smaller pores.

### 2.5.7 Crystallinity in Semi-Crystalline Polymers

Research on batch polymer processing in the last two decades have mainly focused on foaming of amorphous polymers, such as PS, polycarbonate (PC) and poly(methyl methacrylate) (PMMA), and very little work has been done on the foaming of semi-crystalline polymers [71]. Crystallinity is one of the key parameters that need to be considered when foaming semi-crystalline polymers [90]. Novatein behaves like a semi-crystalline polymer, although it has a softening point rather than a distinct melt region.

Baldwin et al. [91] have demonstrated for PET-$CO_2$ systems that crystallinity effects both cell nucleation and growth mechanisms and, therefore, plays a major role in microcellular processing. Furthermore, the crystallinity of PET increased from <5% (initial sample considered to be amorphous) to about 30% when the concentration of $CO_2$ was increased (saturation pressure: 5.52 MPa, sorption time: 25 h, saturation temperature: 20 °C). The heterogeneous nature of the semi-crystalline polymer matrix causes the bubble nucleation to be non-homogeneous throughout the sample. Furthermore, the polymer-gas mixture formed during microcellular processing was not uniform since the gas does not dissolve in the crystals. Cell growth is also limited because crystallinity severely increases the matrix stiffness, which densifies and degrades the cellular structure [71; 90]. When viewed under the SEM, highly crystallized material such as polycarbonate (PCL) [92] and polylactic acid (PLA) [93] have chaotic foam morphologies containing un-foamed regions. To address these issues, Colton [94] produced microcellular structures of semi-crystalline PP by processing in the molten amorphous state, above the melting point.

The polymer-gas solution formation process is much more complex with semi-crystalline polymers compared with amorphous resins. The effect of the dissolution of gas molecules into the polymer is another issue in the foaming process of semi-crystalline polymers. In amorphous polymers, this process causes significant plasticization and actively lowers the $T_g$. If the processing temperature is close to the $T_g$ of the neat amorphous polymer, a rapid viscosity increase is induced when gas is depleted from the gas-swollen melt. The impact of crystallization on cell formation during desorption of the polymer matrix can be investigated using a non-invasive

monitoring technique, such as ultrasound measurement [95]. The chain mobility is enhanced with the increase of the free volume of the polymer by the dissolved molecules (swell), which modifies the crystallization onset and the kinetics. The cellular structure of semi-crystalline polymer foams is relatively difficult to control compared to that of amorphous polymer foam. A study carried out by Reignier et al. [71] emphasizes the importance of crystallization kinetics and crystallization temperature to the processability of semi-crystalline polymers. Solubility of gas in a polymer is a linear function of crystallinity, since gas cannot dissolve in the crystalline phase, and increasing the crystalline fraction decreases the overall solubility of the system.

The foam morphology is also influenced by the presence of a crystalline phase in a polymer due to interactions between $CO_2$ and the polymer [96-98]. Furthermore, $CO_2$ sorption does not occur in the crystalline phase resulting in denser structures [90; 99-101]. There are two main impacts crystallinity has on cell density and the mechanisms governing microcellular nucleation.

First, crystalline foams have an increased cell density which is believed to be the result of heterogeneous nucleation, with the crystals acting as nucleating particles. Previous studies have shown that the preferential site for microvoid nucleation is the interface between the crystalline and amorphous regions since this is a higher energy region and the free energy barrier is lower [91]. On the other hand, Handa et al. [102] claimed that classical heterogeneous nucleation cannot be applied in the case of semi-crystalline polymers since the amorphous and semi-crystalline region boundaries are not well defined. Furthermore, the surface energy of the crystallized region was found to be lower than its amorphous counterpart.

Second, crystallinity impacts cell size and the mechanism governing cell growth. Baldwin et al. [91] explains that this is due to the increased matrix stiffness associated with crystallization, which causes an abrupt decrease in cell size. The cell growth mechanism is controlled primarily by the viscoelastic properties of the polymer matrix, rather than gas diffusion kinetics. The addition of talc drastically affects the matrix stiffness by increasing the crystallization temperature, resulting in different cellular morphologies [71].

During PLA foam process, cell coalescence and cell rupture can occur during cell growth because of PLA's inherently low melt strength. PLA's low melt strength also facilitates gas loss during foam expansion, causing severe shrinkage. An effective way to overcome these weak viscoelastic properties is to enhance PLA's crystallization kinetics during foam processing [103]. Crystallization during foaming can increase PLA's ability to expand by minimising cell coalescence and gas loss. However, high crystallinity will also suppress foam expansion due to excessive stiffness and less gas dissolution. On the other hand, heterogeneous cell nucleation theory states that cell nucleation will be promoted around the nucleated crystals through local pressure variations, thus improving final cell density. Taki et al. [104] studied the cell nucleation mechanism of poly-L-lactide acid (PLLA) with $CO_2$ in a batch process and found that the presence of spherulites in the PLLA matrix promoted the number of cell nuclei. They explained that the growing spherulites expelled dissolved $CO_2$ from the interface, leading to an increased concentration of $CO_2$, which caused cell nucleation to occur around the spherulites. Liao et al. [105] studied various crystallinities and crystallite sizes on the foaming of PLLA. They found that a higher foam density was achieved in areas with high concentrations of crystals with large sizes. Meaning that increased stiffness in the highly crystalline domain restricted cell growth and expansion.

#### 2.5.7.1 Effect of Talc on Crystallization

Heterogeneous nucleation allows better control of the cell nucleation process; in many cases, this is obtained by using a mineral nucleating agent such as talc [106]. However, their introduction in polymer formulations could also affect the crystallization behaviour of semi-crystalline polymers. To investigate this issue, classical DSC can be used to investigate the crystallization behaviour of NTP in the presence of talc. Reignier et al. [71] found that the crystallization temperature of PCL increased with small increments in talc concentrations. A small addition of 0.5% talc increased the melt crystallization peak from 32 °C to ≈ 39.5 °C. The conclusion reached from these results was that talc particles not only nucleate crystal formation, but they also speed up the crystallization kinetics through a volume effect.

For polymer-$CO_2$ systems nucleated with talc, foam density (g/cm$^3$) decreases linearly and cell size (µm) increases as foaming temperature increases [71]. The increase in cell size with foaming temperature is due to the viscosity decrease in the matrix material, meaning there is less resistance to cell growth. Cell population density (cells/cm$^3$) is also proportional to density. Ameli et al. [107] studied foam injection moulding behaviour of PLA with up to 5 wt.% talc. They found that the addition of talc improved crystallinity and promoted crystallization kinetics, which led to more uniform cell morphology, larger cell density and smaller cell sizes.

## 2.5.8 Methods of Improving Foamability

### 2.5.8.1 Organic Solvents

A study by Tsivintzelis et al. [88] investigated the use of $CO_2$-ethanol supercritical mixtures as blowing agents to foam polycaprolactone (PCL). Their results revealed that the difficulties involved in foaming crystalline polymers can be overcome with the addition of small amounts of organic solvents. When pure $CO_2$ was used as a blowing agent, the porous structure was non-uniform and consisted of regions with different pore sizes and pore densities. However, when small amount of ethanol was added the structure was more uniform and had larger pore sizes. This is due to the softening of the polymer matrix upon the addition of ethanol. Furthermore, a pronounced viscosity reduction is expected to occur due to the sorption of $CO_2$ and ethanol into the polymer matrix. This simplifies the growth of pores and facilitates the coalescence of neighbouring pores, resulting in larger pores and decreased bulk foam density.

If ethanol is added it is important to consider the possibility of polymer degradation. This can be investigated by measuring the intrinsic viscosity of the polymer samples in chloroform at ≈ 25°C by a calibrated Cannon Fenske viscometer [88]. If no major differences in intrinsic viscosity are observed among the foamed sample and unprocessed polymer, then no significant degradation has occurred.

#### 2.5.8.2 Talc

The study by Reignier et al. [71] also investigated the use of talc and its effect on crystallization. Talc is an efficient nucleating agent commonly used to produce fine-cell thermoplastic foams with a high cell density. It was found that talc modified the nucleation of both crystallites and cells, producing smaller cells and a more uniform cell size distribution. Also, the presence of talc had little effect on the proportion of small and open versus large and closed cells. As the concentration of talc increased, cell size decreased and cell density increased [71].

#### 2.5.8.3 Chain Extenders

A limitation in foaming of polymers is poor melt properties. One of the most investigated means of improving melt strength and elasticity is to modify the molecular structure by using a chain extender. Chain extension can improve both crystallinity and rheological properties of polymers [90]. Chain extension involves reacting functional molecules such as hydroxyl, anhydride, amine, isocyanate, and carboxylic acid, with the carboxyl or hydroxyl-end of polymer chains. The use of an epoxy functionalized chain extender was recently reported to give rise to branched structures improving significantly the processing window and material properties [108-110].

Advantages in using chain extenders is that, at low foaming temperatures (i.e. $T_F$ = 110 °C), the cellular structure is finer when chain extenders are increased. Highly chain extended samples also have higher cell population densities, shifting from macro cellular scale ($10^4$ cells $cm^{-3}$) to micro cellular scale ($10^{10}$ cells $cm^{-3}$) [90].

Weak melt strength is the result of gas loss which leads to reduced cell expansion and denser foams. Rheological properties improve because the melt strength is less sensitive to temperature and allows foaming at higher temperatures. Strain hardening plays an important role and prevents cells from collapsing. A disadvantage is that melt viscoelasticity increases by the chain extension process, which drastically reduces the cell expansion potential, as reported in Corre et al. [90]. A lower cell extension would reduce the risk of neighbouring cells coalescing, thus leading to higher cell densities and smaller cell diameters.

## 2.6 References


[1] *Biodegradable Polymers and Plastics*. (2003). New York: Kluwer Academic/Plenum Publishers.

[2] Utracki, L. A., & Wilkie, C. A. (2014). *Polymer blends handbook*. Springer Reference.

[3] Audic, J.-L., Chaufer, B., & Daufin, G. (2003). Non-food applications of milk components and dairy co-products: A review. *Lait, 83*(6), 417-438.

[4] Barone, J. R., & Arikan, O. (2007). Composting and biodegradation of thermally processed feather keratin polymer. *Polymer Degradation and Stability, 92*(5), 859-867.

[5] Cuq, B., Gontard, N., & Guilbert, S. (1998). Proteins as Agricultural Polymers for Packaging Production. *Cereal Chemistry, 75*(1), 1-9.

[6] Flieger, M., Kantorová, M., Prell, A., Řezanka, T., & Votruba, J. (2003). Biodegradable plastics from renewable sources. *Folia Microbiologica, 48*(1), 27-44.

[7] Hatti-Kaul, R., Törnvall, U., Gustafsson, L., & Börjesson, P. (2007). Industrial biotechnology for the production of bio-based chemicals – a cradle-to-grave perspective. *Trends in Biotechnology, 25*(3), 119-124.

[8] Hernandez-Izquierdo, V. M., Reid, D. S., McHugh, T. H., De J. Berrios, J., & Krochta, J. M. (2008). Thermal Transitions and Extrusion of Glycerol-Plasticized Whey Protein Mixtures. *Journal of Food Science, 73*(4), E169-E175.

[9] Ralston, B. E., & Osswald, T. A. (2005). *Creating Sustainability for the Environment*. Presented at the Global Plastics Environmental Conference (GPEC 2005).

[10] Verbeek, C. J. R., & van den Berg, L. E. (2010). Extrusion Processing and Properties of Protein-Based Thermoplastics. *Macromolecular Materials and Engineering, 295*(1), 10-21.

[11] Dee, K. C., Puleo, D. A., & Bizios, R. (2003). Proteins. In *An Introduction To Tissue-Biomaterial Interactions* (pp. 15-35). John Wiley & Sons, Inc.

[12] Jerez, A., Partal, P., Martínez, I., Gallegos, C., & Guerrero, A. (2007). Protein-based bioplastics: effect of thermo-mechanical processing. *Rheologica Acta, 46*(5), 711-720.

[13] De Graaf, L. A. (2000). Denaturation of proteins from a non-food perspective. *Journal of Biotechnology, 79*(3), 299-306.

[14] De Graaf, L. A., Harmsen, P. F. H., Vereijken, J. M., & Mönikes, M. (2001). Requirements for non-food applications of pea proteins A Review. *Food / Nahrung, 45*(6), 408-411.

[15] Jerez, A., Partal, P., Martínez, I., Gallegos, C., & Guerrero, A. (2007). Egg white-based bioplastics developed by thermomechanical processing. *Journal of Food Engineering, 82*(4), 608-617.

[16] Domenek, S., Morel, M.-H., Redl, A., & Guilbert, S. (2003). Thermosetting of wheat protein based bioplastics: modeling of mechanism and material properties. *Macromolecular Symposia, 197*(1), 181-192.

[17] *New Zealand Trade and Enterprise*. (2014). Meat. Retrieved June 10 2014, from https://www.nzte.govt.nz/en/buy/our-sectors/food-and-beverage/meat/.

[18] Low, A., Verbeek, C. J. R., & Lay, M. C. (2014). Treating Bloodmeal with Peracetic Acid to Produce a Bioplastic Feedstock. *Macromolecular Materials and Engineering, 299*(1), 75-84.

[19] Verbeek, C. R., & van den Berg, L. (2011). Development of Proteinous Bioplastics Using Bloodmeal. *Journal of Polymers and the Environment, 19*(1), 1-10.

[20] *Wallace Corporation Limited*. (2014). Blood Meal. Retrieved June 10, 2014, from http://www.wallace.co.nz/Rendering/Blood+Meal.html.

[21] Marsilla, K. I. K., & Verbeek, C. J. R. (2013). Properties of Bloodmeal/Linear Low-density Polyethylene Blends Compatibilized with Maleic Anhydride Grafted Polyethylene. *Journal of Applied Polymer Science, 130*(3), 1890-1897.

[22] Verbeek, C. J. R., & van den Berg, L. E. (2012). Structural changes as a result of processing in thermoplastic bloodmeal. *Journal of Applied Polymer Science, 125*(S2), E347-E355.

[23] Hicks, T., Verbeek, C. J. R., Lay, M. C., & Manley-Harris, M. (2013). The Role of Peracetic Acid in Bloodmeal Decoloring. *Journal of the American Oil Chemists' Society, 90*(10), 1577-1587.

[24] Ku Marsilla, K. I., & Verbeek, C. J. R. (2014). Mechanical Properties of Thermoplastic Protein From Bloodmeal and Polyester Blends. *Macromolecular Materials and Engineering* n/a-n/a.

[25] Verbeek, C. J. R., & van den Berg, L. E. (2011). Mechanical Properties and Water Absorption of Thermoplastic Bloodmeal. *Macromolecular Materials and Engineering, 296*(6), 524-534.

[26] Verbeek, C. R., Hicks, T., & Langdon, A. (2012). Odorous Compounds in Bioplastics Derived from Bloodmeal. *Journal of the American Oil Chemists' Society, 89*(3), 529-540.

[27] Verbeek, C. R., Hicks, T., & Langdon, A. (2012). Biodegradation of Bloodmeal-Based Thermoplastics in Green-Waste Composting. *Journal of Polymers and the Environment, 20*(1), 53-62.

[28] Verbeek, C. R., & Koppel, N. (2012). Moisture sorption and plasticization of bloodmeal-based thermoplastics. *Journal of Materials Science, 47*(3), 1187-1195.

[29] Pickering, K. L., Verbeek, C. J. R., Viljoen, C., & Van Den Berg, L. E. (2010). Plastics material.

[30] Bier, J. M., Verbeek, C. J. R., & Lay, M. C. (2014). Thermal and Mechanical Properties of Bloodmeal-Based Thermoplastics Plasticized with Tri(ethylene glycol). *Macromolecular Materials and Engineering, 299*(1), 85-95.

[31] Di Gioia, L., & Guilbert, S. (1999). Corn Protein-Based Thermoplastic Resins: Effect of Some Polar and Amphiphilic Plasticizers. *Journal of Agricultural and Food Chemistry, 47*(3), 1254-1261.

[32] Smith, M. J., & Verbeek, C. J. (2016). Impact Modification and Fracture Mechanisms of Core–Shell Particle Reinforced Thermoplastic Protein. *Macromolecular Materials and Engineering, 301*(8), 992-1003.

[33] Ku Marsilla, K., & Verbeek, C. J. (2014). Mechanical properties of thermoplastic protein from bloodmeal and polyester blends. *Macromolecular Materials and Engineering, 299*(7), 885-895.

[34] Ku- Marsilla, K., & Verbeek, C. J. R. (2015). Compatibilization of Protein Thermoplastics and Polybutylene Succinate Blends. *Macromolecular Materials and Engineering, 300*(2), 161-171.

[35] Kuo, S.-W. (2012). Miscibility enhancement of polymer blends through multiple hydrogen bonding interactions. In V. Mittal (Ed.), *Functional Polymer Blends: Synthesis, Properties, and Performance* (pp. 27-52). Baton Rouge, LA: Chapman and Hall/CRC.

[36] Zhang, J., Jiang, L., Zhu, L., Jane, J.-l., & Mungara, P. (2006). Morphology and properties of soy protein and polylactide blends. *Biomacromolecules, 7*(5), 1551-1561.

[37] Zhu, R., Liu, H., & Zhang, J. (2012). Compatibilizing Effects of Maleated Poly(lactic acid) (PLA) on Properties of PLA/Soy Protein Composites. *Industrial and Engineering Chemistry Research 51*(22), 7786-7792.

[38] Wang, H., Sun, X., & Seib, P. (2001). Strengthening blends of poly (lactic acid) and starch with methylenediphenyl diisocyanate. *Journal of applied polymer science, 82*(7), 1761-1767.

[39] Orozco, V. H., Brostow, W., Chonkaew, W., & Lopez, B. L. (2009) Preparation and Characterization of Poly (Lactic Acid)- g- Maleic Anhydride+ Starch Blends. In *Macromolecular symposia* (Vol. 277, pp. 69-80): Wiley Online Library.

[40] Zhang, J.-F., & Sun, X. (2004). Mechanical Properties of Poly(lactic acid)/Starch Composites Compatibilized by Maleic Anhydride. *Biomacromolecules, 5*(4), 1446-1451.

[41] Fowlks, A. C., & Narayan, R. (2010). The effect of maleated polylactic acid (PLA) as an interfacial modifier in PLA- talc composites. *Journal of applied polymer science, 118*(5), 2810-2820.

[42] Petersson, L., Oksman, K., & Mathew, A. (2006). Using maleic anhydride grafted poly (lactic acid) as a compatibilizer in poly (lactic acid)/layered- silicate nanocomposites. *Journal of applied polymer science, 102*(2), 1852-1862.

[43] Qian, S., Mao, H., Sheng, K., Lu, J., Luo, Y., & Hou, C. (2013). Effect of low-concentration alkali solution pretreatment on the properties of bamboo particles reinforced poly (lactic acid) composites. *Journal of Applied Polymer Science, 130*(3), 1667-1674.

[44] Fischer, L., & Peissker, F. (1998). A covalent two-step immobilization technique using itaconic anhydride. *Applied microbiology and biotechnology, 49*(2), 129-135.

[45] Verbeek, C., & Hanipah, S. (2010). Grafting itaconic anhydride onto polyethylene using extrusion. *Journal of applied polymer science, 116*(6), 3118-3126.

[46] Ku Marsilla, K. I., & Verbeek, C. J. R. (2015). Modification of poly(lactic acid) using itaconic anhydride by reactive extrusion. *European Polymer Journal, 67*, 213-223.

[47] S.T. Lee and N.S Ramesh. (2004). *Polymeric Foams: Mechanisms and Materials*. Boca Raton: CRC Press.

[48] *Handbook of Polymeric Foams and Foam Technology*. (1991). Munich: Hanser.

[49] *Foam Extrusion: Principles and Practice*. (2000). Boca Raton: CRC Press.

[50] Lee, S.-T., & Scholz, D. (Eds.). (2009). *Polymeric Foams: Technology and Developments in Regulation, Process, and Products*. Boca Raton, FL: CRC Press.

[51] Hilyard, N. C., & Cunningham, A. (1994). *Low Density Cellular Plastics: Physical Basis of Behaviour*. London: Chapman & Hall.

[52] Bailey, F. E. (1991). *Polymeric Foams*. New York: Hanser.

[53] Blander, M., & Katz, J. L. (1975). Bubble nucleation in liquids. *AIChE Journal, 21*(5), 833-848.

[54] Byon, S. K., & Youn, J. R. (1990). Ultrasonic processing of thermoplastic foam. *Polymer Engineering & Science, 30*(3), 147-152.

[55] Cole, R. (1974). Boiling Nucleation. In P. H. James & F. I. Thomas (Eds.), *Advances in Heat Transfer* (Vol. Volume 10, pp. 85-166). Elsevier.

[56] Cole, R. (1986). Bubble nucleation, growth and departure in boiling heat transfer. In *Handbook of Heat and Mass Transfer*. Houston, TX: Gulf Publishing.

[57] Colton, J. S., & Suh, N. P. (1987). The nucleation of microcellular thermoplastic foam with additives: Part I: Theoretical considerations. *Polymer Engineering and Science, 27*(7), 485-492.

[58] Han, J. H., & Dae Han, C. (1990). Bubble nucleation in polymeric liquids. II. theoretical considerations. *Journal of Polymer Science Part B: Polymer Physics, 28*(5), 743-761.

[59] Lee, S. T. (2000). *Foam Extrusion: Principles and Practice*. Boca Raton, FL: CRC Press.

[60] Ramesh, N. S., Rasmussen, D. H., & Campbell, G. A. (1994). The heterogeneous nucleation of microcellular foams assisted by the survival of microvoids in polymers containing low glass transition particles. Part I: Mathematical modeling and numerical simulation. *Polymer Engineering & Science, 34*(22), 1685-1697.

[61] Springer, G. S. (1979). Homogeneous Nucleation. In F. I. Thomas & P. H. James (Eds.), *Advances in Heat Transfer* (Vol. Volume 14, pp. 281-346). Elsevier.

[62] Yang, H.-H., & Han, C. D. (1984). The effect of nucleating agents on the foam extrusion characteristics. *Journal of Applied Polymer Science, 29*(12), 4465-4470.

[63] Einstein, A. (1910). Theorie der Opaleszenz von homogenen Flüssigkeiten und Flüssigkeitsgemischen in der Nähe des kritischen Zustandes. *Annalen der Physik, 338*(16), 1275-1298.

[64] Uhlmann, D. R., & Chalmers, B. (1965). The Energetics of Nucleation. *Industrial & Engineering Chemistry, 57*(9), 19-31.

[65] Kang, D. J., Xu, D., Zhang, Z. X., Pal, K., Bang, D. S., & Kim, J. K. (2009). Well- Controlled Microcellular Biodegradable PLA/Silk Composite Foams Using Supercritical CO2. *Macromolecular Materials and Engineering, 294*(9), 620-624.

[66] Pilla, S., Kramschuster, A., Lee, J., Auer, G. K., Gong, S., & Turng, L.-S. (2009). Microcellular and solid polylactide–flax fiber composites. *Composite Interfaces, 16*(7-9), 869-890.

[67] Hamza, R., Zhang Xiaodong, D., Macosko Christopher, W., Stevens, R., & Listemann, M. (1997). Imaging Open-Cell Polyurethane Foam via Confocal Microscopy. In *Polymeric Foams* (Vol. 669, pp. 165-177). American Chemical Society.

[68] Gibson, L. J., & Ashby, M. F. (1988). *Cellular Solids*. Oxford, London: Pergamon.

[69] Hampson, R., F., Kurylo, M., J., & Sander, S., P. (1989). Evaluated Rate Constants for Selected HCFC's and HFC's with OH and O($^1$D). In *Scientific*

*Assessment of Stratospheric Ozone* (Vol. 2). Earth System Research Laboratory. Retrieved from http://www.esrl.noaa.gov/csd/assessments/ozone/1989/report.html.

[70] Morita, K., Uchiki, K., & Shinoda, H. (1993). High polymer network.

[71] Reignier, J., Gendron, R., & Champagne, M. F. (2007). Autoclave Foaming of Poly(ε-Caprolactone) Using Carbon Dioxide: Impact of Crystallization on Cell Structure. *Journal of Cellular Plastics, 43*(6), 459-489.

[72] Plastic Engineering Associates Licensing, I. (Compiler) (2008). *Turbo-Screws Technology for PLA Foam*.

[73] Pontiff, T. M. (1997) Factors affecting foam cell nucleation in direct gassed foam extrusion. In *FOAMPLAS* (pp. 251-261). Mainz, Germany.

[74] Scholz, D. (1999) 25 Years endothermic blowing or foaming agents - Is that enough? In *Structural Plastics Conference*. Boston, MA.

[75] Scholz, D. (1987). *The position of endothermic nucleating and blowing agents in thermoplastic foams*. Presented at the Ausplace Conference.

[76] Sjöqvist, M., & Gatenholm, P. (2007). Effect of Water Content in Potato Amylopectin Starch on Microwave Foaming Process. *Polymer Environment*.

[77] Fleming, G. K., & Koros, W. J. (1986). Dilation of polymers by sorption of carbon dioxide at elevated pressures. 1. Silicone rubber and unconditioned polycarbonate. *Macromolecules, 19*(8), 2285-2291.

[78] Hirose, T., Mizoguchi, K., & Kamiya, Y. (1986). Dilation of polyethylene by sorption of carbon dioxide. *Journal of Polymer Science Part B: Polymer Physics, 24*(9), 2107-2115.

[79] Sefcik, M. D. (1986). Dilation of polycarbonate by carbon dioxide. *Journal of Polymer Science Part B: Polymer Physics, 24*(5), 935-956.

[80] Wissinger, R. G., & Paulaitis, M. E. (1987). Swelling and sorption in polymer–CO2 mixtures at elevated pressures. *Journal of Polymer Science Part B: Polymer Physics, 25*(12), 2497-2510.

[81] Chiou, J. S., Barlow, J. W., & Paul, D. R. (1985). Plasticization of glassy polymers by CO2. *Journal of Applied Polymer Science, 30*(6), 2633-2642.

[82] Sefcik, M. D. (1986). Dilation and plasticization of polystyrene by carbon dioxide. *Journal of Polymer Science Part B: Polymer Physics, 24*(5), 957-971.

[83] Wang, W.-C. V., Kramer, E. J., & Sachse, W. H. (1982). Effects of high-pressure CO2 on the glass transition temperature and mechanical properties of polystyrene. *Journal of Polymer Science: Polymer Physics Edition, 20*(8), 1371-1384.

[84] Berens, A. R., & Huvard, G. S. (1989). Interaction of Polymers with Near-Critical Carbon Dioxide. In *Supercritical Fluid Science and Technology* (Vol. 406, pp. 207-223). American Chemical Society.

[85] Goel, S. K., & Beckman, E. J. (1994). Generation of microcellular polymeric foams using supercritical carbon dioxide. I: Effect of pressure and temperature on nucleation. *Polymer Engineering & Science, 34*(14), 1137-1147.

[86] Rouholamin, D., Smith, P., & Ghassemieh, E. (2013). Control of morphological properties of porous biodegradable scaffolds processed by supercritical CO2 foaming. *Journal of Materials Science, 48*(8), 3254-3263.

[87] Tsivintzelis, I., Angelopoulou, A. G., & Panayiotou, C. (2007). Foaming of polymers with supercritical CO2: An experimental and theoretical study. *Polymer, 48*(20), 5928-5939.

[88] Tsivintzelis, I., Pavlidou, E., & Panayiotou, C. (2007). Biodegradable polymer foams prepared with supercritical CO2–ethanol mixtures as blowing agents. *The Journal of Supercritical Fluids, 42*(2), 265-272.

[89] Guo, Q., Wang, J., Park, C. B., & Ohshima, M. (2006). A Microcellular Foaming Simulation System with a High Pressure-Drop Rate. *Industrial & Engineering Chemistry Research, 45*(18), 6153-6161.

[90] Corre, Y.-M., Maazouz, A., Duchet, J., & Reignier, J. (2011). Batch foaming of chain extended PLA with supercritical CO2: Influence of the rheological properties and the process parameters on the cellular structure. *The Journal of Supercritical Fluids, 58*(1), 177-188.

[91] Baldwin, D. F., Shimbo, M., & Suh, N. P. (1995). The Role of Gas Dissolution and Induced Crystallization During Microcellular Polymer Processing: A Study of Poly (Ethylene Terephthalate) and Carbon Dioxide Systems. *Journal of Engineering Materials and Technology, 117*(1), 62-74.

[92] Mascia, L., Re, G. D., Ponti, P. P., Bologna, S., Giacomo, G. D., & Haworth, B. (2006). Crystallization effects on autoclave foaming of polycarbonate using supercritical carbon dioxide. *Advances in Polymer Technology, 25*(4), 225-235.

[93] Zhai, W., Ko, Y., Zhu, W., Wong, A., & Park, C. (2009). A Study of the Crystallization, Melting, and Foaming Behaviors of Polylactic Acid in Compressed CO2. *International Journal of Molecular Sciences, 10*(12), 5381-5397.

[94] Colton, J. S. (1989). The Nucleation of Microcellular Foams in Semi Crystalline Thermoplastics. *Materials and Manufacturing Processes, 4*(2), 253-262.

[95] Reignier, J., Tatibouët, J., & Gendron, R. (2006). Batch foaming of poly(ε-caprolactone) using carbon dioxide: Impact of crystallization on cell nucleation as probed by ultrasonic measurements. *Polymer, 47*(14), 5012-5024.

[96] Sadowski, G. (2006). Phase Behavior of Polymer Systems in High-Pressure Carbon Dioxide. In *Supercritical Carbon Dioxide* (pp. 15-35). Wiley-VCH Verlag GmbH & Co. KGaA.

[97] Shieh, Y.-T., Su, J.-H., Manivannan, G., Lee, P. H. C., Sawan, S. P., & Dale Spall, W. (1996). Interaction of supercritical carbon dioxide with polymers. I. Crystalline polymers. *Journal of Applied Polymer Science, 59*(4), 695-705.

[98] Shieh, Y.-T., Su, J.-H., Manivannan, G., Lee, P. H. C., Sawan, S. P., & Dale Spall, W. (1996). Interaction of supercritical carbon dioxide with polymers. II. Amorphous polymers. *Journal of Applied Polymer Science, 59*(4), 707-717.

[99] Baldwin, D. F., Park, C. B., & Suh, N. P. (1996). A microcellular processing study of poly(ethylene terephthalate) in the amorphous and semicrystalline states. Part I: Microcell nucleation. *Polymer Engineering & Science, 36*(11), 1437-1445.

[100] Baldwin, D. F., Park, C. B., & Suh, N. P. (1996). A microcellular processing study of poly(ethylene terephthalate) in the amorphous and semicrystalline states. Part II: Cell growth and process design. *Polymer Engineering and Science, 36*(11), 1446-1453.

[101] Doroudiani, S., Park, C. B., & Kortschot, M. T. (1996). Effect of the crystallinity and morphology on the microcellular foam structure of semicrystalline polymers. *Polymer Engineering and Science, 36*(21), 2645-2662.

[102] Handa, Y. P., Zhang, Z., Nawaby, V., & Tan, J. (2001). Gas Solubility in and Foamability of Various Forms of Syndiotactic Polystyrene. *Cellular Polymers, 20*(4), 241-253.

[103] Iannace, S., & Park, C. B. (2015). *Biofoams: Science and Applications of Bio-based Cellular and Porous Materials*. CRC Press.

[104] Taki, K., Kitano, D., & Ohshima, M. (2011). Effect of growing crystalline phase on bubble nucleation in poly (L-lactide)/CO2 batch foaming. *Industrial & Engineering Chemistry Research, 50*(6), 3247-3252.

[105] Liao, X., Nawaby, A. V., & Whitfield, P. S. (2010). Carbon dioxide- induced crystallization in poly (L- lactic acid) and its effect on foam morphologies. *Polymer international, 59*(12), 1709-1718.

[106] Park, C. B., Cheung, L. K., & Song, S. W. (1998). The effect of talc on cell nucleation in extrusion foam processing of polypropylene with CO2 and isopentane. *Cellular Polymers, 17*(4), 221-251.

[107] Ameli, A., Jahani, D., Nofar, M., Jung, P. U., & Park, C. B. (2013). Processing and characterization of solid and foamed injection-molded polylactide with talc. *Journal of Cellular Plastics, 49*(4), 351-374.

[108] Mihai, M., Huneault, M. A., & Favis, B. D. (2010). Rheology and extrusion foaming of chain-branched poly(lactic acid). *Polymer Engineering & Science, 50*(3), 629-642.

[109] Pilla, S., Kim, S. G., Auer, G. K., Gong, S., & Park, C. B. (2009). Microcellular extrusion-foaming of polylactide with chain-extender. *Polymer Engineering & Science, 49*(8), 1653-1660.

[110] Pilla, S., Kramschuster, A., Yang, L., Lee, J., Gong, S., & Turng, L.-S. (2009). Microcellular injection-molding of polylactide with chain-extender. *Materials Science and Engineering: C, 29*(4), 1258-1265.

# 3

# Morphology and Mechanical Properties of Itaconic Anhydride Grafted Poly(lactic acid) and Thermoplastic Protein Blends

A journal article published in

***International Polymer Processing***

By

A. S. Walallavita, C. J. R. Verbeek, & M. C. Lay

**Morphology and Mechanical Properties of Itaconic Anhydride Grafted Poly(lactic acid) and Thermoplastic Protein Blends**

In Chapter 3, itaconic anhydride grafted PLA blended with thermoplastic protein was investigated using reactive extrusion, for the first time. The results were used to determine the effectiveness of a compatibilizer in Novatein-PLA blends and the improvement in Novatein's mechanical properties when blended. The formation of a co-continuous morphology at equal proportions of Novatein and PLA was also examined using SEM and further characterised using DMA and XRD. The findings of this chapter contributed to the production of Novatein-PLA batch foams, later discussed in Chapter 4.

As first author of this paper, I prepared the initial draft manuscript, which was refined and edited in consultation with my supervisors, who have been credited as co-authors.

Morphology and Mechanical Properties of Itaconic Anhydride Grafted Poly(lactic acid) and Thermoplastic Protein Blends, previously published in International Polymer Processing (Carl Hanser Verlag, Munich, Germany).

*A. S. Walallavita, C. J. R. Verbeek*, M. C. Lay*

*Department of Engineering, School of Science and Engineering, University of Waikato, Hamilton, New Zealand*

# Morphology and Mechanical Properties of Itaconic Anhydride Grafted Poly(lactic acid) and Thermoplastic Protein Blends

*Blends between Novatein thermoplastic protein and polylactic acid (PLA) have been prepared by reactive extrusion using itaconic anhydride grafted PLA. At equal proportions of Novatein and PLA, the absence of a compatibilizer formed a dispersed phase morphology of Novatein in PLA and the incorporation of compatibilizer formed a co-continuous morphology. Incorporating PLA in Novatein can improve the tensile strength of Novatein by 42 % and the impact strength by 36 % at an equal proportion blend (50/50) in the presence of a compatibilizer. Thermal analysis revealed that 50/50 was the phase inversion point, above and below this composition the material behaved similarly. The effect of compatibilizer was evident in wide-angle X-ray scattering. In the absence of compatibilizer three phases were detected: crystalline Novatein, amorphous Novatein, and amorphous PLA phases. With compatibilizer, the blend was moving towards two phases: crystalline Novatein, and an amorphous blend of Novatein and PLA. Itaconic anhydride grafted PLA improved miscibility between Novatein and PLA, and its use can potentially lead to the production of Novatein/PLA foams.*

## 1 Introduction

Polymer foams are an unprecedented necessity in everyday life particularly in applications such as packaging where light weight and mechanical integrity are critical. The global market for synthetic polymer foams totalled 19.1 million tonnes in 2013, and is expected to grow to 25.3 million tonnes by 2019 (Smithers Pira, 2016). Furthermore, the packaging market is expected to reach $975 billion by 2018 (Smithers Pira, 2016). Like most polymer industries, polymer foams used in packaging are petroleum derived; examples include polyvinyl chloride, polyethylene, polypropylene, and polystyrene. The large and increasing volume of foamed materials in landfills has sparked interest toward more sustainable materials which can be utilized in high-volume situations. Biopolymer foams are one such alternative to solve the packaging disposal problem.

The popularity of polylactic acid (PLA) as a renewable biopolymer continues to increase because of its processing and performance features which allows PLA to compete with petroleum-based polymers (Parker et al., 2011b). PLA can be foamed using non-toxic carbon dioxide and has thermal and mechanical properties competitively similar to that of expanded polystyrene (Parker et al., 2011a; Witt and Shah, 2012). Biopolymers can also be directly extracted from natural raw materials such as proteins; Novatein Thermoplastic Protein (NTP) is one such example. Novatein is the only commercial thermoplastic protein that can be extruded and injection molded into a variety of agricultural products such as plant pots, weasand clips and weed mat pegs (Pickering et al., 2010). However, foaming Novatein is a new area of study which has never been investigated. The foamability of a material is related to the rheological properties of the melt, i. e. the polymer needs to withstand the stretching forces during bubble growth and hold the newly formed cellular structure. This is also known as strain hardening behavior and is a fundamental characteristic in the foaming process (Marrazzo et al., 2007). Inducing a cellular structure in Novatein is difficult because of its low melt strength. However, the foamability of Novatein could potentially be improved by blending with a biopolymer that can successfully be foamed, such as PLA.

Producing a foamed material by blending two polymers has been reported in the literature. Bao et al. (Bao et al., 2013) induced a nanocellular foam structure in a blend of polycarbonate (PC) and PLA. The method utilizes the high glass transition temperature ($T_g$) and/or high crystallinity of one of the polymers, in this case PC, to supress cell growth because of its high viscosity. As a result, cell nucleation occurs in the PLA phase which has a low $T_g$ and low crystallinity and higher sorption of blowing agent (carbon dioxide). Furthermore, the interface of the two phases acts as heterogeneous nucleation sites thereby increasing cell density. Polymer blends have structural non-homogeneity (soft and hard regions) which can aid foaming (Park et al., 2005). During cell growth the cell walls thin; soft regions are used to create pores which interconnect cells while hard regions maintain the overall cell structure and prevent cells from completely coalescing (Kohlhoff and Ohshima, 2011).

* Mail address: Casparus Johannes Reinhard Verbeek, Department of Engineering, School of Science and Engineering, University of Waikato, Hamilton 3240, New Zealand
E-mail: jverbeek@waikato.ac.nz

The properties of polymer blends are dependent on the composition, structure, and interactions of the components (Ku-Marsilla and Verbeek, 2015). Weak interfacial adhesion and thermodynamic incompatibility between two components can lead to poor mechanical properties of the blend. These issues can be addressed with the use of a compatibilizer. The main advantage of using compatibilizers in polymer blends is coalescence suppression of the dispersed domains which is achieved by stabilizing the interface. In recent years, grafting a reactive moiety such as maleic anhydride (MA) has led to improved interfacial modification between immiscible natural polymers and PLA (Fowlks and Narayan, 2010; Orozco et al., 2009; Petersson et al., 2006; Zhang and Sun, 2004). Zhu et al. (2012) found the tensile strength of soy protein blends had increased by 19 % when PLA was grafted with MA (PLA-g-MA). PLA-g-MA was also used as a compatibilizer for thermoplastic starch blends (Huneault and Li, 2007). Blend morphology without compatibilizer was coarse and starch particle size ranged from 5 to 30 μm. Blends comprising PLA-g-MA showed a well dispersed and finer phase size (1 to 3 μm) and significantly improved ductility. MA is widely available and has a low tendency to homopolymerize making MA the most commonly used monomer for grafting reactions, yet its reaction with proteins may result in unstable amide bonds that can easily be hydrolysed (Ku Marsilla and Verbeek, 2015). An alternative to MA is itaconic anhydride (IA) which is less harmful and prepared from renewable resources (Pesetskii et al., 2002; Verbeek and Hanipah, 2010; Yazdani-Pedram et al., 2003). IA is extremely stable when reacted with proteins as it can be used for acetylating cysteine, lysine, and tyrosine (Fischer and Peissker, 1998). Previous work has shown that itaconic anhydride can be grafted onto PLA (PLA-g-IA) using dicumyl peroxide as the radical initiator (Ku Marsilla and Verbeek, 2015). IA has also been successfully grafted onto polyethylene with a high degree of grafting (Verbeek and Hanipah, 2010). In the case of Novatein and PLA, using a renewable monomer such as IA can lead to a 100 % bio-derived blend.

In this study, the compatibilizing effect of IA/DCP on blends of Novatein and PLA has been investigated. The evolution of morphology, the mechanical properties and thermal analysis in the presence of a compatibilizer have been observed to determine whether IA/DCP has improved miscibility between Novatein and PLA. The findings of this study will ultimately lead to the production of Novatein/PLA foams.

## 2 Methodology

### *2.1 Materials*

Novatein was obtained from Aduro Biopolymers, Hamilton, New Zealand (Aduro Biopolymers, 2016) and stored at >4 °C for a minimum of 24 h. The Novatein formulation contains an amphiphilic plasticizer, tri(ethylene glycol) (TEG), which is an effective plasticizer for bloodmeal thermoplastics (Bier et al., 2014). Analytical grade itaconic anhydride (IA) and dicumyl peroxide (DCP) were purchased from Sigma Aldrich and used as received. A fully amorphous PLA grade (4060D) in pellet form was obtained from NatureWorks LLC and used as received.

### *2.2 Preparation of PLA Grafted Itaconic Anhydride (PLA-g-IA)*

PLA-g-IA was prepared by dissolving 40 grams of itaconic anhydride (molecular weight 112.08 g/mol) and 7.5 grams of dicumyl peroxide (molecular weight 270.37 g/mol) in 30 ml dehydrated acetone. The solution was poured over 952.5 grams of PLA and kept in the fume hood for approximately 2 h before oven drying at 50 °C for 3 h. Different concentrations of IA and DCP have been analysed previously (Ku Marsilla and Verbeek, 2015); for this study, the amount of IA/DCP grafted onto PLA was fixed at 5 wt.% for all blends which gives a grafting degree of 0.45 %. The material was then reactive extruded to ensure that there is no residue unreacted IA. A LabTech twin screw extruder with L/D ratio of 44 : 1 was used for grafting with a temperature profile of 145, 145, 165, 165, 180, 180, 180, 180, 160, 160, 155 °C. Screws were co-rotating and maintained at a constant speed of 150 $min^{-1}$ for all experiments. A vacuum port was attached at the 7$^{th}$ heating zone to remove potential harmful vapours. The extrudate was collected in a water bath to prevent crystallization and subsequently pelletized. PLA-g-IA was dried below 50 °C overnight before blending with Novatein.

### *2.3 Preparation of Novatein/PLA Blends*

Blends were extruded using the same extruder used for grafting. Novatein was used as received from Aduro Biopolymers (Aduro Biopolymers, 2016). PLA pellets without compatibilizer were oven dried at 45 °C for 4 h to a moisture content of less than 250 ppm to minimise hydrolysis during melt processing. PLA with and without compatibilizer was extruded with Novatein according to the blend ratios listed in Table 1. Blends which contain compatibilizer are indicated with "IA/DCP" at the end of the blend ratio designation (i.e. 90-10 IA/DCP, 70-30 IA/DCP, 50-50 IA/DCP, 30-70 IA/DCP). Temperature profiles varied between 70 °C at the feed and 175 °C at the die according to the ratio of Novatein and PLA in the blend. A relative torque of 50 to 60 % was maintained by adjusting the mass flow rate of the feed. Standard tensile and impact bars were prepared using an injection molding machine (model Boy 35A, Boy Machines Inc., Exton, USA).

| Sample name | Novatein wt.% | PLA wt.% |
|---|---|---|
| Novatein | 100 | 0 |
| 90-10 | 90 | 10 |
| 70-30 | 70 | 30 |
| 50-50 | 50 | 50 |
| 30-70 | 30 | 70 |
| PLA | 0 | 100 |

*Table 1. Novatein/PLA blend compositions. Samples with compatibilizer are indicated with IA/DCP in their sample name and contain 4.2 wt.% IA and 0.8 wt.% DCP*

### 2.4 Analysis

Fracture surfaces of tensile and impact tested bars were viewed using a field emission scanning electron microscope (SEM), model S-4700, Hitachi, Tokyo, Japan. Specimens were coated with platinum using an ion sputter (model E-1030, Hitachi) before scanning at an accelerating voltage of 3 kV. The binary blend phase separation was observed using Energy Dispersive X-Ray Spectroscopy (SEM-EDS). To better illustrate Novatein morphology, chloroform ($CHCl_3$) was used to extract the PLA phase in injection molded test specimens. Blends were kept in $CHCl_3$ in the fume hood until all of the PLA phase had been dissolved. The resulting surface morphology was viewed under SEM, rather than tensile tested fracture surfaces.

A testing machine (model 33R4204, Instron, Norwood, USA) was used for tensile testing at an extension rate of 5 mm/min and extensometer gauge length of 50 mm. Injection molded specimens were conditioned at 23 °C and 50 % relative humidity for 7 days prior to tensile testing according to ASTM D638-86. Specimens were tested in groups of five directly after removal from the conditioning chamber. Impact testing bars ($80 \times 10 \times 4$ mm$^3$) were produced from the injection molder and conditioned at 23 °C and 50 % relative humidity for 7 days. A minimum of ten impact bars were notched in accordance with ISO 2818 and Charpy edgewise impact strength (ISO 179) was measured using a pendulum impact system (model Ray-Ran, Ray-Ran Test Equipment, Nuneaton, UK). Velocity of impact was 2.9 m/s, energy was 2 J and hammer weight was 0.475 kg.

Water absorption of Novatein/PLA blends was measured over ten days and each sample was measured in replicas of five. All samples were oven dried at 70 °C until constant weight was reached and then immersed in water at room temperature for ten days. Samples were removed and blotted with tissue paper to remove excess water before being weighed. Water absorption was calculated on a dry sample basis.

Dynamic mechanical properties of Novatein/PLA blends were investigated using a DMA 8000 (Perkin Elmer, Waltham, USA) fitted with a high temperature furnace and controlled with Pyris software version 11.1.1.0492 (Perkin Elmer). DMA specimens ($30 \times 6.5 \times 3$ mm$^3$) were cut from injection molded samples and tested using a single cantilever fixture at 1 Hz and free length of 12.5 mm at temperatures –80 to 150 °C.

Differential scanning calorimetry (DSC) was conducted using a DSC 8500 (Perkin Elmer) and analysed using Pyris software version 11.1.1.0492. Approximately 5 mg of sample was placed into a crimp sealed aluminium pan and run under constant nitrogen purge gas. Specimens were heated from 25 to 200 °C at 20 °C/min and held for 5 min at 200 °C, before being cooled to 25 °C at 20 °C/min.

Wide angle X-ray scattering was carried out using a X-ray diffractometer (PANalytical Empyrean, Almelo, The Netherlands) using $CuK_{\alpha 1}$ radiation and a generator voltage of 45 kV and a current of 40 mA at ambient temperature. Samples were extruded, granulated, and powdered before mounting on XRD sample holders. Data was collected at a step size of 0.0131° in the 2θ range from 5° to 40°. A fixed 7.5 mm anti-scatter slit was used with soller slit of 0.04 rad.

## 3 Results and Discussion

### 3.1 Morphology

The properties of polymer blends are greatly influenced by the morphology; i.e. shape, size, and distribution of the components. Polymer blend morphologies can generally be categorised into three classes: dispersed, continuous, and co-continuous phases (Prochazka et al., 2002; Veenstra et al., 2000a; Veenstra et al., 2000b; Willemse, 1999). Co-continuous morphologies are mainly formed around the point of phase inversion, at which the matrix is hardly distinguishable from the dispersed phase. The role of a compatibilizer is to reduce interfacial tension by stabilizing the morphology which in turn leads to a co-continuous morphology (Ku-Marsilla and Verbeek, 2015).

Figure 1 shows SEM images of tensile tested fracture surfaces of Novatein/PLA blends at different compositions, with and without compatibilizer. Neat PLA and Novatein/PLA blends exhibited brittle failure as the fracture surfaces showed little sign of plastic deformation. In the absence of a compatibilizer, a dispersed phase morphology has formed where spherical Novatein domains are imbedded in a PLA matrix (Fig. 1C, E and G). The separate phases were observed using SEM-EDS. Dispersed phase morphology is a result of poor interfacial adhesion which in turn leads to the propagation of cracks (Fig. 1E). Ku-Marsilla and Verbeek (2015) also observed poor interfacial adhesion between Novatein and PBS in the absence of a compatibilizer. Liu et al. (2010) observed that soy protein dispersion and domain sizes did not drastically change upon the addition of polymeric methylene diphenyl diisocyanate (pMDI) but compatibilization resulted in less visible cracks and voids, indicating that pMDI improved interfacial bonding between PLA and soy protein.

The morphology of Novatein/PLA blends with compatibilizer (Fig. 1D, F and H) showed fewer agglomerated Novatein particles and phase separation was less visible. The morphology at 70-30 IA/DCP and 30-70 IA/DCP was very similar, and was further explored using thermal analysis (discussed in sections 3.3 and 3.4).

In equal proportions of Novatein and PLA-g-IA (Fig. 1H) the Novatein phase was virtually indistinguishable within the matrix. The compatibilizing action of IA/DCP has improved interfacial adhesion for the 50-50 blend which caused a 49 % increase in tensile strength over neat Novatein, discussed in section 3.2.

Zhu et al. (2012) found that large soy protein particles caused a severe stress concentration within the matrix which allowed cracks to propagate through the weak interfaces. However, upon the addition of PLA-g-MA, the soy protein phase became finer and an improvement in tensile strength from 45 to 53 MPa was observed. For Novatein/PLA and even soy/PLA blends, the tensile strength of the blends was inferior to neat PLA because of weak interfacial adhesion even in the presence of a compatibilizer. Poor interfacial adhesion leads to debonding at the interface at a stress level smaller than that of matrix yielding.

To better understand the dispersed and co-continuous phase morphologies, chloroform was used to dissolve the PLA phase and resulting SEM images are presented in Fig. 2. Chloroform did not dissolve Novatein and the sample remained intact (Ta-

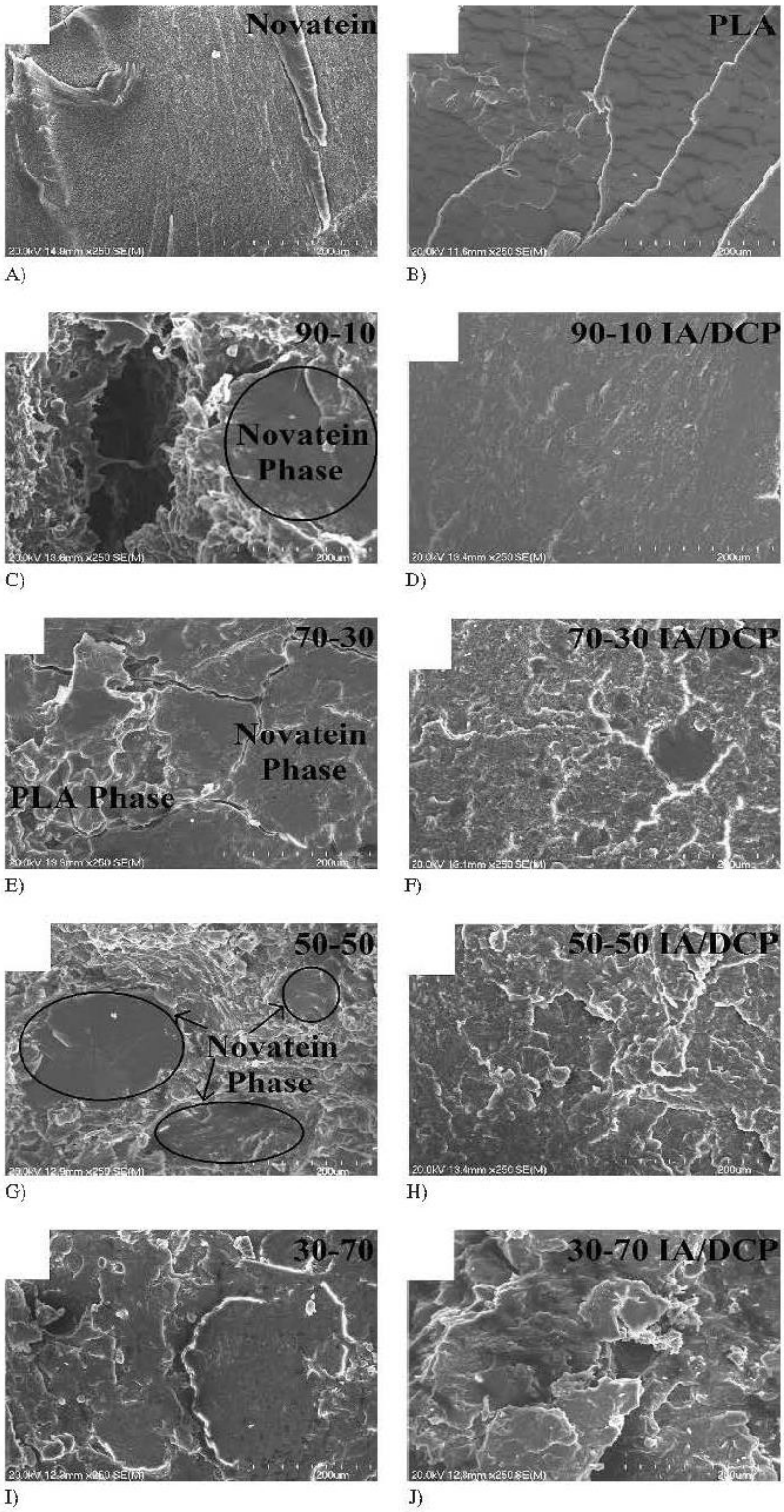


*Fig. 1. SEM images of tensile tested fracture surfaces at magnification × 250, A) Novatein, B) PLA, C) 90-10, D) 90-10 IA/DCP, E) 70-30, F) 70-30 IA/DCP, G) 50-50, H) 50-50 IA/DCP, I) 30-70, J) 30-70 IA/DCP*

ble 2). At a Novatein/PLA composition of 90-10 and 70-30 (Fig. 2A to D), Novatein was the continuous phase and the dispersed PLA domains were dissolved. At higher compositions of PLA (30-70), the sample was no longer self-supporting as the PLA phase was the continuous phase which dissolved in chloroform (SEM image not shown). Sample collapse upon solvent extraction was also observed in a study by Veenstra et al. (2000b). They explained that this could be due to a transition morphology in between a co-continuous and dispersed morphology. This explains why a dispersed droplet morphology was not observed in the fracture surfaces of 30-70 blends (Fig. 1I and J). The morphology was neither co-continuous or dispersed but rather a transition between the two morphologies. Veenstra et al. (2000b) have also proven that co-continuous morphologies are not formed at a single volume fraction (i.e. the point of phase inversion) but rather over a range of volume fractions.

A clear visualization of the compatibilizing action of IA/DCP was prominent at a 50-50 ratio of Novatein and PLA

| Sample | Weight loss % |
|---|---|
| Novatein | 0 |
| 90-10 | 9.5 |
| 90-10 IA/DCP | 9 |
| 70-30 | 31 |
| 70-30 IA/DCP | 30.3 |
| 50-50 | 53 |
| 50-50 IA/DCP | 51.5 |
| 30-70 | 68.2 |
| 30-70 IA/DCP | 71 |
| PLA | 100 |

*Table 2. Percent weight loss of sample after digestion with chloroform*

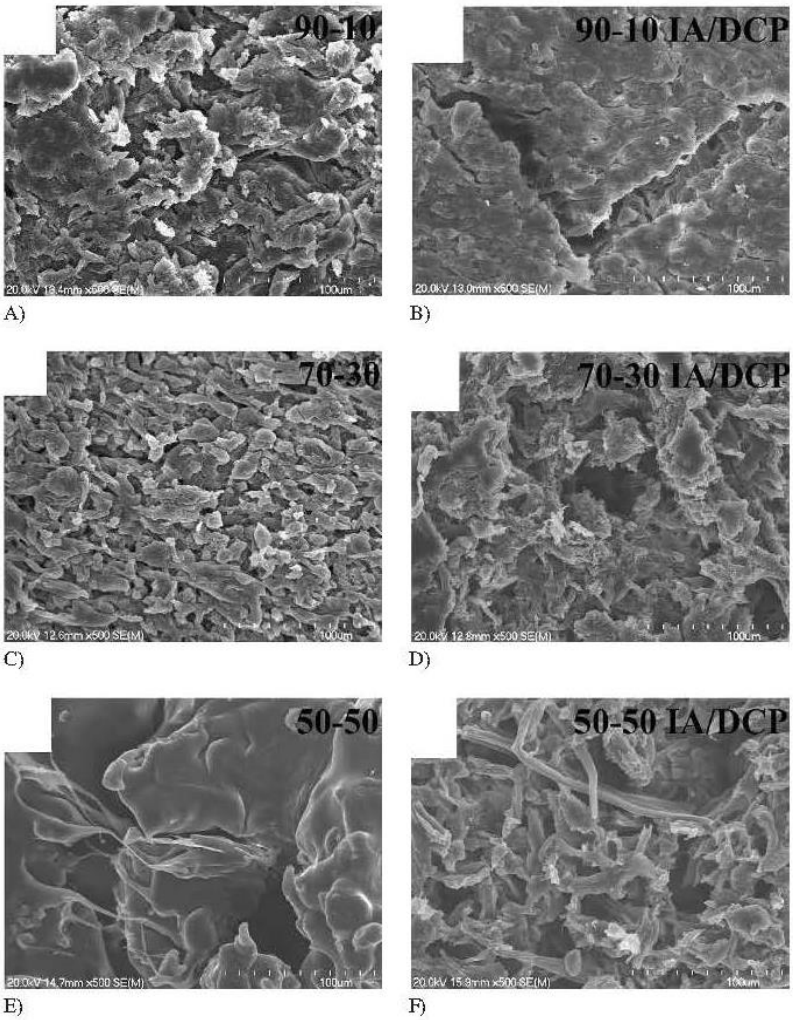


*Fig. 2. SEM images of digested surfaces at magnification × 500, A) 90-10, B) 90-10 IA/DCP, C) 70-30, D) 70-30 IA/DCP, E) 50-50, F) 50-50 IA/DCP*

(Fig. 2E and F). In the absence of compatibilizer (Fig. 2E), the specimen turned to sludge in the presence of chloroform. This indicated that in the absence of compatibilizer the morphology was dispersed which could no longer remain intact as the PLA was removed. However, the incorporation of a compatibilizer developed a fine co-continuous morphology (Fig. 2F). IA/DCP compatibilization has led to improved interfacial bonding between the two phases which also explains the improved tensile strength observed for the 50-50 blend (section 3.2). A co-continuous morphology is ideal for foaming to induce cell nucleation and growth evenly throughout the sample. Figure 2F shows the presence of fine threads, which was also observed in soy protein and PLA blends after chloroform digestion of the PLA phase (Liu et al., 2010). The study found that in the presence of compatibilizer, the soy protein phase changed from round particles to fine threads which led to an improvement in tensile strength because of stress transfer from the matrix to the elongated threads. The improved mechanical properties of Novatein/PLA at 50-50 IA/DCP ratio discussed in the next section could be a result of these fine threads since they were not observed in other blend morphologies.

### *3.2 Mechanical Properties*

The tensile strength of Novatein and PLA were 17.4 and 54.6 MPa, respectively (Fig. 3A). Blending Novatein and PLA at ratios of 90-10 and 70-30 reduced the tensile strength to below that of neat Novatein. This is common when blending two incompatible polymers with little adhesion between phases. The size of the dispersed phase initially drops with the addition of a copolymer which eventually attains an equilibrium value at high concentrations of the copolymer (Zhu et al., 2012). A study by Martin and Avérous (2001) on thermoplastic starch (TPS) and PLA blends showed a reduction in tensile strength, elongation at break, and impact resistance in all blends compared with pure TPS and PLA. They proposed that the weak mechanical properties were due to poor interfacial adhesion between the two phases. Morphology analysis of TPS/PLA 75/25 (wt.%) blend showed a continuous phase of TPS with large, non-uniform PLA domains. The tensile strength was highest at a 50-50 ratio of Novatein and PLA including a compatibilizer. Zhu et al. (2012) found that grafting PLA with MA increased tensile strength and elongation of soy protein blends by 19 and 21 %, respectively, compared to blends without PLA-g-MA. A reduction in elongation of Novatein and PLA blends were observed compared to neat PLA because the inclusion of Novatein as the dispersed phase constrains PLA chain movement (Fig. 3B).

Elongation, or strain at break, are largely controlled by sample defects such as cracks and voids. During sample deformation these defects form localized high stress regions which can lead to premature sample failure (Liu et al., 2010). Upon the addition of compatibilizer the interfacial bonding between Novatein and PLA matrix has enhanced, meaning there were less interfacial cracks and lower stress concentration gradients in the sample. All Novatein and PLA blends showed an improvement in elongation upon the incorporation of a compatibilizer.

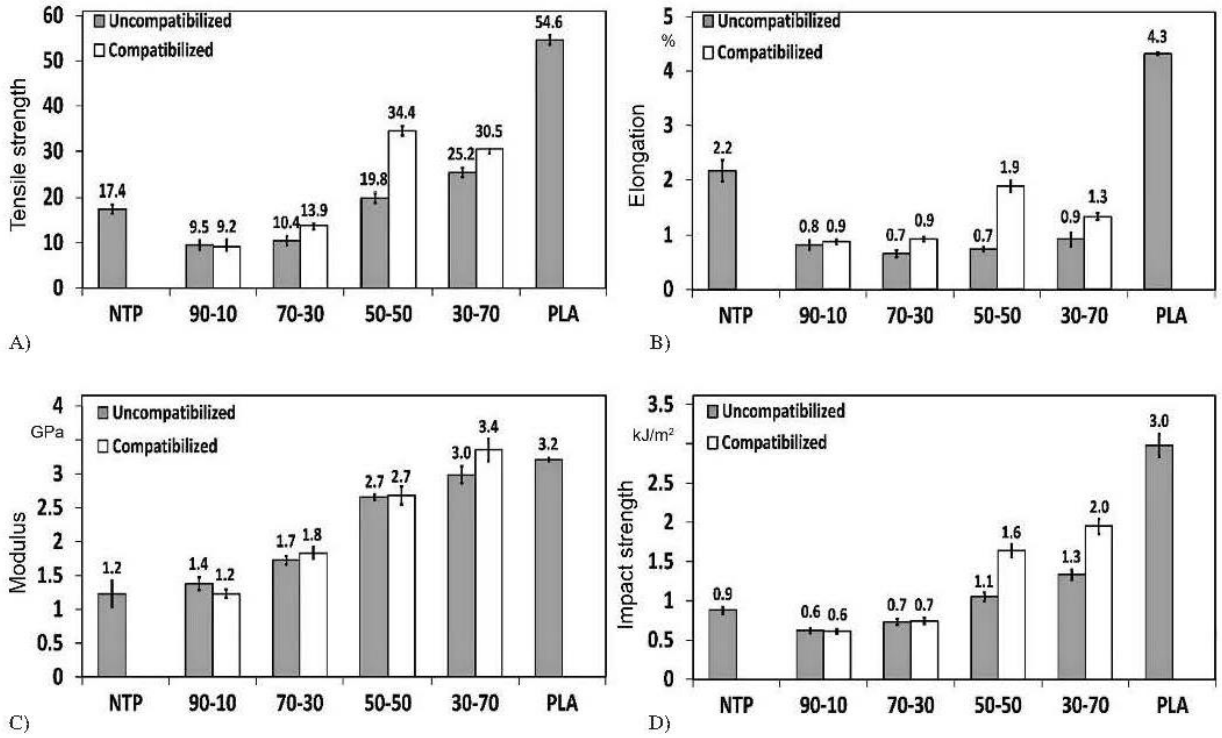


*Fig. 3. Tensile strength (A), percent elongation (B), secant modulus (C) and impact strength (D) of Novatein/PLA blends*

The secant modulus of Novatein was lowest and gradually increased with increasing amounts of PLA (Fig. 3C). The modulus of the 30-70 IA/DCP blend was even slightly higher than pure PLA. The modulus of a material is calculated within the linear elastic region of the material's deformation which involves vibrational and reversible movement of polymer chains (Liu et al., 2010). In the initial part of deformation, the vibrational/reversible movement of the polymer chains was impacted by the compatibilization effects which lead to a slight increase in modulus upon the addition of IA and DCP. Compatibilization made very little difference with any of the blends and would suggest that changes in morphology had little effect on the average stiffness of these blends.

Similar to tensile strength, the notched Charpy impact strength also dropped relative to neat NTP for the 90-10 and 70-30 blends (Fig. 3D). Neat PLA displayed brittle behavior and with the addition of Novatein the sample became even more brittle. However, at a PLA ratio of 50 wt.% and above, the impact strength was greater than Novatein. The addition of IA and DCP only had a slight effect on improving the impact strength of Novatein/PLA blends, except for the 50-50 blend ratio which showed 36 % improvement upon compatibilization with IA/DCP. Improved impact strength is a result of a co-continuous morphology (Veenstra et al., 2000b). Compatibilization was only effective at 50 % Novatein or above. Including a compatibilizer changed the morphology sufficiently to alter the fracture behavior of the material. Novatein and PLA are both very brittle with low impact strength and this was also reflected in their blends.

The mechanical properties of Novatein and Novatein/PLA blends did not outperform neat PLA, except for the secant modulus of 30-70 IA/DCP which was slightly higher than neat PLA. However, the properties of neat Novatein significantly improved with the incorporation of PLA, especially at 50 wt.% PLA with compatibilizer.

The manner in which water absorption will occur in blends with PLA will also be influenced by the blend's morphology. Novatein is a hydrophilic polymer and absorbs 50 wt.% of water in just 24 h (Fig. 4). Blending Novatein with a hydrophobic polymer such as PLA could drastically alter its water resistance. The incorporation of a compatibilizer slightly reduced the rate of water absorption and was most noticeable at the 50-50 blend ratio. Without compatibilizer, PLA was dispersed and water was able to reach the Novatein domains relatively unobstructed. With compatibilizer, the blend formed a co-continuous morphology, obstructing water diffusion, which led to better water resistance. Improving the water resistance of Novatein could widen its use in many agricultural and packaging applications which involves exposure to moisture.

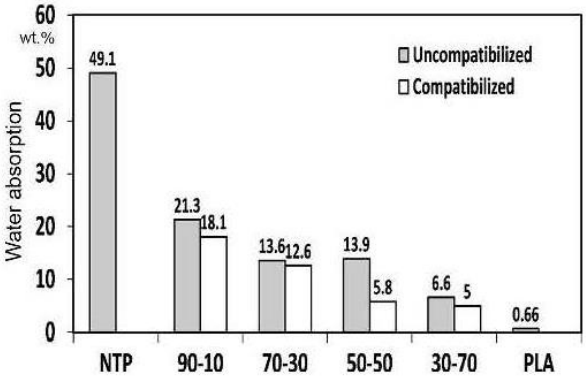


*Fig. 4. Water absorption of Novatein/PLA blends after ten days*

### *3.3 Dynamic Mechanical Analysis (DMA)*

Figure 5 shows the loss modulus and tan δ as a function of temperature for Novatein, PLA and the blends. Quenching PLA after extrusion allowed the material to remain amorphous. During a thermal scan neat PLA became very soft above its α-transition (69 °C) and showed a large damping peak. Novatein and PLA have similar $T_g$s between 60 to 70 °C and Novatein also shows a β transition at –20 °C (Bier et al., 2013). The damping peak of PLA in the blends was greatly reduced compared to neat PLA which is a result of the Novatein phase restricting chain motion of the matrix polymer, thereby leading to less damping. The presence of TEG in Novatein can cause a small decrease in $T_g$ because hydrophilic plasticizers such as TEG disrupt protein-protein interactions by binding to hydrophilic amino acid side groups (Verbeek and Koppel, 2012). Above 50 % Novatein, blends with compatibilizer demonstrated slightly lower damping and narrower peaks compared to blends without compatibilizer, and according to Zhu et al. (2012) this is indicative of stronger interaction between the two phases.

Temperature dependence of the loss modulus (E″) is also presented in Fig. 5. The pure components showed peaks at 67 °C which shifted to about 10 °C lower when the two components were blended, which may be a result of higher local plasticization caused by segregation effects in the amorphous zones (Li and Huneault, 2007). The intensity of the peaks also moved to an intermediate value of that of the pure components. PLA showed two E″ peaks which were thought to be a result of thermal history. At higher ratios of PLA in the blend, the peaks became sharper and significantly increased in intensity (more than the pure components), suggesting a tighter range in PLA chain mobility. In section 3.1 it was observed that the morphology of 70-30 IA/DCP (Fig. 1F) and 30-70 IA/DCP (Fig. 1J) was similar, which can also be explained in light of the loss modulus. The chloroform dissolution of these two blends showed that in the presence of compatibilizer, 70-30 and 30-70 formed continuous phase morphologies. 70-30 was continuous in the Novatein phase (Fig. 2D) and 30-70 was continuous in the PLA phase which disintegrated in the presence of chloroform. As a result, a peak in loss modulus was present in the range of 36–38 °C for 70-30 and 30-70 with compatibilizer. At 50-50, a peak at 24 °C was observed for the blend without compatibilizer which had a dispersed phase morphology (Fig. 2E). 50-50 IA/DCP formed a co-continuous phase morphology (Fig. 2F) and no E″ peaks were observed except for a $T_g$ at 52 °C. This indicated that the 50-50 blend composition formed a phase inversion point, above and below this composition range (i.e. 70-30 and 30-70) thermal and morphology analysis showed that the blends behaved similarly.

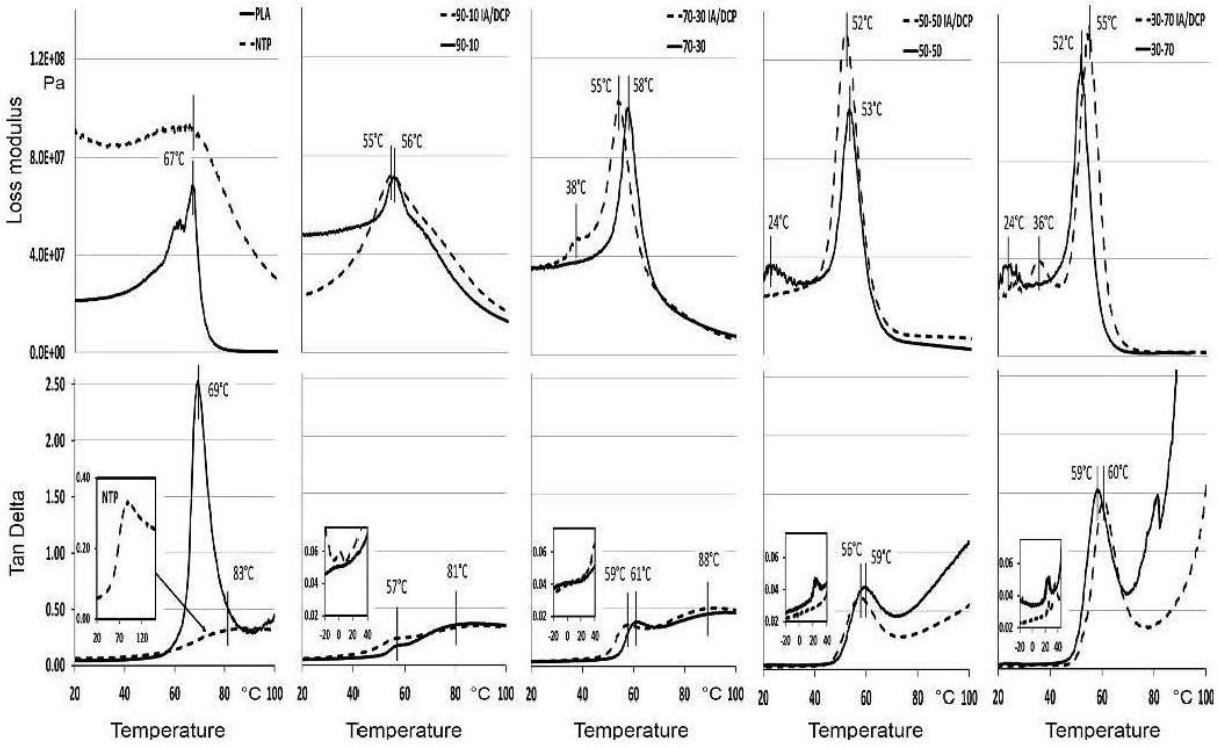


*Fig. 5. Loss modulus, storage modulus, and tan δ of Novatein, PLA, and blends*

### *3.4 Differential Scanning Calorimetry (DSC)*

The measurement of a single $T_g$ as a function of composition in DSC is generally an indication of a miscible polymer blend (Utracki and Wilkie, 2014). However, for the current system, both polymers had similar $T_g$s and virtually no conclusions can be drawn on this basis. DSC curves for the current system is shown in Fig. 6, and $T_g$, peak temperature and change in enthalpy is presented in Table 3. Thermal history was not removed except for pure PLA, to assess the properties of the blends as they would be used for foaming. All samples showed an endothermic peak at $T_g$ which represents excess enthalpic relaxations, representing the degree of packing of amorphous chains (Gao et al., 2014). During the first heating scan two peaks were observed for PLA at 59.8 and 63.7 °C (Fig. 6). During the second heating scan (not shown), the two peaks disappeared and was replaced by a single faint endotherm at 55 °C, and no melting peak was observed because the grade of PLA used was amorphous.

The first heating scan for Novatein detected the $T_g$ (peak labelled "a" in Fig. 6) closely followed by an endotherm. Previous studies have also detected this endotherm as relaxation behavior where internal readjustments of the tightly packed chain structure take place through cooperative molecular motion (Ku-Marsilla and Verbeek, 2015). PLA showed a $T_g$ at 58.3 °C which dropped by 10 °C when 30 wt.% Novatein was added. This depression in $T_g$ was also observed in the DMA re-

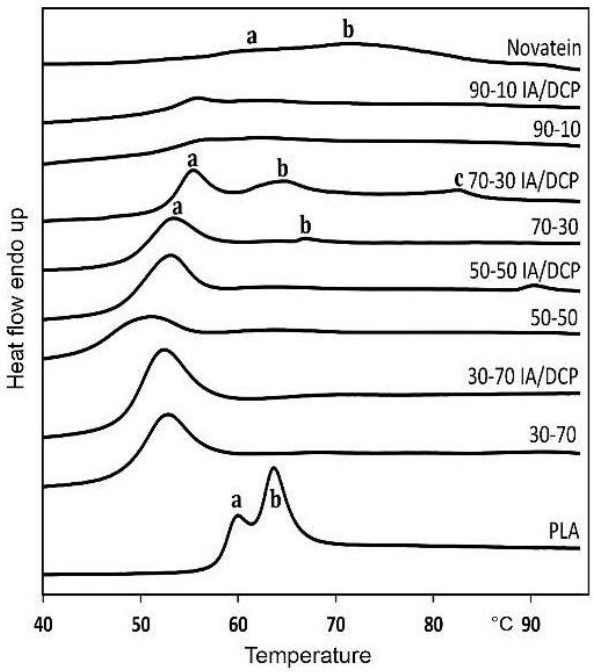


*Fig. 6. Glass transition ($T_g$) of Novatein, PLA, and blends based on the first heating scan*

| Blends | $T_g$ °C | Peak temperature C | | | ΔH* J/g | | |
|---|---|---|---|---|---|---|---|
| Novatein | 58.6 | 60.1[a] | 72.2[b] | | – | | |
| 90-10 IA/DCP | 53.1 | 55.7 | | | 0.04 | | |
| 90-10 | 53.8 | 56.1 | | | 0.02 | | |
| 70-30 IA/DCP | 53.1 | 55.3[a] | 64.9[b] | 82.6[c] | 0.42[a] | 0.06[b] | 0.04[c] |
| 70-30 | 49.9 | 53.1[a] | 66.8[b] | | 0.64[a] | 0.01[b] | |
| 50-50 IA/DCP | 48.9 | 52.9 | | | 1.56 | | |
| 50-50 | 46.1 | 50.3 | | | 1.02 | | |
| 30-70 IA/DCP | 48.8 | 52.2 | | | 3.03 | | |
| 30-70 | 48.6 | 52.6 | | | 2.63 | | |
| PLA | 58.3 | 59.8[a] | 63.7[b] | | 0.60[a] | 2.34[b] | |

[a, b, c] Represents the peaks labelled in Fig. 6. *data corrected for the percentage of PLA in the blend

*Table 3. Glass transition, peak temperature, and change in enthalpy of Novatein/PLA blends*

sults in section 3.3. Similar observations were made by Zhang et al. (2004) for PLA/soy protein blends; they attributed this to be a result of residual moisturee in the blends which plasticizes PLA and increases the flexibility of the molecules. Furthermore, the lowering of PLA $T_g$ when blended with Novatein could also be a result of the plasticizer in Novatein, triethylene glycol (TEG). TEG is an effective plasticizer for Novatein because it increases flexibility and reduces intermolecular interactions between polymer chains (Verbeek and Koppel, 2012). During compounding, the migration of small molecules such as TEG and water from the Novatein phase to PLA can result in lowering of the $T_g$. This was also found by Zhu et al. (2012) in PLA and soy protein blends. However, this drop in $T_g$ due to plasticizer is less pronounced than the drop in $T_g$ due to blending Novatein and PLA. The desired effect of plasticizer is to lower $T_g$ without compromising tensile strength and modulus (Vanin et al., 2005). This has been achieved with Novatein/PLA blends, $T_g$ was lowest (Table 3) and tensile strength and modulus were high (Fig. 3) at 50-50 composition. For Novatein/PLA blends, DSC results agreed with DMA in that the 50-50 composition was the point of phase inversion. Above and below this composition range (70-30 and 30-70) the materials showed similar $T_g$. Once again, the effect of compatibilizer was evident at 70-30 and 50-50 composition which had a slightly higher $T_g$ compared to uncompatibilized blends. An increase in $T_g$ with compatibilizer was also observed by Zhu et al. (2012) and was thought to be as a result of improved interaction between the protein and the PLA phase.

### *3.5 Wide Angle X-Ray Scattering (WAXS)*

Pure PLA showed an amorphous peak at 15° 2θ and no crystals and long-range order were detected (Fig. 7A). Bloodmeal is semi-crystalline with randomly distributed β-sheets and helices representing the crystalline phase (Hicks et al., 2014). The peak at 9° 2θ corresponds to inter- β-sheet and helical spacing, while the peak at 19° 2θ is attributed to repeated distances within each structure (Fig. 7A). Hydrogen bonding in α-helices occurs along the protein backbone and is intra-molecular, while hydrogen bonding in β-sheets occurs between aligned chain segments and can be either inter- or intra-molecular (Bier et al., 2014; Elshemey et al., 2010).

The summation of pure Novatein and PLA diffractograms (Fig. 7A) closely resembled that of the 50-50 curve without compatibilizer (Fig. 7D). This would suggest that the blend exists as three phases: crystalline Novatein, amorphous Novatein, and amorphous PLA. The broad shoulder in the range 15° and 17° 2θ could be attributed to the dominant amorphous character of PLA, similar observation was made by Mittal el al. in PLA-polycaprolactone blends (Mittal et al., 2015).

With a compatibilizer, the additive diffractogram no longer represented that of the compatibilized blend. The peak at 9° 2θ was present suggesting that the separate amorphous PLA phase must have been partly dissolved in the amorphous Novatein phase, resulting in a single amorphous halo not obscuring the peak at 9° 2θ. As observed in DMA and DSC, 50-50 represented a critical point. Above this composition (70-30) the inter-molecular peak was present and below this composition (30-70) the peak at 9° 2θ mostly disappeared. At 30-70 Novatein/PLA, it was difficult to detect Novatein and the curve was similar to pure PLA. This would suggest that the material behavior would be dominated by the matrix material (present in greater proportion), except for the 50-50 case where a co-continuous phase formed. WAXS confirmed that itaconic anhydride was an effective compatibilizer, which is evident from the change in diffractograms between compatibilized and uncompatibilised blends. In all cases, the inter-spacing peak at 9° 2θ became more prominent as amorphous PLA was dissolved into the amorphous Novatein phase.

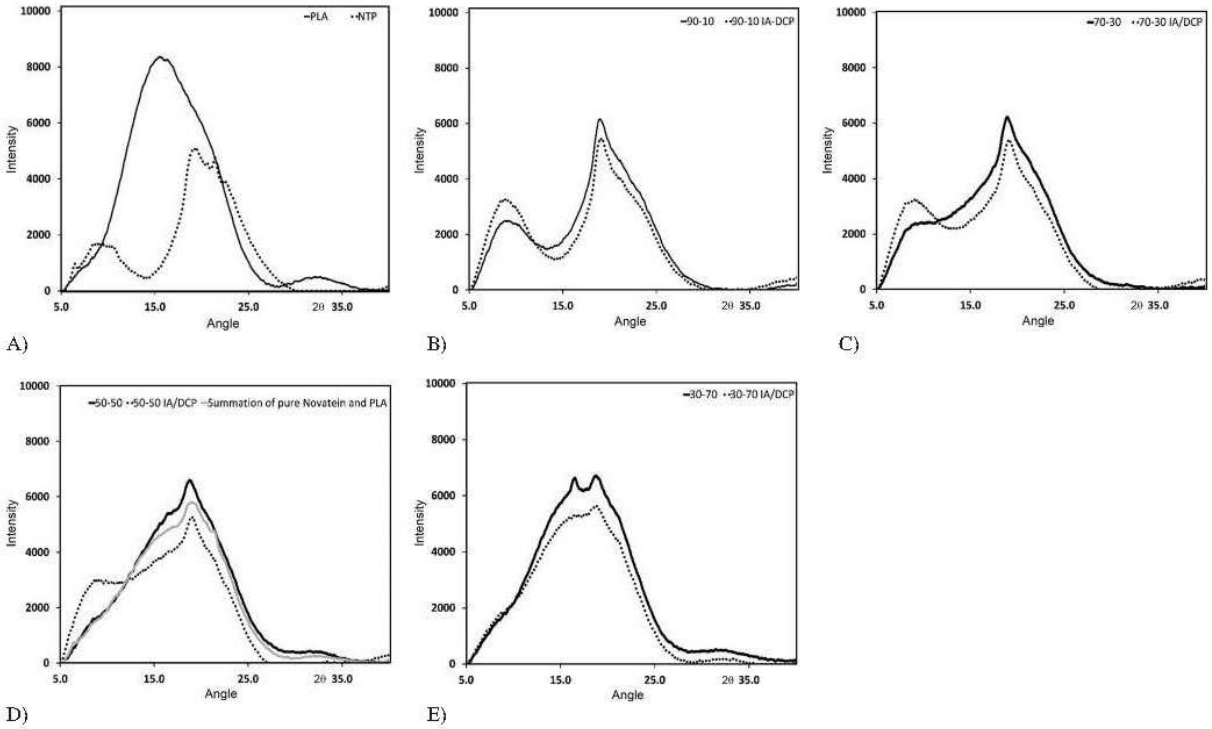


*Fig. 7. XRD of pure polymers, blends, and summation of Novatein and PLA*

## 4 Conclusions

Blends between Novatein and PLA were successfully produced using reactive extrusion and the compatibilizing effect of itaconic anhydride was confirmed. Fewer agglomerated Novatein particles and less phase separation were visible in the presence of a compatibilizer. At 50-50 Novatein/PLA, a dispersed morphology was observed in the absence of compatibilizer which caused the material to disintegrate in chloroform. Upon the addition of IA/DCP, the 50-50 blend stayed intact which was thought to be a result of co-continuous morphology.

Tensile strength improved by 42 % and impact strength improved by 36 % when PLA was grafted with itaconic anhydride at 50-50 composition. In addition, the morphology also influenced water absorption. Without compatibilizer, PLA was dispersed and water molecules were able to dissolve the Novatein domains. With compatibilizer, the blend formed a co-continuous morphology which was able to obstruct water diffusion.

The loss modulus in DMA also showed a difference in behavior at 50-50 with and without compatibilizer. Two peaks ($T_g$ and shorter range chain movements) were observed at 50-50 without compatibilizer which had a dispersed phase morphology, and one peak ($T_g$) was observed at 50-50 with compatibilizer which had a co-continuous phase morphology. This indicated that 50-50 formed a phase inversion point. Furthermore, it was concluded that blends either existed as a three phase system (excluding a compatibilizer) or a two phase system (in the presence of a compatibilizer) because PLA was absorbed into the amorphous phase of Novatein.

## References

Aduro Biopolymers, Novatein, http://www.adurobiopolymers.com/Novatein (2016)

Bao, D., Liao, X., He, T., Yang, Q. and Li, G., "Preparation of Nanocellular Foams from Polycarbonate/Poly(lactic acid) Blend by Using Supercritical Carbon Dioxide," J. Polym. Res., **20**, 1 10 (2013), DOI:10.1007/s10965-013-0290-6

Bier, J. M., Verbeek, C. J. R. and Lay, M. C., "Identifying Transition Temperatures in Bloodmeal-Based Thermoplastics Using Material Pocket DMTA," J. Therm. Anal. Calorim., **112**, 1303 1315 (2013), DOI:10.1007/s10973-012-2680-0

Bier, J. M., Verbeek, C. J. R. and Lay, M. C., "Thermal and Mechanical Properties of Bloodmeal-Based Thermoplastics Plasticized with Tri(ethylene glycol)," Macromol. Mater. Eng., **299**, 85 95 (2014), DOI:10.1002/mame.201200460

Bier, J. M., Verbeek, C. J. R. and Lay, M. C., "Thermal Transitions and Structural Relaxations in Protein-Based Thermoplastics," Macromol. Mater. Eng., **299**, 524 539 (2014), DOI:10.1002/mame.201300248

Elshemey, W., Elfiky, A. and Gawad, W., "Correlation to Protein Conformation of Wide-Angle X-ray Scatter Parameters," Protein J., **29**, 545 550 (2010), PMid:21046443; DOI:10.1007/s10930-010-9291-z

Fischer, L., Peissker, F., "A Covalent Two-Step Immobilization Technique Using Itaconic Anhydride," Appl. Microbiol. Biotechnol., **49**, 129 135 (1998), DOI:10.1007/s002530051148

Fowlks, A. C., Narayan, R., "The Effect of Maleated Polylactic Acid (PLA) as an Interfacial Modifier in PLA-Talc Composites," J. Appl. Polym. Sci., **118**, 2810 2820 (2010), DOI:10.1002/app.32380

Gao, C., Bao, X., Yu, L., Liu, H., Simon, G. P., Chen, L. and Liu, X., "Thermal Properties and Miscibility of Semi-Crystalline and Amorphous PLA Blends," J. Appl. Polym. Sci., **131** (2014), DOI:10.1002/app.41205

Hicks, T., Verbeek, C. J., Lay, M. C. and Bier, J. M., "Effect of Oxidative Treatment on the Secondary Structure of Decoloured Bloodmeal," RSC Adv., **4**, 31201–31209 (2014), DOI:10.1039/C4RA03890H

Huneault, M. A., Li, H., "Morphology and Properties of Compatibilized Polylactide/Thermoplastic Starch Blends," Polymer **48**, 270–280 (2007), DOI:10.1016/j.polymer.2006.11.023

Kohlhoff, D., Ohshima, M., "Open Cell Microcellular Foams of Polylactic Acid (PLA)-based Blends with Semi-Interpenetrating Polymer Networks," Macromol. Mater. Eng., **296**, 770–777 (2011), DOI:10.1002/mame.201000371

Ku Marsilla, K. I., Verbeek, C. J. R., "Modification of Poly(lactic acid) Using Itaconic Anhydride by Reactive Extrusion," Eur. Polym. J., **67**, 213–223 (2015), DOI:10.1016/j.eurpolymj.2015.03.054

Ku-Marsilla, K., Verbeek, C. J. R., "Compatibilization of Protein Thermoplastics and Polybutylene Succinate Blends," Macromol. Mater. Eng., **300**, 161–171 (2015), DOI:10.1002/mame.201400141

Li, H., Huneault, M. A., "Effect of Nucleation and Plasticization on the Crystallization of Poly (Lactic Acid)," Polymer, **48**, 6855–6866 (2007), DOI:10.1016/j.polymer.2007.09.020

Liu, B., Jiang, L., Liu, H. and Zhang, J., "Synergetic Effect of Dual Compatibilizers on in situ Formed Poly(lactic acid)/Soy Protein Composites," Ind. Eng. Chem. Res., **49**, 6399–6406 (2010), DOI:10.1021/ie100218t

Marrazzo, C., Maio, E. D. and Iannace, S., "Foaming of Synthetic and Natural Biodegradable Polymers," J. Cell. Plast., **43**, 123–133 (2007), DOI:10.1177/0021955x06073214

Martin, O., Averous, L., "Poly(lactic acid): Plasticization and Properties of Biodegradable Multiphase Systems," Polymer **42**, 6209–6219 (2001), DOI:10.1016/S0032-3861(01)00086-6

Mittal, V., Akhtar, T., Luckachan, G. and Matsko, N., "PLA, TPS and PCL Binary and Ternary Blends: Structural Characterization and Time-Dependent Morphological Changes," Colloid. Polym. Sci., **293**, 573–585 (2015), DOI:10.1007/s00396-014-3458-7

Orozco, V. H., Brostow, W., Chonkaew, W. and Lopez, B. L., "Preparation and Characterization of Poly(lactic acid)-g-Maleic Anhydride+ Starch Blends," Macromol. Symp., **277**, 69–80 (2009), DOI:10.1002/masy.200950309

Park, C. B., Padareva, V., Lee, P. C. and Naguib, H. E., "Extruded Open-Celled LDPE-Based Foams Using Non-Homogeneous Melt Structure," J. Polym. Eng., **25**, 239–260 (2005), DOI:10.1515/polyeng.2005.25.3.239

Parker, K., Garancher, J. P., Shah, S., Weal, S. and Fernyhough, A., "Polylactic Acid (PLA) Foams for Packaging Applications," in Handbook of Bioplastics and Biocomposites Engineering Applications, S. Pilla (Ed.), Wiley, Hoboken, p. 161–175 (2011b), DOI:10.1002/9781118203699.ch6

Parker, K., Garancher, J.-P., Shah, S. and Fernyhough, A., "Expanded Polylactic Acid – an Eco-Friendly Alternative to Polystyrene Foam," J. Cell. Plast., **47**, 233–243 (2011a), DOI:10.1177/0021955x11404833

Pesetskii, S., Jurkowski, B. and Makarenko, O., "Free Radical Grafting of Itaconic Acid and Glycidyl Methacrylate onto PP Initiated by Organic Peroxides," J. Appl. Polym. Sci., **86**, 64–72 (2002), DOI:10.1002/app.10911

Petersson, L., Oksman, K. and Mathew, A., "Using Maleic Anhydride Grafted Poly(lactic acid) as a Compatibilizer in Poly(lactic acid)/Layered-Silicate Nanocomposites," J. Appl. Polym. Sci., **102**, 1852–1862 (2006), DOI:10.1002/app.24121

Pickering, K. L., Verbeek, C. J. R., Viljoen, C. and Van Den Berg, L. E., U. S. Patent 20100234515 A1 (2010)

Prochazka, F., Carrot, C., Castro, M., Celle, C. and Majesté, J., "Phase Inversion and Cocontinuity in Immiscible Polymer Blends," Meeting of the Polymer Processing Society, Guimarães, Portugal (2002)

Smithers Pira, "Global Packaging Market to Reach $975 Billion by 2018," http://www.smitherspira.com/news/2013/december/global-packaging-industry-market-growth-to-2018 (2015)

Utracki, L. A., Wilkie, C. A.: Polymer Blends Handbook, 2nd Edition, Springer, New York (2014), DOI:10.1007/978-94-007-6064-6

Vanin, F., Sobral, P., Menegalli, F., Carvalho, R. and Habitante, A., "Effects of Plasticizers and Their Concentrations on Thermal and Functional Properties of Gelatin-Based Films," Food Hydrocolloids, **19**, 899–907 (2005), DOI:10.1016/j.foodhyd.2004.12.003

Veenstra, H., Van Dam, J. and Posthuma de Boer, A., "On the Coarsening of Co-Continuous Morphologies in Polymer Blends: Effect of Interfacial Tension, Viscosity and Physical Cross-Links," Polymer **41**, 3037–3045 (2000a), DOI:10.1016/S0032-3861(99)00455-3

Veenstra, H., Verkooijen, P. C. J., van Lent, B. J. J., van Dam, J., de Boer, A. P. and Nijhof, A. P. H. J., "On the Mechanical Properties of Co-Continuous Polymer Blends: Experimental and Modelling," Polymer **41**, 1817–1826 (2000b), DOI:10.1016/S0032-3861(99)00337-7

Verbeek, C. J. R., Koppel, N. J., "Moisture Sorption and Plasticization of Bloodmeal-Based Thermoplastics," J. Mater. Sci., **47**, 1187–1195 (2012), DOI:10.1007/s10853-011-5770-7

Verbeek, C., Hanipah, S., "Grafting Itaconic Anhydride onto Polyethylene using Extrusion," J. Appl. Polym. Sci., **116**, 3118–3126 (2010), DOI:10.1002/app.31901

Willemse, R. C., "Co-Continuous Morphologies in Polymer Blends: Stability," Polymer, **40**, 2175–2178 (1999), DOI:10.1016/S0032-3861(98)00430-3

Witt, M. R. J., Shah, S., U. S. Patent 8283389 B2 (2012)

Yazdani-Pedram, M., Vega, H., Retuert, J. and Quijada, R., "Compatibilizers Based on Polypropylene Grafted with Itaconic Acid Derivatives. Effect on Polypropylene/Polyethylene Terephthalate Blends," Polym. Eng. Sci., **43**, 960–964 (2003), DOI:10.1002/pen.10079

Zhang, J.-F., Sun, X., "Mechanical Properties of Poly(lactic acid)/Starch Composites Compatibilized by Maleic Anhydride," Biomacromolecules, **5**, 1446–1451 (2004), PMid:15244463; DOI:10.1021/bm0400022

Zhu, R., Liu, H. and Zhang, J., "Compatibilizing Effects of Maleated Poly(lactic acid) (PLA) on Properties of PLA/Soy Protein Composites," Ind. Eng. Chem. Res., **51**, 7786–7792 (2012), DOI:10.1021/ie300118x

*Date received: August 16, 2016*
*Date accepted: June 26, 2017*

Bibliography
DOI 10.3139/217.3343
Intern. Polymer Processing
XXXIII (2018) 2; page 153–163

ISSN 0930-777X

# 4

# Biopolymer Foams from Novatein Thermoplastic Protein and Poly(lactic acid)

A journal article published in

***Applied Polymer Science***

By

A. S. Walallavita, C. J. R. Verbeek, M. C. Lay

**Biopolymer Foams from Novatein Thermoplastic Protein and Poly(lactic acid)**

In Chapter 4, the Novatein-PLA blends produced in Chapter 3 have been batch foamed using subcritical $CO_2$ with and without compatibilizer, PLA grafted itaconic anhydride. A high-pressure foaming vessel was used to bead foam Novatein-PLA blends, and the effect of $CO_2$ impregnation parameters on resulting foam densities and cell sizes were investigated. This chapter further examines the effect of the differences in crystallinities between Novatein and PLA and how this can lead to a variety of unique foam morphologies with greater cell densities due to heterogeneous nucleation.

As first author of this paper, I prepared the initial draft manuscript, which was refined and edited in consultation with my supervisors, who have been credited as co-authors.

Biopolymer Foams from Novatein Thermoplastic Protein and Poly(lactic acid), previously published in Applied Polymer Science (Wiley, Hoboken, NJ. USA). Reprinted with permission. Rightslink License number 4287830685847.

Journal of Applied Polymer Science

# Biopolymer foams from Novatein thermoplastic protein and poly(lactic acid)

**Anuradha Sammanie Walallavita, Casparus Johannes Reinhard Verbeek, Mark Christopher Lay**
Department of Engineering, School of Science and Engineering, University of Waikato, Hamilton 3240, New Zealand
Correspondence to: A. S. Walallavita (E-mail: anu.walallavita@gmail.com)

**ABSTRACT:** A batch processing method is used to fabricate foams comprising of a blend of poly(lactic acid) (PLA) and Novatein, a protein-based thermoplastic. Various compositions of Novatein/PLA are prepared with and without a compatibilizer, PLA grafted with itaconic anhydride (PLA-g-IA). Pure Novatein cannot form a cellular structure at a foaming temperature of 80 °C, however, in a blend with 50 wt % of PLA, microcells form with smaller cell sizes (3.36 μm) and higher cell density ($8.44 \times 10^{21}$ cells $cm^{-3}$) compared to pure PLA and blends with higher amounts of PLA. The incorporation of 50 wt % of semicrystalline Novatein stiffens the amorphous PLA phase, which restrains cell coalescence and cell collapse in the blends. At a foaming temperature of 140 °C, $NTP_{30}$–$PLA_{70}$ shows a unique interconnected porous morphology which can be attributed to the $CO_2$-induced plasticization effect. © 2017 Wiley Periodicals, Inc. J. Appl. Polym. Sci. **2017**, *134*, 45561.

**KEYWORDS:** biopolymers and renewable polymers; blends; compatibilization; foams; morphology

Received 5 May 2017; accepted 18 July 2017
**DOI: 10.1002/app.45561**

## INTRODUCTION

Environmental concerns regarding greenhouse gases and potential depletion of petrochemicals have led to the demand for sustainable alternatives. The use of natural polymers is generating attention because of their ability to behave as synthetic polymers after plasticization. One such natural polymer which is a nonpotential food source and nonsynthetic source of nitrogen is Novatein thermoplastic protein (NTP).[1] One of the major disadvantages of Novatein is its hydrophilic nature and loss of plasticizer during use, which results in poor mechanical properties. To address these issues, Novatein has been blended with polymers such as poly(butylene succinate) (PBS)[2,3] and poly(lactic acid) (PLA).[4] PLA has good mechanical properties and biodegradability, as a result, it is a popular packaging material. Furthermore, the use of PLA in both synthetic and natural polymer blends have grown significantly.[5–12]

Most polymer blends are immiscible which leads to unsatisfactory phase dispersion and the mechanical properties are weaker than the pure polymer counterparts. As a result, a compatibilizer is used as a third component to improve the interfacial bonding between two polymers. In a previous study,[13] itaconic anhydride (IA) was grafted onto PLA (PLA-g-IA) using dicumyl peroxide (DCP) as the radical initiator. IA is extremely stable when reacted with proteins and has been used for acetylating lysine, cysteine, and tyrosine.[14] Furthermore, IA is derived from renewable resources,[15] and its use as a compatibilizer for Novatein and PLA can produce a 100% bio-derived blend. A blend consisting of Novatein and PLA-g-IA has been produced using reactive extrusion,[4] however, the foaming capability of this blend has not been investigated.

A batch processing method was used to fabricate Novatein/PLA foams. This two-stage process involves saturating the polymer with blowing agent in a high-pressure environment, followed by a temperature rise in a hot fluid bath which leads to cell nucleation and growth. This batch foaming technique has successfully been implemented to foam PLA using subcritical $CO_2$,[16,17] however, batch foaming Novatein is more difficult due to the constraining effects of the crystalline phase and gas desorption occurring in the crystalline domains.

The foaming behavior of semicrystalline and amorphous polymers is very different because there is a nonuniform distribution of absorbed $CO_2$ in the matrix, resulting in diverse morphologies.[18–22] In general, the cell structure of semicrystalline polymers is relatively difficult to control compared to amorphous polymers because they can recrystallize during foaming. This may occur faster upon the dissolution of a gas in the polymer due to the plasticization effect of the gas.[19,23] By definition, crystallization is not expected with amorphous polymers.[19,21,24] Furthermore, nucleation of cells in amorphous polymers occurs homogeneously and the polymer expands uniformly. In semicrystalline polymers, the foam structure is affected by the crystal morphology since absorption and

Table I. Novatein/PLA Blend Compositions

| Sample name | Novatein (wt %) | PLA (wt %) | IA (wt %) | DCP (wt %) |
|---|---|---|---|---|
| Novatein | 100 | 0 | 0 | 0 |
| $NTP_{50}$-$PLA_{50}$ | 50 | 50 | 0 | 0 |
| $NTP_{50}$-$PLA_{50}$-g-IA | 50 | 45 | 4.2 | 0.8 |
| $NTP_{30}$-$PLA_{70}$ | 30 | 70 | 0 | 0 |
| $NTP_{30}$-$PLA_{70}$-g-IA | 30 | 65 | 4.2 | 0.8 |
| $NTP_{10}$-$PLA_{90}$ | 10 | 90 | 0 | 0 |
| $NTP_{10}$-$PLA_{90}$-g-IA | 10 | 85 | 4.2 | 0.8 |
| PLA | 0 | 100 | 0 | 0 |

diffusion take place almost exclusively through the amorphous regions.[22] Zhang *et al.*[25] observed that blends between PLA and poly(ethylene glycol) exhibited smaller cell size and higher cell density compared to the neat counterparts due to the inhibitional effect of crystallization on cell expansion. Higher cell densities were obtained because the crystalline structure served as heterogeneous nucleation sites. According to classical nucleation theory, bubble nucleation preferentially occurs at the interfaces of a multiphase system because of the lower activation energy barrier at these sites, whereas in homogeneous systems, bubble nucleation initiates synchronously throughout the polymer.

Blending is a promising approach which has been implemented to improve the foamability and pore morphology of some polymers. Incorporating 25 wt % of poly(hydroxybutyrate-*co*-valerate) (PHBV) in a blend with PLA resulted in low density foams with finer, more uniform cells when compared to pure PLA.[26] The foamability of thermoplastic gelatin (TPG) foams was improved when blended with PBS and resulting foams had higher cell density and smaller cells when compared to neat TPG foams.[27]

Novatein has been blended with PLA in a previous study, and the morphology and mechanical properties of these blends (before foaming) have been reported.[4] The study concluded that IA grafted PLA improved miscibility between Novatein and PLA, and its use can potentially lead to the production of Novatein/PLA foams. The present study uses an environmentally benign blowing agent, $CO_2$, to induce a cellular structure in Novatein/PLA blends with the aim of improving the foamability of Novatein. Foaming of multiphase systems offers a great opportunity to enhance the properties of porous materials, however, controlling the foaming process can be challenging. It has previously been shown through X-ray diffraction that Novatein and amorphous PLA blends exist as three primary phases: crystalline Novatein, amorphous Novatein, and amorphous PLA, suggesting that foaming would result in a range of morphologies.[4] This study discusses the effect of foaming on the different crystalline regions of the blend and the morphology formed under certain experimental conditions. The outcome of this study can provide a wider understanding about the foaming process and resulting morphologies of semicrystalline and amorphous polymer blends.

## EXPERIMENTAL

### Materials

Novatein was obtained from Aduro Biopolymers[28] and stored at >4 °C for a minimum of 24 h. Analytical grade IA and DCP were purchased from Sigma–Aldrich, St. Louis, Missouri, and used as received. Amorphous PLA grade Ingeo 4060 D in pellet form was obtained from NatureWorks LLC.

### Preparation of PLA-g-IA

PLA-g-IA was prepared by dissolving 40 g of IA (molecular weight 112.08 g/mol) and 7.5 g of DCP (molecular weight 270.37 g/mol) in 30 mL dehydrated acetone. The solution was poured over 952.5 g of PLA and kept in the fume hood for approximately 2 h before oven drying at 50 °C for 3 h. Different concentrations of IA and DCP have been analyzed previously,[13] for this study, the amount of IA/DCP grafted onto PLA was fixed at 5 wt % for all blends which gives a grafting degree of 0.45%. The material was then reactive extruded to ensure that there is no residue unreacted IA. A LabTech twin screw extruder with *L/D* ratio 44:1 was used for grafting with a temperature profile of 145, 145, 165, 165, 180, 180, 180, 180, 160, 160, and 155 °C. Screws were co-rotating and maintained a constant speed of 150 rpm for all experiments. A vacuum port was attached at the 7th heating zone to remove potential harmful vapors. The extrudate was collected in a water bath to prevent crystallization and subsequently pelletized. PLA-g-IA was dried below 50 °C overnight before blending with Novatein.

### Preparation of Novatein/PLA Blends

Blends were extruded using the same extruder used for grafting. Novatein was used as received from Aduro Biopolymers, Hamilton, New Zealand.[28] PLA pellets without compatibilizer was oven dried at 45 °C for 4 h to a moisture content of <250 ppm to minimize hydrolysis during melt processing. PLA with and without compatibilizer was extruded with Novatein according to the formulations listed in Table I. Temperature profiles varied between 70 °C at the feed and 175 °C at the die according to the ratio of Novatein and PLA in the blend. A relative torque 50%–60% was maintained by adjusting the mass flow rate of the feed.

### Batch Foaming

Extruded and granulated samples were sieved to an average sample size of 4 mm and placed in perforated nylon bags tied with string. The nylon bags allowed diffusion of $CO_2$ into the sample and kept the granules secured so $CO_2$ uptake could be determined by mass balance. The nylon bags containing the samples were then placed in a pressure vessel and saturated with subcritical $CO_2$ following the procedure by Witt and Shah.[29] The experimental setup is shown in Figure 1. The

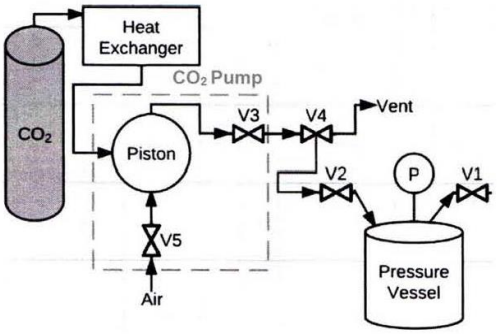


Figure 1. Experimental setup of pressure vessel and liquid $CO_2$ pump. [Color figure can be viewed at wileyonlinelibrary.com]

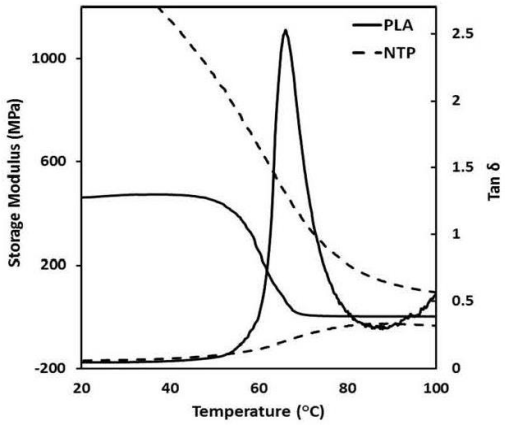


Figure 3. Storage modulus and tan δ of pure Novatein and PLA as a function of temperature.

sample was then placed in a hot fluid bath for 15 s at varying temperatures above the material's $T_g$ (80, 100, 120, 140, and 160 °C), which softens the polymer and gives way to cell nucleation and growth.

### Sorption Experiments

Sorption experiments were carried out to study the saturation concentration of $CO_2$ in Novatein/PLA blends. Samples were placed in the pressure vessel (Figure 1) and saturated at the same pressure and temperature used previously (Batch Foaming section). After periodic impregnation times, pressure was quenched to atmospheric and samples were quickly removed from the pressure vessel and weighed to monitor $CO_2$ sorption. The weight measured was equal to the amount of $CO_2$, which has been absorbed. It was found that a sorption time of 3 h was sufficient to saturate all samples with $CO_2$. Desorption experiments were also carried out. After saturation, the samples were removed and stored at both ambient and freezer temperature conditions (–18 °C). The weight loss of the samples was periodically measured.

### Analysis

The foams produced were characterized by measuring foam density following ASTM Standard D1622. The pore structure was analyzed using images obtained from Hitachi S-4700 field emission scanning electron microscope (SEM). Samples were fractured after immersion in liquid nitrogen to preserve the cellular structure. Specimens were platinum coated using a Hitachi E-1030 Ion Sputter, Hitachi in Tokyo, Japan before viewing under SEM. The mean cell size was measured using Image J software. A minimum of 100 pores were selected from the micrographs for each sample. The cell density of the foamed sample, $N_f$ (cells $cm^{-3}$) was determined using eq. (1)[30,31]:

$$N_f = \left[\frac{nM^2}{A}\right]^{\frac{3}{2}} \quad (1)$$

where $n$ is the number of cells in the region of area, $A$, and $M$ is the magnification factor.

The dynamic viscoelastic properties of the pure polymers were investigated using a Perkin Elmer DMA 8000, Waltham, Massachusetts fitted with a high temperature furnace and controlled with Pyris software version 11.1.1.0492. Dynamic mechanical analysis (DMA) specimens (30 × 6.5 × 3 $mm^3$) were cut from injection molded samples and tested using a single cantilever fixture at 1 Hz and a free length of 12.5 mm at temperatures −80 to 150 °C.

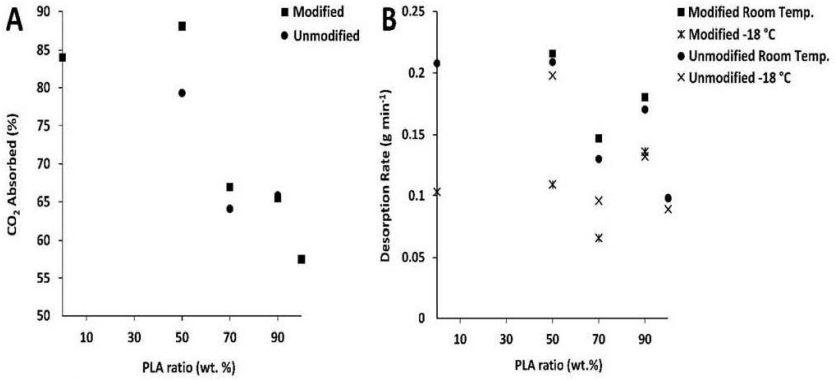


Figure 2. (a) Percentage of $CO_2$ absorbed and (b) desorption rate (g $min^{-1}$) of Novatein/PLA blends.

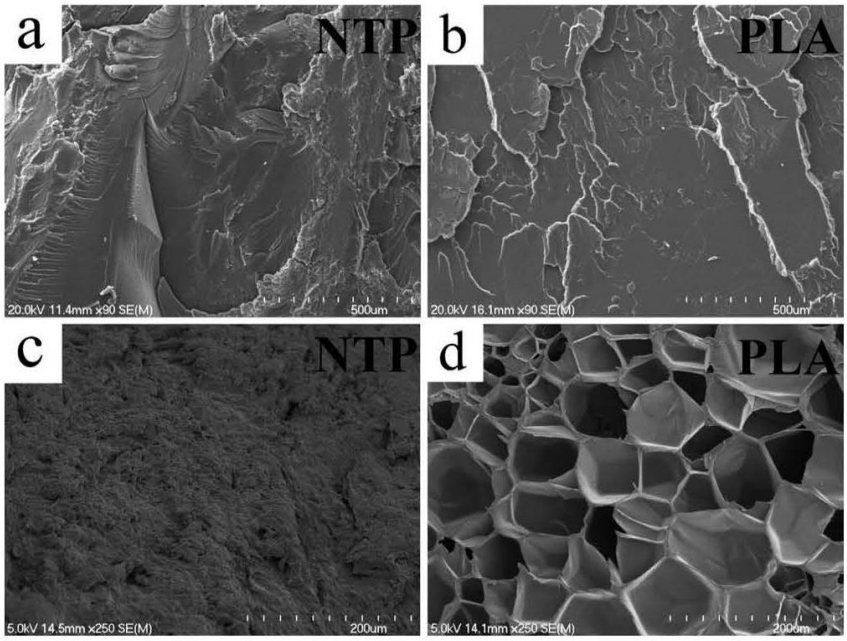


**Figure 4.** SEM micrographs of (a) Novatein and (b) PLA before foaming, (c) Novatein and (d) PLA after foaming at 80 °C with magnification ×250.

## RESULTS AND DISCUSSION

### $CO_2$ Sorption and Desorption

The equilibrium concentration of $CO_2$ in each blend after a saturation time of 3 h is presented in Figure 2(a). Sorption results showed that at a greater content of Novatein, the sample absorbed more $CO_2$ and also lost $CO_2$ at a faster rate. This is because Novatein is very porous and cannot retain the blowing agent as well as a solid matrix. PLA has a strong affinity toward $CO_2$, likely to be a Lewis acid–base interaction between $CO_2$ and the carbonyl group of PLA.[32] Intrinsic gas transport

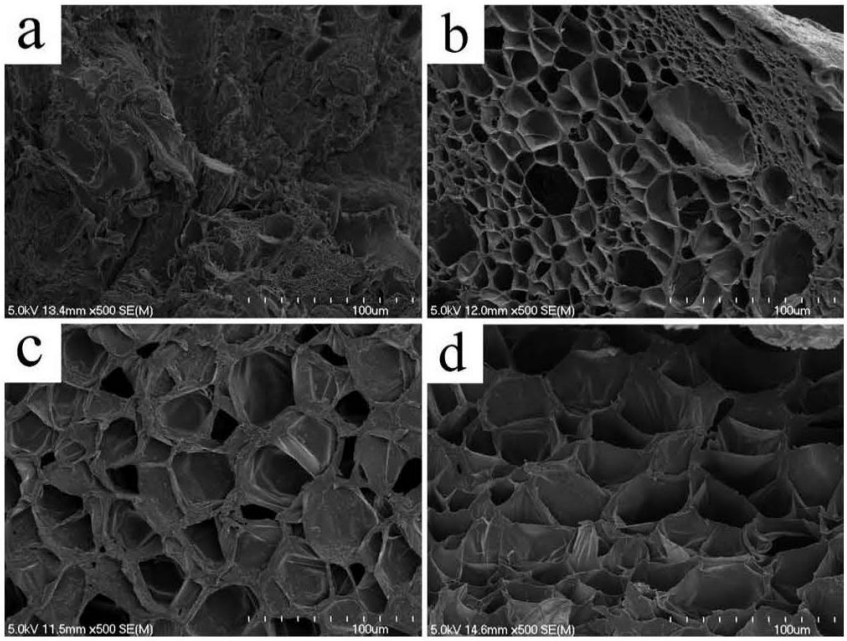


**Figure 5.** SEM micrographs of blends foamed at 80 °C with magnification ×500: (a) $NTP_{50}$–$PLA_{50}$, (b) $NTP_{30}$–$PLA_{70}$, (c) $NTP_{10}$–$PLA_{90}$, and (d) PLA.

Table II. Cell Properties of Blends Foamed at 80 °C with and without IA/DCP as Compatibilizer

| | Cell size (μm) | | Cell density (cells/cm$^3$) | |
|---|---|---|---|---|
| Blend composition (wt %) | Uncompatibilized | Compatibilized | Uncompatibilized | Compatibilized |
| $NTP_{50}$-$PLA_{50}$ | 3.36 | 1.04 | $8.44 \times 10^{21}$ | $1.04 \times 10^{24}$ |
| $NTP_{30}$-$PLA_{70}$ | 22.5 | 6.11 | $1.22 \times 10^{18}$ | $1.32 \times 10^{22}$ |
| $NTP_{10}$-$PLA_{90}$ | 42.7 | 9.69 | $1.88 \times 10^{15}$ | $2.71 \times 10^{18}$ |
| PLA | 55.4 | — | $5.18 \times 10^{14}$ | — |

characteristics in polymers are established by two critical thermodynamic parameters, solubility, and diffusivity of the gas. Gas solubility affects the nucleation of cells and final cell morphology, gas diffusivity controls cell growth. Solubility and diffusivity of $CO_2$ in semicrystalline polymers is a strong function of crystallinity. In amorphous polymers, the nucleation of cells occurs homogeneously and the polymer expands uniformly. Crystallinity reduces the solubility of gas in the polymer as the crystals are considered impermeable. Their presence also adds tortuosity to the path of diffusing molecules, thus reducing the rate of diffusion.[22] $CO_2$ absorption into a polymer induces swelling and plasticization, which causes a depression in $T_g$. Reduction in $T_g$ means there is a higher mobility of the polymer chains, which allows the polymer to crystallize at lower temperatures. During the impregnation process, this increase in crystallinity results in a lower amount of $CO_2$ absorbed as the gas is insoluble in the crystals, and $CO_2$ is gradually expelled from the growing crystallites.

This can lead to a nonhomogeneous $CO_2$ distribution in the polymer matrix as $CO_2$ is trapped in the amorphous intercrystal regions. This $CO_2$ gradient in amorphous and semicrystalline polymer blends causes cell nucleation to occur in localized regions, these observations are presented in the next sections.

Figure 2(b) presents the rates of weight loss of $CO_2$ from the blends in both ambient (room temperature) and freezer (−18 °C) temperature conditions. Weight loss at low temperature was slower than at ambient conditions for all samples, which was expected since diffusion is temperature dependent. It is important that the blends can retain the blowing agent for foaming since the degree of foaming differs depending on the amount of blowing agent at the foaming time. This indicates that the foaming process is controlled by desorption rate, a similar conclusion was achieved by Hao *et al.*[33] in their desorption study of PLA/starch composites. Compatibilized blends were also able to retain $CO_2$ better at −18 °C because of improved surface adhesion. Novatein and PLA phase separation in uncompatibilized blends gives rise to channels for $CO_2$ escape, such formation of voids has previously been reported for polypropylene blends as well.[34]

### Foam Morphologies of Pure Novatein and PLA Samples

DMA was used to measure the storage modulus and loss tangent of the pure polymers before foaming (Figure 3). Novatein and PLA have similar $T_g$s between 60 and 70 °C. The storage modulus of PLA drops steeply above the $T_g$, and that of Novatein comes down gradually over a wider temperature range than PLA. This difference in storage modulus above the $T_g$ indicates a difference in matrix stiffness between the two polymers.[30] The lower the storage modulus, the more potential for bubble growth and higher the expansion ratio.[31] Figure 4 shows the SEM micrographs of pure Novatein and PLA before and after foaming at a foaming temperature of 80 °C. PLA produced a cellular structure with an average cell size of 55.4 μm and an average cell density of $5.18 \times 10^{14}$ cells cm$^{-3}$. The $T_g$ of Novatein was too close to the foaming temperature of 80 °C, therefore, pore nucleation and growth was limited.[35] Furthermore, the matrix stiffness of Novatein was higher than that of PLA (Figure 3) and storage modulus was greater at 80 °C, thus, Novatein was unable to form a cellular structure in this temperature range due to cell growth restrictions. The effect of temperature on foam structure is discussed in the next section. A blend between Novatein and PLA could improve the foamability of Novatein, as similar results have been reported in a study by Oliviero *et al.*[27] on foam blends between TPG and PBS. This study found that once PBS was completely melted at 120 °C, the absence of a crystalline phase and low viscosity led to the nucleation and growth of microcells and the cellular morphology of the blend improved with respect to TPG.

### Effect of Novatein/PLA Composition on Foam Cell Structure

Figure 5 shows the SEM micrographs of foam blends at different Novatein proportions without compatibilizer. All samples were saturated at the same pressure and temperature[29] and

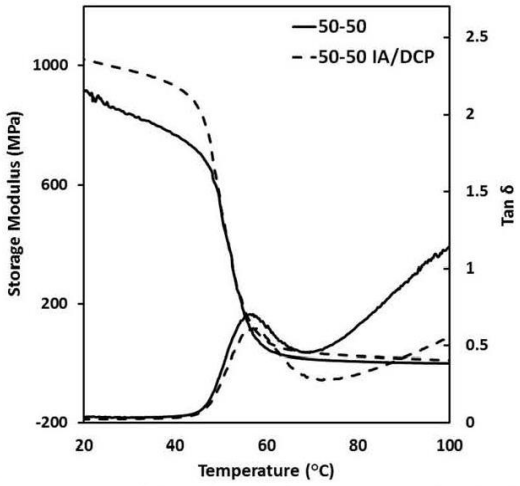


Figure 6. Storage modulus and tan δ of $NTP_{50}$–$PLA_{50}$ with and without compatibilizer as a function of temperature.

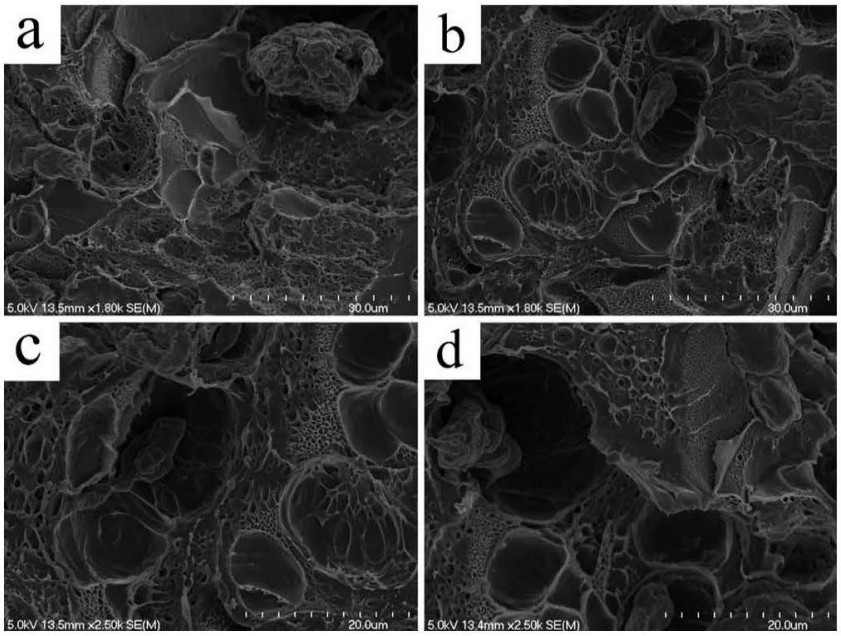


**Figure 7.** Enlarged SEM micrographs of $NTP_{50}$–$PLA_{50}$ foamed at 80 °C with magnifications (a,b) ×1.80k and (c,d) ×2.50k.

foamed at a temperature of 80 °C. Blends that contained more PLA had larger cell sizes, with pure PLA displaying the largest cell size and lowest cell density. Cell sizes were smaller and cell density was higher at the 50:50 ratio of Novatein and PLA (Table II). This was an interesting observation because pure Novatein cannot form a cellular structure at this foaming temperature, however, with 50 wt % of PLA, microcells formed with smaller cell sizes compared to pure PLA and blends with higher amounts of PLA. The DMA curve of the 50–50 blend (Figure 6) resembles closely to that of pure Novatein, indicating that Novatein is the dominant, or continuous phases in most cases. Also at 50 wt % Novatein, the interfacial area is much greater (co-continuous phase), which serve as heterogeneous nucleation sites. According to classical nucleation theory, the surface free energy at heterogeneous nucleation sites is lower[36–40] leading to the observation that at equal proportions of Novatein and PLA a larger number of nano-cells formed. At higher Novatein contents (above 50 wt %), it was difficult to obtain a cellular structure upon foaming (results not shown) because of a high matrix stiffness. Cell growth was restricted due to the stiff Novatein phase. Additionally, the presence of the crystal structure means the amount of $CO_2$ available for bubble growth decreased and the $CO_2$ concentration in the polymer blend remained higher. As a consequence, the dissolved $CO_2$ was used for cell nucleation and cell density increased.[21,41–44] In blends with higher PLA contents, crystallinity is lower and the polymer receives more blowing agent during saturation because of a greater proportion of amorphous regions.[22] The greater amount of dissolved $CO_2$ induced a greater thermodynamic instability and $CO_2$ was used to grow the cells. Therefore, the cell size was greater and cell density was lower in blends with a higher PLA content (Table II).

At a magnification of ×500, the microcellular structure of the $NTP_{50}$–$PLA_{50}$ blend was not visible [Figure 5(a)], however at ×2500 magnification (Figure 7), the presence of nano-sized cells was evident, dispersed around larger cells. These nano-scale cells formed because of differences in crystallinity between both components in the blend. The space for cell growth in the PLA phase is restricted by the stiff Novatein phase. The incorporation of 50 wt % Novatein in PLA has increased the crystallinity of the blend and the matrix stiffness of Novatein was high enough to restrain cell coalescence and cell collapse. Furthermore, the introduction of a crystalline phase from Novatein has created additional interfacial area for nucleation (interface between crystalline and amorphous phases). Increased crystallinity can help stabilize the cellular morphology but also hinders the formation of foams with high porosity.[27] Liao *et al.*[40] blended PLA with polystyrene and observed the restricting effects of PLA on polystyrene expansion. At certain saturation conditions, PLA had high crystallinity and faster rate of gas desorption in the crystalline domains, which prevented PLA from foaming. This constraining effect of the crystalline PLA phase restrained bubble growth in the polystyrene domains. This suggests that confined foaming behavior is brought about by the nature of the second phase in the blend, its intermolecular interactions, and phase structure of the blend.[40] The cell size distribution of pure PLA was broader compared to Novatein–PLA blends (Figure 8). The cell size distribution was the narrowest, and the cell sizes were the smallest at 50 wt % Novatein. Increased chain mobility is favorable for foaming and is brought about by $CO_2$ dissolution which is less pronounced in Novatein. By blending these polymers, Novatein further restricts chain movement, which led to increased cell uniformity with increasing Novatein content. Richards *et al.*[26] also found that adding 25 wt % of PHBV to PLA resulted in foams with finer cells compared to pure PLA.

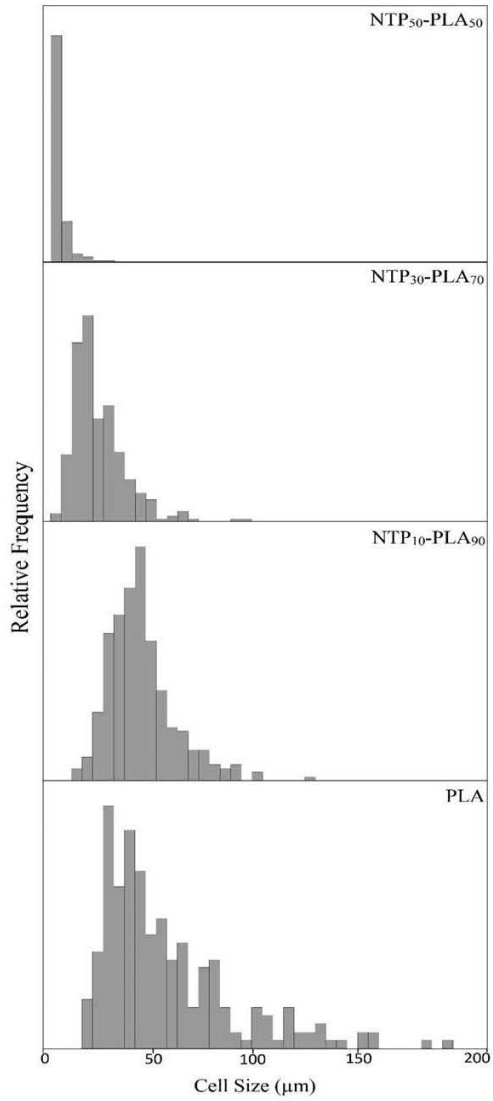


Figure 8. Cell size distribution of uncompatibilized NTP–PLA blends and pure PLA foamed at 80 °C.

### Effect of Compatibilizer on Cell Structure

Upon the addition of compatibilizer, a further reduction in cell size and increase in cell density was observed compared to uncompatibilized blends (Table II). The cell size of compatibilized $NTP_{50}$–$PLA_{50}$ was the lowest and cell density was the highest. The cell size of $NTP_{10}$–$PLA_{90}$ was reduced by 77% when IA/DCP was added as compatibilizer.

Generally, a reduction in intrinsic viscosity (i.e., reduction in average molecular weight) is observed when functional groups are grafted onto PLA in the presence of peroxide initiators (DCP) due to a significant β-sheet scission.[45] However, in the case of PLA-g-IA, the bulky IA functional group expanded the helical structure of PLA and hindered chain mobility, which increased the intrinsic viscosity compared to unmodified PLA.[13] This increase in intrinsic viscosity has suppressed bubble growth in modified blends, which led to a decrease in cell size. Low cell growth rate means the amount of $CO_2$ consumed for cell growth decreased and the concentration of $CO_2$ dissolved in the blend remains higher.[41] This excess of dissolved $CO_2$ was then used for cell nucleation and, as a result, cell density of compatibilized blends was greater.

Figure 9 shows the differences in cell structure between blends with and without compatibilizer. At low magnifications, cell structure is visible in the uncompatibilized blend [Figure 9(a)], in the compatibilized blends cell structure is only visible at much higher magnifications [Figure 9(f)]. With compatibilizer, the cell structure is more uniform and cell size is smaller (Figure 10). This may be due to improved phase morphology upon the addition of compatibilizer. In the absence of compatibilizer, a dispersed phase morphology formed in the unfoamed blends, which was a result of poor interfacial adhesion between the two phases. Poor interfacial adhesion has been reported for Novatein and other protein blends.[3,7] The morphology of unfoamed Novatein/PLA blends with compatibilizer (images not shown) had fewer agglomerated Novatein particles and phase separation was less visible. This suggests a co-continuous or a very finely dispersed morphology since it is difficult to differentiate the matrix from the dispersed phase.[4] This led to more uniform cell nucleation and growth when foaming.

### Effect of Foaming Temperature on Cell Structure

The process of cell nucleation and growth is largely controlled by foaming temperature,[46,47] yet the effect of temperature on foam morphology is complex because it affects gas solubility and diffusion as well as polymer viscosity.[40] For blends that have a higher PLA content, foam density was low at lower foaming temperatures (Figure 11) because PLA domains have a high $CO_2$ gas solubility at low foaming temperatures, which is necessary to favor bubble nucleation and growth.[48] At 50 wt % Novatein, foam density was high at a foaming temperature of 80 °C, but when foaming temperature was increased to 100 °C the foam density decreased. At low foaming temperatures, Novatein's high matrix stiffness hindered foam expansion and only gave way to the formation of small cells (Table II). Most thermoplastic materials foam in a narrow temperature range because the interaction of the blowing agent affects the matrix stiffness.[47] Novatein has a high material stiffness due to its semicrystalline nature, and high temperatures are required to give the polymer chains sufficient energy to move, similar observations have been reported for thermoplastic zein and gelatin foams.[49] At low foaming temperature (80 °C), the stiffness of the blend was too high which prevented cell growth. High matrix stiffness means that when the pressure drop was triggered during the foaming stage, the pressure change did not uniformly propagate through the polymer matrix, leading to foams with high density.[47] Compatibilized blends [Figure 11(b)] showed that the incorporation of 10 wt % Novatein resulted in foams with a lower density than pure PLA. This further emphasizes the effect of heterogeneous nucleation occurring in blends.

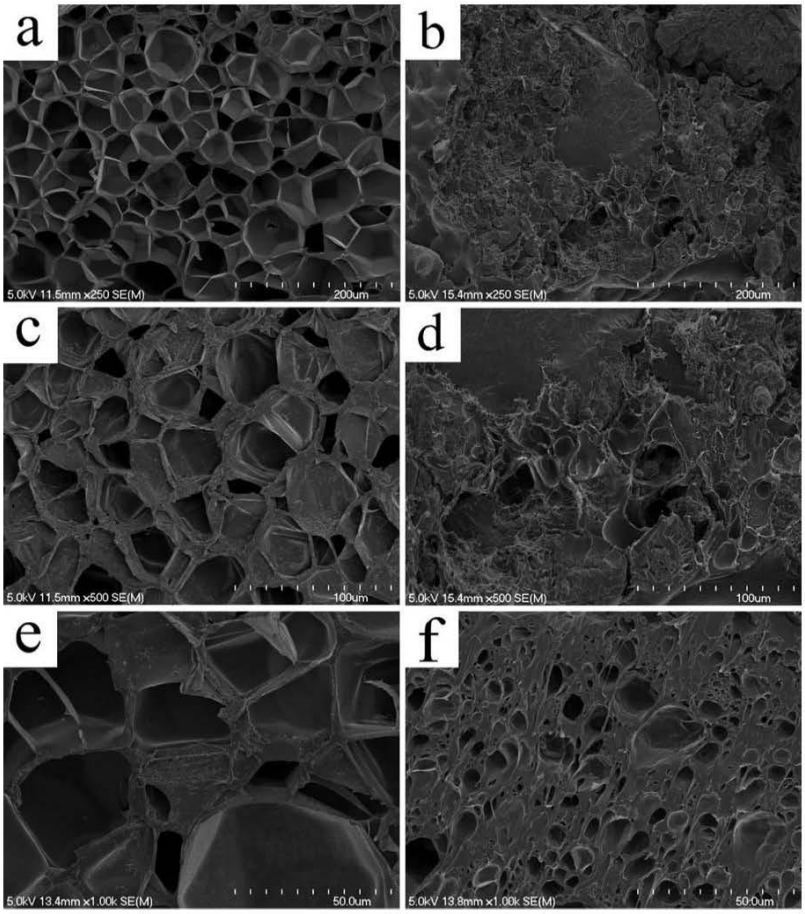


**Figure 9.** SEM micrographs of $NTP_{10}$–$PLA_{90}$ blends foamed at 80 °C: (a) uncompatibilized and (b) compatibilized. (c) and (e) are the enlarged images of (a). (d) and (f) are the enlarged images of (b).

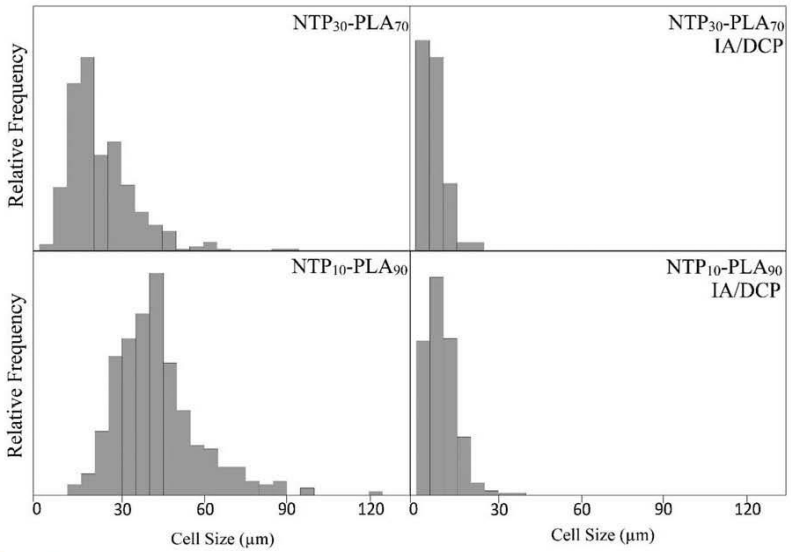


**Figure 10.** Cell size distribution of NTP–PLA blends with and without compatibilizer foamed at 80 °C.

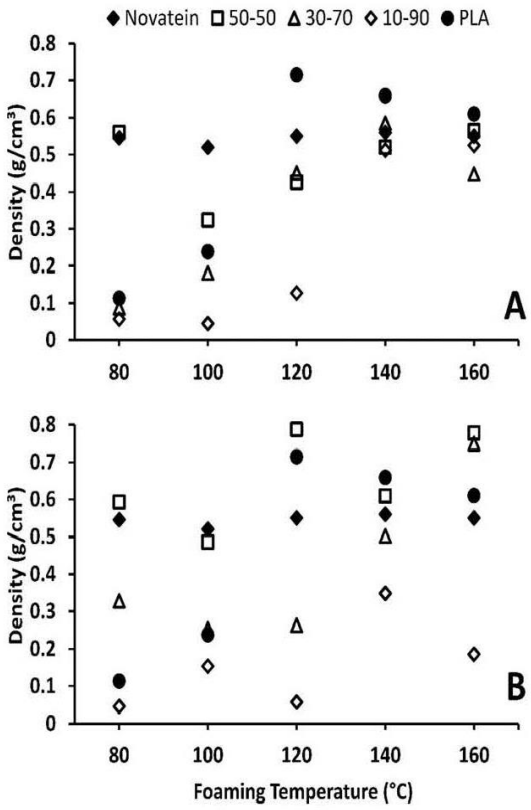


Figure 11. Density of Novatein–PLA foam blends at different foaming temperatures: (a) unmodified and (b) modified with IA/DCP.

Figure 12 shows the SEM images of uncompatibilized Novatein/PLA blends foamed at varying temperatures, at magnifications appropriate for each composition. At a foaming temperature of 140 °C, $NTP_{50}$–$PLA_{50}$ had the smallest cell size of all the blends (1.57 μm) and high cell density ($2.98 \times 10^{22}$ cells $cm^{-3}$). It was expected that increasing the temperature led to a decrease in polymer viscosity.[48] This observation can also be explained in light of blowing agent behavior as foaming temperature changes. At low foaming temperatures, it is difficult for cells to nucleate because there is reduced thermal energy. This leaves an excess of $CO_2$ in the polymer matrix which is then used for growing the few cells which are present, resulting in larger cell sizes. At higher temperatures there is greater thermal energy and the blowing agent is used for cell nucleation, which means less $CO_2$ is present to promote cell growth.[26] When the temperature was increased to 160 °C, it was difficult to obtain a foam structure in most Novatein/PLA blends which could be attributed to high crystallinity at high foaming temperatures.[48] In compatibilized blends, small cell structures were observed at the foaming temperature of 160 °C (Figure 13). This may be due to improved interfacial adhesion which makes the co-continuous blend morphology stable for cell nucleation even at high temperatures. Pure PLA had a high density when foamed at high temperatures because the $CO_2$-plasticized PLA matrix becomes too weak to withstand cell expansion and the low melt strength resulted in gas loss and denser foams.[21] At 140 °C, $NTP_{30}$–$PLA_{70}$ showed a unique interconnected porous morphology with a pore size of 3.29 μm and a cell density of $6.72 \times 10^{22}$ cells $cm^{-3}$ (Figure 14). Interconnected pore morphology was also observed in compatibilized blends at foaming temperatures 140 and 160 °C (Figure 13). This interconnected porous morphology has often been observed in other studies with PLA[25,48,50] and can be attributed to the $CO_2$-induced

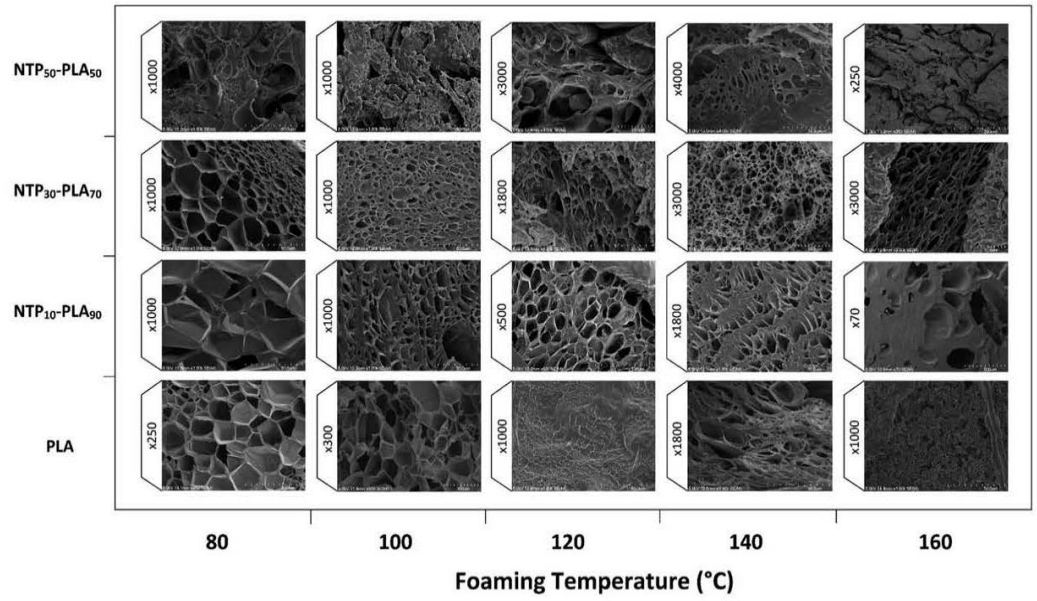


Figure 12. SEM images at various magnifications of Novatein/PLA blends foamed at different temperatures.

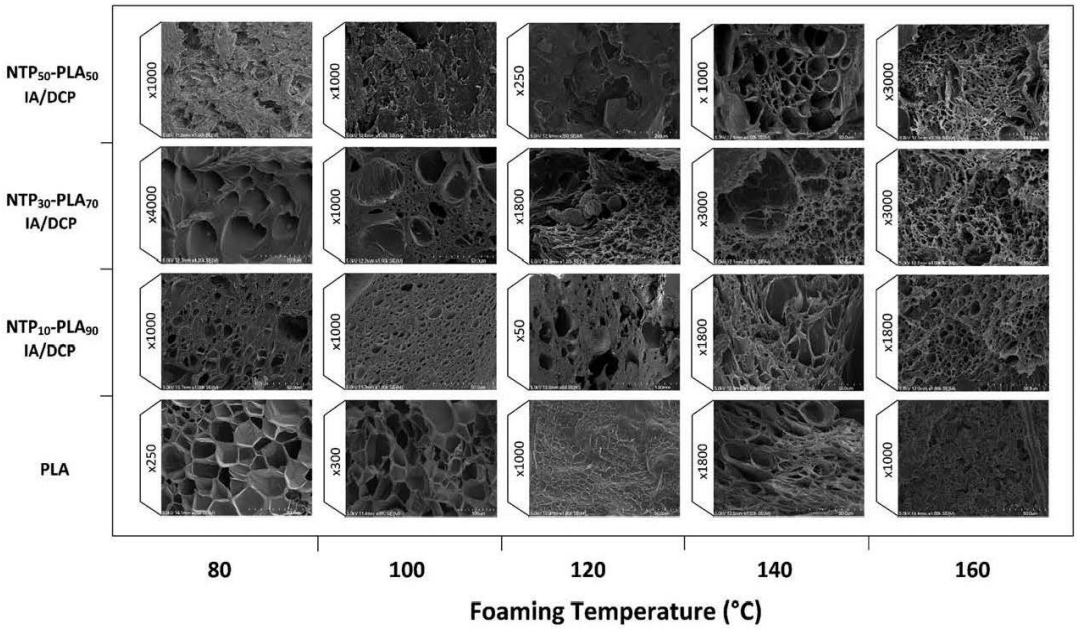


**Figure 13.** SEM images at various magnifications of compatibilized Novatein/PLA blends foamed at different temperatures.

plasticization effect. This plasticization effect significantly reduces the elasticity and viscosity of the matrix, which decreases pore-wall strength and results in pore breakage and an interconnected structure.[50] Figure 14(d) shows a cellular structure appearing in Novatein regions (detected using SEM-EDS, Madison, Wisconsin) surrounded by a foamed PLA matrix.

## CONCLUSIONS

The foaming capability of Novatein has been improved with the incorporation of PLA. Nano-scale cells were observed in blends with 50 wt % Novatein due to the constraining effects of the semicrystalline Novatein phase on PLA expansion. A further reduction in cell size and increase in cell density was observed

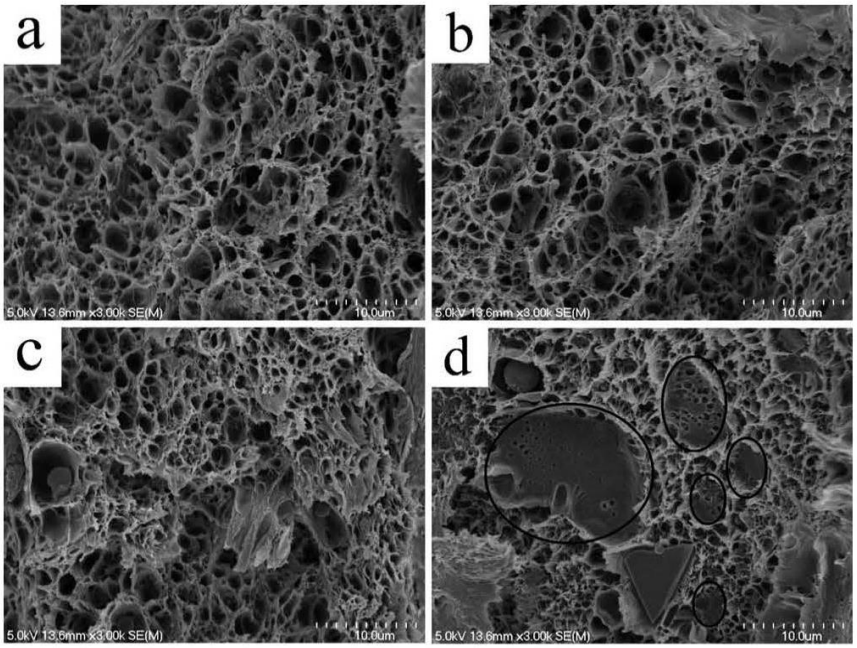


**Figure 14.** SEM images showing interconnected pores of $NTP_{30}$–$PLA_{70}$ foamed at 140 °C with magnification ×3000.

upon the addition of compatibilizer due to the higher crystallinity of grafted PLA. The co-continuous morphology obtained upon the addition of compatibilizer led to the development of foams with more uniform cell sizes. A high foaming temperature was required to foam the stiff Novatein regions of the blend. Co-continuous morphology in compatibilized blends was stable for cell nucleation even at high temperatures. The addition of 10 wt % Novatein in a blend with PLA has led to the development of low density foams due to heterogeneous nucleation. The outcome of this study can be employed in the development of Novatein/PLA foams, which find use in agricultural packaging applications.

## REFERENCES


1. Pickering, K. L.; Verbeek, C. J. R; Viljoen, C.; Van Den Berg, L. E. U.S. Pat. 8277553 B2 (**2010**).
2. Ku Marsilla, K. I.; Verbeek, C. J. R. *Macromol. Mater. Eng.* **2014**, *299*, 885.
3. Ku Marsilla, K. I.; Verbeek, C. J. R. *Macromol. Mater. Eng.* **2015**, *300*, 161.
4. Walallavita, A.; Verbeek, C. J. R.; Lay, M. *Int. Polym. Process* **2017**, to appear.
5. Fowlks, A. C.; Narayan, R. *J. Appl. Polym. Sci.* **2010**, *118*, 2810.
6. Huneault, M. A.; Li, H. *Polymer* **2007**, *48*, 270.
7. Liu, B.; Jiang, L.; Liu, H.; Zhang, J. *Ind. Eng. Chem. Res.* **2010**, *49*, 6399.
8. Mittal, V.; Akhtar, T.; Luckachan, G.; Matsko, N. *Colloid. Polym. Sci.* **2015**, *293*, 573.
9. Petersson, L.; Oksman, K.; Mathew, A. *J. Appl. Polym. Sci.* **2006**, *102*, 1852.
10. Zhang, J.; Jiang, L.; Zhu, L.; Jane, J.-l.; Mungara, P. *Biomacromolecules* **2006**, *7*, 1551.
11. Zhang, J.-F.; Sun, X. *Biomacromolecules* **2004**, *5*, 1446.
12. Zhu, R.; Liu, H.; Zhang, J. *Ind. Eng. Chem. Res.* **2012**, *51*, 7786.
13. Ku Marsilla, K. I.; Verbeek, C. J. R. *Eur. Polym. J.* **2015**, *67*, 213.
14. Fischer, L.; Peissker, F. *Appl. Microbiol. Biotechnol.* **1998**, *49*, 129.
15. Yazdani-Pedram, M.; Vega, H.; Retuert, J.; Quijada, R. *Polym. Eng. Sci.* **2003**, *43*, 960.
16. Parker, K.; Garancher, J. P.; Shah, S.; Weal, S.; Fernyhough, A. In Handbook of Bioplastics and Biocomposites Engineering Applications; Pilla, S., Ed.; Wiley: Hoboken, NJ, **2011**; p 161.
17. Parker, K.; Garancher, J.-P.; Shah, S.; Fernyhough, A. *J. Cell. Plast.* **2011**, *47*, 233.
18. Baldwin, D. F.; Park, C. B.; Suh, N. P. *Polym. Eng. Sci.* **1996**, *36*, 1446.
19. Liao, X.; Nawaby, A. V.; Handa, Y. P. *Cell. Polym.* **2007**, *26*, 69.
20. Liao, X.; Nawaby, A. V.; Whitfield, P.; Day, M.; Champagne, M.; Denault, J. *Biomacromolecules* **2006**, *7*, 2937.
21. Corre, Y.-M.; Maazouz, A.; Duchet, J.; Reignier, J. *J. Supercrit. Fluids* **2011**, *58*, 177.
22. Doroudiani, S.; Park, C. B.; Kortschot, M. T. *Polym. Eng. Sci.* **1996**, *36*, 2645.
23. Handa, Y. P.; Zhang, Z.; Wong, B. *Macromolecules* **1997**, *30*, 8499.
24. Handa, Y. P.; Roovers, J.; Wang, F. *Macromolecules* **1994**, *27*, 5511.
25. Zhang, W.; Chen, B.; Zhao, H.; Yu, P.; Fu, D.; Wen, J.; Peng, X. *J. Appl. Polym. Sci.* **2013**, *130*, 3066.
26. Richards, E.; Rizvi, R.; Chow, A.; Naguib, H. *J. Polym. Environ.* **2008**, *16*, 258.
27. Oliviero, M.; Sorrentino, L.; Cafiero, L.; Galzerano, B.; Sorrentino, A.; Iannace, S. *J. Appl. Polym. Sci.* **2015**, *132*, DOI: 10.1002/app.42704.
28. Aduro Biopolymers. http://www.adurobiopolymers.com/Novatein.
29. Witt, M. R. J.; Shah, S. U.S. Pat. 8283389 B2 (**2012**).
30. Bao, D.; Liao, X.; He, T.; Yang, Q.; Li, G. *J. Polym. Res.* **2013**, *20*, 1.
31. Nemoto, T.; Takagi, J.; Ohshima, M. *Polym. Eng. Sci.* **2010**, *50*, 2408.
32. Nalawade, S.; Picchioni, F.; Janssen, L.; Grijpma, D.; Feijen, J. *J. Appl. Polym. Sci.* **2008**, *109*, 3376.
33. Hao, A.; Geng, Y.; Xu, Q.; Lu, Z.; Yu, L. *J. Appl. Polym. Sci.* **2008**, *109*, 2679.
34. Thomann, R.; Wang, C.; Kressler, J.; Mülhaupt, R. *Macromol. Chem. Phys.* **1996**, *197*, 1085.
35. Salerno, A.; Oliviero, M.; Maio, E.; Iannace, S.; Netti, P. A. *J. Mater. Sci. Mater. Med.* **2009**, *20*, 2043.
36. Biresaw, G.; Carriere, C.; Willett, J. *J. Appl. Polym. Sci.* **2004**, *94*, 65.
37. Colton, J. S.; Suh, N. P. *Polym. Eng. Sci.* **1987**, *27*, 485.
38. Colton, J. S.; Suh, N. P. *Polym. Eng. Sci.* **1987**, *27*, 500.
39. Goel, S. K.; Beckman, E. J. *Polym. Eng. Sci.* **1994**, *34*, 1148.
40. Liao, X.; Zhang, H.; Wang, Y.; Wu, L.; Li, G. *RSC Adv.* **2014**, *4*, 45109.
41. Kohlhoff, D.; Ohshima, M. *Macromol. Mater. Eng.* **2011**, *296*, 770.
42. Baldwin, D. F.; Shimbo, M.; Suh, N. P. *J. Eng. Mater. Technol.* **1995**, *117*, 62.
43. Mascia, L.; Re, G. D.; Ponti, P. P.; Bologna, S.; Giacomo, G. D.; Haworth, B. *Adv. Polym. Tech.* **2006**, *25*, 225.
44. Reignier, J.; Gendron, R.; Champagne, M. F. *J. Cell. Plast.* **2007**, *43*, 459.
45. Ma, P.; Jiang, L.; Ye, T.; Dong, W.; Chen, M. *Polymers* **2014**, *6*, 1528.
46. Naguib, H. E.; Park, C. B.; Reichelt, N. *J. Appl. Polym. Sci.* **2004**, *91*, 2661.
47. Zhao, N.; Zhu, C.; Howe Mark, L.; Park, C. B.; Li, Q. *J. Appl. Polym. Sci.* **2015**, *132*, DOI: 10.1002/app.42551.
48. Liao, X.; Nawaby, A. V. *J. Polym. Res.* **2012**, *19*, 1.
49. Salerno, A.; Oliviero, M.; Di Maio, E.; Iannace, S. *Int. Polym. Proc.* **2007**, *22*, 480.
50. Chen, B.-Y.; Wang, Y.-S.; Mi, H.-Y.; Yu, P.; Kuang, T.-R.; Peng, X.-F.; Wen, J.-S. *J. Appl. Polym. Sci.* **2014**, *131*, DOI: 10.1002/app.41181.

# 5

# Concluding Remarks

# Concluding Remarks

In this work, blends between Novatein thermoplastic protein and PLA were produced using reactive extrusion, with and without compatibilizer, PLA-g-IA. The properties of these blends were studied at different compositions of Novatein and PLA/PLA-g-IA. These blends were then subsequently foamed using sub-critical $CO_2$ as blowing agent in a batch foaming apparatus.

Novatein and PLA are immiscible and blending resulted in poor adhesion and dispersed phase morphologies. Upon the addition of compatibilizer, fewer agglomerated Novatein particles were visible and phase separation was improved. To better understand the dispersed and co-continuous phase morphologies, chloroform was used to dissolve the PLA phase, keeping the Novatein phase intact. The compatibilizing action of IA/DCP was visible at a 50-50 ratio of Novatein and PLA. In the absence of compatibilizer, a dispersed phase morphology was formed indicative of sample disintegration in the presence of chloroform. However, upon the addition of compatibilizer, the sample remained intact with chloroform, suggesting a co-continuous morphology. This was also evident in the mechanical properties of compatibilized blends.

Blending Novatein and PLA at ratios of 90-10 and 70-30 reduced the tensile strength to below that of neat Novatein, which is common when blending incompatible polymers with little adhesion between phases. At Novatein-PLA ratio of 50-50 however, the tensile and impact strength improved by 42% and 36%, respectively. Including a compatibilizer improved the elongation (strain at break) of all blends due to improved interfacial bonding and lower stress concentration gradients. The mechanical properties of blends did not outperform neat PLA, except for the secant modulus at 30-70 Novatein/PLA-g-IA, which was slightly higher than neat PLA. However, the properties of neat Novatein was significantly improved by blending with PLA at a 50-50 ratio with compatibilizer.

Above 50% Novatein, blends with compatibilizer demonstrated narrower peaks in DMA and less damping compared to blends without compatibilizer, which is once again indicative of stronger interaction between the phases. Both DMA and DSC results showed that a Novatein-PLA ratio of 50-50 was the phase inversion point, above and below this composition the thermal behaviour of the material was similar. XRD showed that the summation of pure Novatein and PLA diffractograms closely resembled that of the 50-50 curve without compatibilizer, suggesting that the blend existed as three phases: crystalline Novatein, amorphous Novatein, and amorphous PLA. With compatibilizer, however, the additive diffractogram was different to compatibilized 50-50 suggesting that the separate amorphous PLA phase must have partly dissolved in the amorphous Novatein phase.

Reactive extrusion was used to successfully produce blends between Novatein and PLA, and the compatibilizing effect of IA was confirmed. IA grafted PLA improved miscibility between Novatein and PLA, and mechanical properties of neat Novatein was enhanced upon the addition of 50% PLA-g-IA. The promising results obtained by blending Novatein and PLA led to the production of batch foams with the aim of improving the foamability of Novatein. Foaming the different crystalline regions of the blend and resulting morphologies under certain experimental conditions were investigated.

$CO_2$ desorption results showed that compatibilized Novatein-PLA blends were able to retain $CO_2$ better because of improved surface adhesion. Uncompatibilized blends gave rise to channels for $CO_2$ escape. Pure Novatein cannot form a cellular structure at a foaming temperature of 80 °C due to cell growth restrictions. The $T_g$ of Novatein was too close to the foaming temperature of 80 °C and the matrix stiffness of Novatein is higher than PLA. However, when Novatein was blended with 50 wt. % PLA, microcells formed with smaller cell sizes (3.36 µm) and higher cell density ($8.44 \times 10^{21}$ cells $cm^{-3}$) compared to pure PLA and blends with higher amounts of PLA. The DMA curve of the 50-50 blend resembled closely to that of pure Novatein, indicating that Novatein was the continuous phase in most cases. Also, at 50 wt.% Novatein, the interfacial area is much greater (co-continuous phase), which served as heterogeneous nucleation sites.

The presence of nano-cells was also visible in the 50-50 blend which formed due to differences in crystallinity between both components in the blend. The incorporation of 50 wt.% Novatein increased the crystallinity of the blend and the matrix stiffness of Novatein was high enough to restrain cell coalescence and cell collapse. Furthermore, the introduction of the interface between the crystalline and amorphous phases has created additional interfacial areal for nucleation.

Upon the addition of compatibilizer, a further increase in cell density and reduction in cell size was observed compared to uncompatibilized blends. More uniform cell nucleation and growth were observed in compatibilized blends due to improved phase morphology. Compatibilized blends showed that the incorporation of 10 wt.% Novatein resulted in foams with a lower density than pure PLA. Foaming temperature also affected cell nucleation and growth in Novatein-PLA blends. PLA domains have a high $CO_2$ gas solubility at foaming temperatures of 80 °C. Novatein domains, however, have a high matrix stiffness which hindered foam expansion up until the foaming temperature was increased to 100 °C. When foaming temperature was further increased to 140 °C, the reduced polymer viscosity led to smallest cell size (1.57 µm) and high cell density ($2.98 \times 10^{22}$ cells $cm^{-3}$) of the 50-50 blend.

Blending Novatein with PLA in the presence of compatibilizer IA, improved the morphology, mechanical properties, and foamability of Novatein. Results from this study can be implemented to broaden the applications of Novatein into agricultural packaging applications. Recommendations for future work include rheology analysis to better understand the specific interactions which occur upon mixing. This changes the free volume of the blend and the degree of entanglement, which in turn affect the flow behaviour. Furthermore, other methods of foaming Novatein-PLA blends can be investigated, such as injection foaming. The stiff Novatein phase requires high temperature and pressure conditions to induce a cellular structure, which can be achieved using injection foaming methods. Novatein is currently being commercialized into various products such as plant pots, weasand clips, and Port Jacksons. Producing a foamed material from Novatein and other biodegradable polymer blends such as PLA would offer valuable alternatives to current Novatein products with improved properties.

# 6

# Appendices

**Book Chapter**

*Book Title:* Advances in Physicochemical Properties of Biopolymers: Part 2
*Editors:* M. Masuelli, D. Renard
*Publishers:* Bentham Books
*Chapter Title:* Protein Plastic Foams
*Authors:* C. Gavin, M. C. Lay, C. J. R. Verbeek, A. Walallavita

**Full Paper Conference**

*Title:* Blending Novatein thermoplastic protein with PLA for carbon dioxide assisted batch foaming
*Authors:* A. Walallavita, C. J. R. Verbeek, M. C. Lay
*Category:* Oral presentation by A. Walallavita, full paper conference
*Publishers:* AIP Conference Proceedings
*Conference:* 31st International Conference of the Polymer Processing Society. June 7 – 11, 2015. Jeju, South Korea.
*RightsLink number:* 4316710759219

**Conference Participation**

1. *Title:* Properties of Blends between Poly(lactic acid) and Novatein Thermoplastic Protein
   *Authors:* A. Walallavita, C. J. R. Verbeek, M. C. Lay
   *Category:* Poster presentation by A. Walallavita, extended abstract
   *Conference:* Bioprocessing Network Conference. September 21-22, 2015. Wellington, New Zealand.

2. *Title:* Compatibilizing Effects of Itaconic Anhydride on Blends between Poly(lactic acid) and Novatein Thermoplastic Protein
   *Authors:* A. Walallavita, C. J. R. Verbeek, M. C. Lay

*Category:* Oral presentation by A. Walallavita, extended abstract

*Conference:* 32nd International Conference of the Polymer Processing Society. June 25-29, 2016. Lyon, France.

**3.** *Title:* Biopolymer Foam Blends of Poly(lactic acid) and Novatein Thermoplastic Protein

*Authors:* A. Walallavita, C. J. R. Verbeek, M. C. Lay

*Category:* Keynote speech by A. Walallavita, extended abstract

*Conference:* Europe/Africa Conference of the Polymer Processing Society. June 26-29, 2017. Dresden, Germany.

# Protein Plastic Foams

An invited book chapter

By

C. Gavin, M. C. Lay, C. J. R. Verbeek, A. S. Walallavita[1]

Published in

***Advances in Physicochemical Properties of Biopolymers***

[1]Although I was not first author of this work, it has been included in the appendix of this thesis as it provides the reader useful literature on protein foams used in various plastic applications. As co-author, I prepared the first draft of the sections on batch foaming, and together with the other authors, revised and edited the entire manuscript into the form accepted for publication.

CHAPTER 9

# Protein Plastic Foams

**Chanelle Gavin, Mark C. Lay*, Casparus J.R. Verbeek*** and **Anuradha Walallavita**

*School of Engineering, Faculty of Science and Engineering, University of Waikato, Hamilton, New Zealand*

**Abstract:** The development of protein-based biopolymers has been driven by the increasing global demand for polymer products, the need for sustainable practice within this industry and the availability of low cost by-products, such as high protein content meals. The continuing development of new and existing protein-based biopolymers will enable these materials to help supplement the increasing global demand for polymer products and to develop new markets with their niche applications. To date various compositions of protein-based biopolymers have been successfully used to produce injection moulded articles, films and foams. Biopolymers typically display poor foaming behavior and commonly produce foams with irregular morphology and high densities. Protein-based biopolymers are no exception, therefore it is important to fully understand how the foaming mechanisms of bubble nucleation, growth and stabilization are affected by the inherently different properties of these materials.

This chapter aims to review the production of stable protein-based foams for use in applications such as cushioning, insulation and packaging through a variety of methods. The review specifically focuses on the production of protein-based foams through thermosetting, the emerging role of proteins as a renewable substitute in polyurethane production and the application of thermoplastic foam technologies to protein-based thermoplastics, with an emphasis on batch and extrusion foaming methods. The similarities and differences between the production of traditional foams and those produced from proteins are highlighted here. Discussion of foam morphologies, properties and processing conditions is also included. Overall, this chapter intends to provide the reader with a greater understanding of the existing research and the current challenges associated with the production of protein-based thermoplastic and thermoset foams.

**Keywords:** Batch foaming, Extrusion foaming, Polyurethane foams, Protein biopolymers, Protein foams, Thermoplastic proteins, Thermoset foams.

* **Corresponding authors Mark C. Lay and Casparus J.R. Verbeek:** School of Engineering, Faculty of Science and Engineering, University of Waikato, Hamilton, New Zealand; Tel: +64 7 856 2889; E-mails: mark.lay@waikato.ac.nz, johan.verbeek@waikato.ac.nz

**Martin Masuelli & Denis Renard (Eds.)**

## INTRODUCTION

This review examines the application of protein-based biopolymers to the polymer foam industry and discusses potential manufacturing methods for stable protein-based foams intended for use as packaging, insulation or cushioning. Until now, reviews regarding protein foaming have typically been limited to those relevant to the food industry with very little emphasis on their application to or use in thermoset or thermoplastic foams [1]. However with increasing interest in thermoplastic proteins for producing injection molded articles and films it is only logical that the industry also begins to assess the foaming ability of these materials on a wider scale.

The development of protein-based foams with similar or enhanced properties in comparison to their traditional polymer counterparts creates an entirely new market at the intersection of the polymer foam industry and the growing biopolymers sector. Recent reports regarding the polymer processing sector show that the global demand for polymer foam products is increasing, such that by 2019 it is predicted that the sector will generate 25 million tons of material. This represents an increase in production of nearly 32% on the 2013 figures, when the industry totaled 19 million tons (equivalent to $USD 87 billion) [2]. The majority of materials consumed by this sector are non-renewable and/or non-biodegradable including polyurethane, polystyrene and polyolefin materials such as polypropylene and polyethylene [2].

Traditional polymeric materials are being supplemented, and to some extent replaced, by biopolymers to address issues regarding the sustainability of this industry. The leading biopolymers are currently starch and PLA, however the use of protein-based biopolymers is also increasing, especially within the US [3]. Combined, this sector is expected to generate $USD 3.67 billion in revenue in 2018 [4, 5]. Unfortunately, the economics relating to the proportion of these materials which are foamed are as yet unpublished, hence the exact size and value of this market is unknown. Furthermore, a number of barriers exist for these and other biopolymer foams including consumer acceptance, poor thermal stability and the associated difficulty and cost of manufacture [6].

In general, the production of foamed polymeric products involves the introduction of a gaseous phase to the polymer system through chemical blowing agents (CBA) or physical blowing agents (PBA), the expansion or evolution of this gas due to changes in physical parameters such as pressure or temperature and the subsequent solidification of the resulting structure (usually by temperature changes or crosslinking) before the cells rupture or collapse due to condensation of the gaseous phase [7, 8]. Following stabilization the blowing agent is

eventually replaced by air as the gaseous species exchange across the cellular matrix (Fig. **1**). This phenomenon has been extensively studied and reviewed with respect to polyurethane, polystyrene, polypropylene and polyethylene foams where the behavior of these materials can be predicted relatively well in relation to physical foaming behavior; however the foaming mechanisms of bubble nucleation, growth and stabilization are yet to be fully understood.

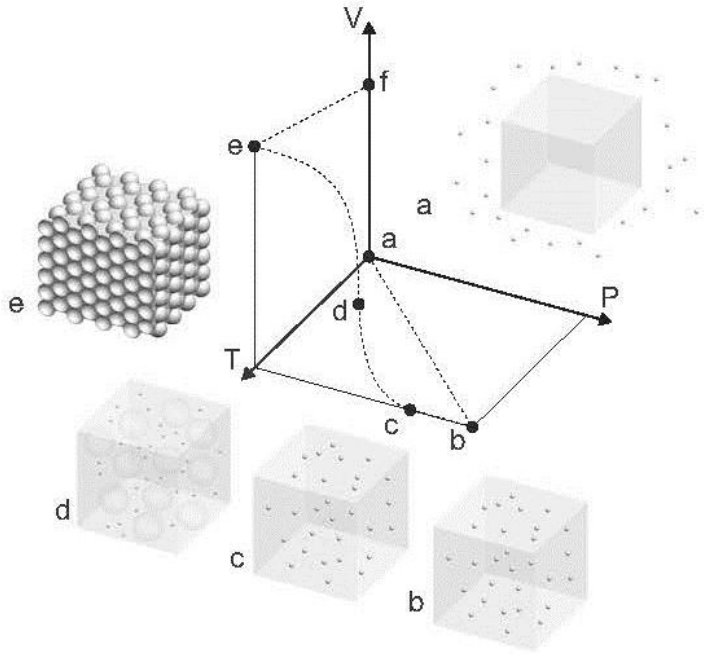


**Fig. (1).** Polymeric foaming process represented using a pressure, volume, and temperature diagram [7], with each stage shown by a letter and picture. The polymer and gas (**A**) is heated and pressurised to saturate the polymer (**B**), which is then depressurised so the gas changes phase and nucleates in the polymer (**C**), and as pressure drops, the remaining gas diffuses into the bubbles and the bubbles grow (**D**), until the final expanded foam is produced (**E**), and cooled (**F**).

Furthermore, the behavior of protein based biopolymers is still being characterized in relation to their structure, reactivity and processing ability. These are all related to their primary structure (amino acid sequence) and secondary structure (α-helices and β-sheets). Research is limited regarding the behavior of proteins within foaming systems. The properties of these materials, including poor rheological properties, low solubility of blowing agents and diffusion behaviour, severely hinder the foaming process. Consequently foamed biopolymers typically demonstrate non-uniform morphology and high density [6].

To date, efforts have been made to foam proteins through thermosetting methods

based on existing knowledge of the crosslinking behavior of casein and formaldehyde (although the possibility of using glutaraldehyde has also been noted) [9]. Aldehydes can react with the amine group from lysine and amino acids with side chains including cysteine, tyrosine, histidine, tryptophan, and arginine (Fig. **2**). Cereal and animal-based proteins are typically high in these amino acids, which enables good crosslinking. In comparison, glutaraldehyde is more selective reacting with lysine, cysteine, histidine, and tyrosine residues only [10]. Reaction with either crosslinking agent reduces the proportion of hydrophilic amino acids in protein blends and consequently these materials display lower water absorption capacities, thereby improving the properties of the resulting foams.

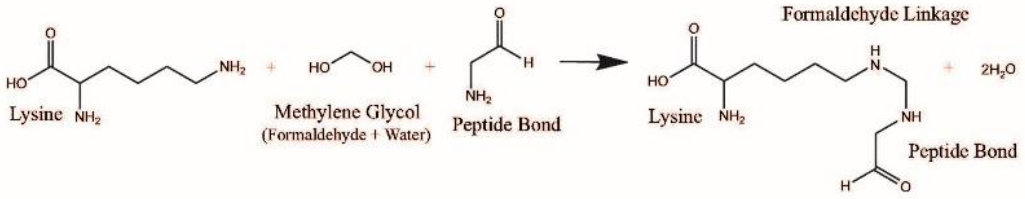


**Fig. (2).** Protein formaldehyde reaction chemistry [11]. Reproduced with permission, see note[1].

Proteins are also finding applications in polyurethane products in an effort to reduce production costs and increase the renewable fraction. Proteins are naturally reactive with these systems and the reactions are self-catalytic in water blown systems demonstrating how the unique chemistry of protein biopolymers, *i.e.* the presence of amide groups, can benefit this part of the market as well.

The increased interest in the production of value-added thermoplastic materials from waste animal and plant proteins has led to investigations regarding their extrudability, injection moulding capacity, film forming ability and recently their foaming ability. These protein based biopolymers have great potential to replace traditional thermoplastic materials in applications such as packaging as they can remain biodegradable after processing.

To enable thermoplastic processing, most proteins need to be blended with denaturants and plasticisers to disrupt protein bonding, lower the glass transition temperature ($T_g$) and enable chain mobility. A variety of proteins have been successfully utilized to produce thermoplastics although only a small proportion of these have been foamed *via* thermoplastic methods, which will be discussed in depth in this review.

This chapter will review the production and properties of thermoset protein foams, the role these protein biopolymers have in polyurethane systems, the production of thermoplastic proteins and thermoplastic foaming. The application

of these materials to these techniques is discussed by drawing on existing knowledge of these systems and protein behavior in general. This review includes an overview of the efforts to foam both plant and animal proteins including: zein, gluten, collagen, myofibrillar and bloodmeal and how these materials differ from traditional thermoplastic materials with respect to their physiochemistry. The underlying principles governing the foaming phenomenon are also briefly discussed including bubble nucleation, growth and stabilization. Attention is given to the factors which govern the foaming ability of these materials such as crystallinity, glass transition temperature, molecular weight distribution and the melt behavior including shear viscosity, extensional rheology, melt strength, surface tension and strain hardening behavior.

## PROTEINS AND THEIR SOURCES

Proteins are genetically encoded molecules found in living organisms where they perform vital structural or functional roles. However, these molecules find secondary applications within the plastics industry. Proteins which have been identified as possible plastic feedstocks include: animal proteins, milk (casein and whey), collagen, gelatin, keratin, egg white, myofibrillar and bloodmeal; and plant and cereal sources. While the structure of animal proteins is very diverse, as they carry out a wide range of biological functions, the proteins found in plants can be described as more or less analogous to each other with most acting as storage proteins. For example, zein is the major prolamine protein in corn/maize while kafirin is analogous, performing the same function in sorghum. Other plant proteins which have been recognised as potential feedstocks include wheat gluten, soy, sunflower, barley and peanut proteins.

Proteins are long chains of amino acids, a fraction of which are folded into structured regions containing α-helices, β-sheets and β-strands while the rest remains amorphous. Their structure is held together by hydrogen bonds, hydrophobic interactions, covalent bonds, ionic interactions and van der Waals forces. Some proteins can be readily incorporated into foams, for example native/soluble proteins can be mixed in solution and mechanically whipped or aerated to produce foams which can be set by a combination of cooking and drying. The available amide groups on native proteins and peptides can also enable them to react with isocyanates to produce polyurethane foams.

Other proteins can be manipulated to behave like thermoplastic protein by adding plasticisers and denaturants which reduce the existing bonding within and between polymer chains to reduce their glass transition temperature (dried proteins have glass transition temperatures >180°C). Sodium sulphite or sodium bisulphite break cysteine-cysteine covalent bonds between chains [12], while

compounds like urea and sodium dodecyl sulphate disrupt hydrogen bonding and hydrophobic interactions respectively [13]. Plasticisers also disrupt hydrogen bonding and increase the free volume between chains allowing greater mobility [13].

Typical plasticisers include glycerol, triethylene glycol, water and other compounds which contain large proportions of hydroxyl groups [13]. This treatment is required to enable these materials to be extruded below their thermal degradation temperature. However these materials can still crosslink during processing leading to excessive pressure and torque in some cases [12]. Thermoplastic proteins have been produced from bloodmeal [14 - 18], gelatin [19, 20], keratin [21, 22], soy [23 - 26], kafirin [27], and zein [20, 27 - 30].

The feasibility of incorporating these molecules into protein-based thermoplastics is dependent upon a combination of the cost and continuity of supply of the proteins and their processability. These heteropolymers each display unique biochemistry which enables them to perform their primary role. Their structure and function of these molecules has been extensively reviewed elsewhere, although only briefly for application in bioplastics. Due to the large amount of available literature on these materials the structures, sources and function of these molecules will not be reviewed here; instead their application shall be the focus.

## THERMOSET PROTEIN-BASED FOAMS

Protein foams (*e.g.* from whey or egg white) can be produced through thermosetting methods where the foamed structure is stabilized by crosslinking the protein chains by heating (*e.g.* meringue/pavlova) or chemical reagents (typically aldehydes).

In the food industry protein foaming is usually conducted by mechanical mixing (whipping) of a protein in a liquid phase to incorporate the air phase [31]. The resulting foam is dependent upon the physical-chemical properties of the solution such as viscosity, surface tension, and surface elasticity [32]. This is dependent on: (i) aggregation properties, protein-protein interactions, (ii) hydration properties, protein-water interactions and (iii) interfacial properties, such as surface tension [33].

Solidified whey protein foams have been produced from whey mixed with NaCl, $Na_2CO_3$ and water by high speed mechanical whipping and baking in an oven at 160°C for 40-50 minutes [33]. Whey foam blends with starch, gluten, and soy protein have also been produced. Such products are of interest to the food industry as whey has a high nutritional value and reasonable cost [34]. However whey protein is seldomly used alone in applications other than food because it is brittle

and has limited mechanical strength. These properties can be improved by blending whey with cross linking agents, plasticizers or other polymers such as alginate [35].

The compressive and flexural strength of hot moulded starch-based foams have been improved by adding gluten and zein proteins [36] while adding palm oil provides water resistance. Foamed combinations of sunflower protein, cassava starch and cellulose fibres have also been produced with densities of 0.45-0.51 $g/cm^3$ [37].

Thermoset plastic foams have also been produced *via* chemical reaction through mechanical mixing of a solution of egg albumin, 37% formaldehyde (cross linking agent) and camphor (waxy plasticizer). Once mixed the material was microwaved for 4-10 minutes to cure and partially dry the resulting foam. The foams had densities between 0.18-0.39 $g/cm^3$, a porosity of 77-79% and thermal conductivities between 0.06-0.065 W/mK, with little dependence of the thermal conductivity on foam density [38]. Blends with higher water content resulted in a softer material which was more elastic. Increasing the formaldehyde content gave a more rigid foam and camphor acted as an external plasticiser which resulted in more elastic and softer foams. An optimal formulation was 4 g camphor, 30 g water, and 8 g formaldehyde to 15 g of albumin protein, and a curing time of four minutes. Adding glycerol enabled foams to retain their elasticity over the course of two months [38]. Foam flexibility was temperature dependent for glycerol containing foams but not for foams produced without this plasticizer [39].

## PROTEINS INCORPORATED INTO POLYURETHANE FOAMS

Polyurethane foams require different processing technologies and have different cell morphologies compared to thermoplastic foams and other thermosets previously described. In general, polyurethane foams contain mainly polyurethane chains with some polyurea blocks and foaming is strongly linked to surface tension effects. Foam formation is governed by the reaction (Fig. **3**) between a diisocyanate and a diol to form a urethane linkage [40]. Carbon dioxide is evolved as a blowing agent through the reaction of water (1-4%) with the diisocyanate monomer. Amide groups on both terminals of the monomer also react with diisocyanate monomers to form urea linkages. Recently, research has been conducted to incorporate protein isolates, concentrates and meals into polyurethane foams due to the availability of reactive amino acid groups which can reduce production costs and give unique morphologies. To date, protein products have been successfully incorporated into both flexible [40, 41] and rigid polyurethane products [42, 43].

Flexible polyurethane foams have been produced with soy protein isolate (SPI),

concentrate (SPC) or defatted soy flower (DFS) in concentrations between 0-30 wt% with varying purity (50-90%) [41]. These proteins were mixed with glycerol/propylene oxide polyether triol, a tertiary amine as catalyst, a surfactant, triethnolamine as a crosslinking agent and water (to evolve $CO_2$ as a blowing agent). Polymeric methylene-4,4'-diphenyldiisocyanate (pMDI) was used as the isocyanate component and the foam was allowed to rise for one hour at room temperature and cured at 25°C for one week.

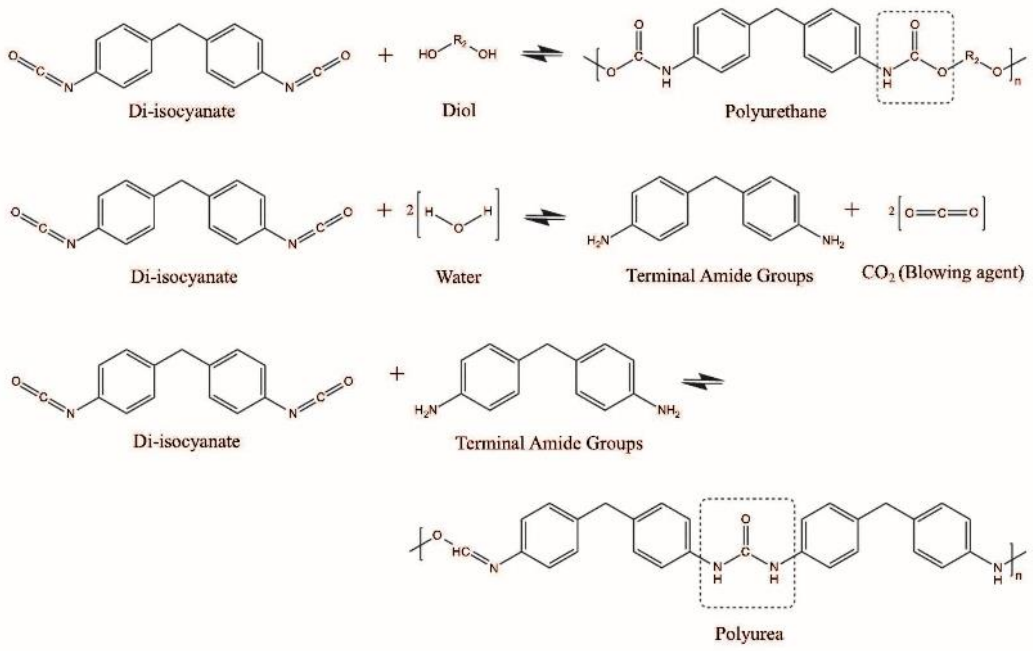


**Fig. (3).** Polyurethane reaction chemistry [8].

Foam density increased with higher contents of soy protein products. Foams containing DFS had a greater expansion ratio than those containing SPI or SPC due to the lower availability of active hydrogen atoms in DFS for reaction with the isocyanate. Foams containing up to 20% SPI demonstrated a higher compressive strength before reaching a plateau. This plateau was due to the protein reacting with all of the available isocyanate, resulting in a lower level of isocyanate available to evolve carbon dioxide and the excess protein weakened the foam structure. Furthermore, all foams containing soy protein products in this study showed greater resilience in comparison to polyurethane, suggesting that these may be suitable for packaging or cushioning applications [41].

A similar study produced polyurethane foams containing SPI, soy fiber and corn starch with toluene di-isocyanate (TDI) and demonstrated that using protein rather

than carbohydrates (starch) produced foams with better properties [40]. At lower amounts of additives (10%), foams containing SPI had a greater resilience compared to the other two formulations at the same level. At 20 wt% all formulations displayed similar resilience while 30% resulted in higher resilience for the soy based foams (SPI and soy fibre) than corn starch.

SPI and soybean meal (SM) have also been used to produce rigid polyurethane foams [43]. This was achieved by blending polyol (PEG-400), catalyst (DABCO), foam stabiliser (L-6865), water, crosslinker (triethanolamine) and protein (SM or SPI in either an activated or non-activated state). Polymeric isocyanate (PAPI-200) was then added and the mixture stirred before curing at room temperature for 30 minutes and aged at 35°C for 24 hours [43]. Up to 30% activated SM gave rigid foams with better thermal and mechanical properties than foams with SPI. Activation of the soybean meal *via* alkali treatment and sulphur bonding reduction increased availability of reactive protein groups to react with isocyanate, increasing foam density. Fibres in SM gave a more compact structure causing higher foam densities (67.6 kg/m$^3$ at 30 wt% SM) compared to foams with SPI (65.3 kg/m$^3$) [43].

The compressive strength of foams increased with increasing SM and SPI and foams containing activated fractions demonstrated higher compressive strength (348 and 262 kPa respectively at 30 wt%) than those which were not activated (242 and 221 kPa respectively) [43]. The polysaccharide and fibre fractions in SM (absent in SPI) may have helped increase compressive strength. Activated SM and SPI gave foams with smaller cell sizes, resulting in lower thermal conductivities, 0.0265 W/mK for activated SM at 30 wt% compared to 0.0312 W/mK for inactivated SM. SM based foams had lower thermal conductivities than those with SPI [43].

Similar thermal conductivities were achieved by another study which used soy flours (SF). SF has a protein content of 50-53% compared to 46% for SM from the previous study. Polyurethane foams containing SF were prepared in a similar manner. Typical thermal conductivities for these foams with 30% SF with the same blowing agent concentration were between 0.0263-0.0266 W/mK [42]. Densities for 30% SF polyurethane foams were 43.3-38.0 kg/m$^3$ which is lower than those from SM. Compressive strengths were also reported and ranged from 247-265 kPa which is comparable to the non-activated (native) SM polyurethane foams previously described.

A study investigated the use of algal protein, a co-product of the biofuels industry, with polyurethane. The algal proteins were first extracted, hydrolysed and the soluble peptides and amino acids retained for freeze drying. The freeze dried

material was then reacted with diamine and ethylene carbonate to produce the necessary polyol structure required for producing polyurethane. The algae polyol was then combined at a concentration of 5% with the other polyols, surfactant, water and isocyanate to produce the polyurethane foam. The algal polyols were high in hydroxyl content and very compatible with other polyols. The polymerisation process was self-catalytic and gave a rigid polyurethane foam which was less flammable than traditional polyurethane foams [44]. The resulting cellular structure was irregular open cell pores with a cell size of $0.6 \pm 0.23$ mm. Compared to the reference foam from commercial polyols, there was no change in core density (53 kg/m$^3$) but there was a decrease in resiliency, tensile strength, elongation and compressive strength when algal polyol was incorporated.

A review of the applications for a natural silk protein called sericin suggests that this protein may also behave favourably in polyurethane systems. A large number of Japanese patents are cited for the incorporation of sericin into polyurethane foams [45], however there is little available literature on these foaming systems.

## THERMOPLASTIC FOAMING PRINCIPLES

The mechanisms which define foaming of thermoplastic polymers are bubble nucleation, growth and stabilisation and have been reviewed at length elsewhere for traditional systems. However, to briefly summarise, the creation of a foamed product is dependent upon the development of gas bubbles within a liquid/melt or softened phase. These bubbles must grow and stabilise to result in a permanent cellular product [46 - 48]. These processes are thermodynamically controlled and polymer must exhibit suitable rheology to successfully produce a cell structure [8].

Initial bubble formation is referred to as cell nucleation. From a thermodynamic perspective, the evolution of gas bubbles within a polymer melt requires instabilities, *i.e.* the presence of a driving force [8]. During bubble nucleation the decrease in the free energy of the system which occurs with the development of the gaseous phase (molecules have a lower Gibb's free energy when present as a distinct phase rather than as individual molecules) provides this driver [49]. Later, as the cells grow to reach a stable state, there is a corresponding increase in Gibb's free energy as new interfaces are formed [47]. Overall, the free energy of the system is said to increase during the foaming process.

Polymer melts can be described as either homogenous or heterogenous which affects the nucleation mechanism. Self-nucleation occurs when a homogenous melt (the primary phase) develops gas bubbles (a secondary phase) without external assistance. In reality, self-nucleation is very seldomly achieved as such a process would encounter a large activation energy barrier. However, should a

number of dissolved gas molecules cluster together, it is theoretically possible [47, 48]. Polymer melts typically contain additives (usually talc 1-3%) or impurities resulting in an inhomogeneous system to which homogenous nucleation theory cannot be directly applied. The presence of these particles and cavities reduces the activation energy required to achieve a stable nucleus, therefore foaming more commonly occurs *via* this mechanism [47 - 50]. The efficiency of the nucleating agent depends on the type and shape of the nucleating particles as well as the interfacial tension between the polymer and nucleating agent [50].

Once nucleated, cells grow as gas continues to diffuse from the polymer into the cells. Growth ceases when the cells are stabilized (through cooling) or when they rupture (*i.e.* the polymer is unable to contain the gas). Bubble coalescence and rupture will continue to occur simultaneously with bubble growth. A permanent cellular product will only result if the cell structure can be stabilised. Typically, a foamed structure becomes stabilised through the cooling process which raises the viscosity of the polymer melt. Eventually, the expansion ceases and the cellular structure appears to stabilize when the polymer has cooled sufficiently to return to a solid state [51].

## FACTORS WHICH AFFECT THERMOPLASTIC FOAMING

Excluding processing conditions, the foaming ability of biopolymers and proteins is similar to that of traditional polymers. Factors which affect foaming include: solubility and diffusivity of the gaseous phase, melt rheology, melt strength and strain hardening behaviour, all of which can be related to the crystallinity of the material. The relationship between these effects are well established with traditional polymers and can easily be manipulated. An improvement of foaming ability has been linked to the introduction of branching, or through increasing the molecular weight distribution in traditional systems [6]. This section aims to discuss the material properties which affect foaming ability in relation to foaming in general and to highlight the factors which are more important in batch and extrusion foaming respectively before these methods are discussed in depth.

### Crystallinity and Thermal Transitions in Polymers and Proteins

Polymers are described as either amorphous, semi-crystalline or crystalline depending upon the degree of ordered structures they contain. For traditional polymers, crystallinity is defined by the proportion of ordered regions called lamellae made by regular folding of the polymer chain. The subsequent production of spherulites from these lamellae results in larger crystalline structures which can reach up to several millimetres in size [15, 52]. In protein thermoplastics, the semi-crystalline nature of these materials is determined by the

secondary structure of the proteins and the relative proportion of α-helices and β-sheets in comparison to less structured regions such as random coils. The crystalline regions within protein polymers are smaller than those observed in traditional polymers, approximately 10 nm in size, but have been shown to dictate the processing temperature of protein thermoplastics and the ability of these materials to form stable products [15, 53].

During processing, ordered regions are disrupted through the addition of heat which enables the production of a melt. At the melting temperature ($T_m$) complete disruption of these ordered structures occurs in the case of traditional polymers. The semi-crystalline nature and the transitional behaviour of protein-based polymers has been extensively reviewed in comparison to the responses demonstrated by traditional polymers [15].

Dry proteins typically display glass transition temperatures which are close to their degradation temperature. This is overcome when denaturants and plasticisers are added to lower the $T_g$. A denaturing temperature ($T_d$) is typically observed in protein biopolymers which is often very similar to the representative melt temperature observed in semi-crystalline polymers.

Above the $T_d$ protein polymers will either unfold to a less ordered conformation associated with the partial dissociation of these ordered structures (α-helices and β-sheets) or the increased temperature can induce the production of these ordered regions, mainly β-sheets, known as aggregation. For protein polymers these transitions can be poorly defined, occurring over a broad temperature range, and depend upon the degree of hydrogen bonding, electrostatic forces and hydrophobic interactions which exist within the protein. Therefore, these transitions are protein dependent.

It is important to emphasize the production of a protein thermoplastic melt does not necessarily indicate the complete disruption of α-helices and β-sheet conformations to an amorphous phase (unlike traditional thermoplastics) and in some cases may promote the formation of β-sheets [15]. However, mechanical shear may result in a reduction or dispersion of these crystalline regions, enabling a thermoplastic melt. The crystallinity of a protein-based thermoplastic affects the melt, the corresponding rheological properties and its behaviour with respect to solubility and diffusivity of gases. The stabilisation of foams will also be effected by the ability of these materials to recreate these ordered regions on cooling to freeze the resulting foam structure.

**Solubility and Diffusivity**

Foaming relies on the introduction and retention of a gaseous phase within a

polymer matrix. The solubility and diffusivity of gases strongly influences the foaming ability of these materials. Gases can be incorporated through the use of either physical blowing agents (PBA) or chemical blowing agents (CBA). Common PBAs used to include chlorofluorocarbons (CFC), hydrochlorofluorocarbons (HCFC), and hydrocarbons such as pentane and butane. However, there has been a recent migration towards more environmentally benign agents such as $CO_2$, $O_2$ and $N_2$. Azodicarbonamide, sodium bicarbonate or sodium bicarbonate/citric acid systems are examples of CBAs where gases are evolved by heating to decompose the CBA.

Factors which affect solubility and diffusivity within polymer systems have been reported as the phase of the polymer (molten or glassy), the structure and degree of crosslinking, crystallinity of the polymer and type, concentration and behaviour of plasticisers and fillers. An excellent review [54] defines the relationship between solubility and diffusivity of gases within polymers for foaming. The production of a fine cell homogenous foam is produced by the complete dissolution of the gaseous phase while partial dissolution results in a heterogeneous foam structure.

Normally, the solubility of a gas can be improved by increasing pressure and decreasing temperature. However, $CO_2$ or $N_2$ in a polymeric systems does not necessarily behave as expected. For example, the solubility of $CO_2$ has been observed to decrease with an increase in temperature while $N_2$ displays an increase in solubility with temperature in polystyrene. Consequently they are often used as a blend during batch foaming, for example 75% vol. $N_2$ and 25% vol. $CO_2$ for zein proteins [6].

The crystallinity of the polymer dictates the gas its solubility and diffusivity as the crystalline regions oppose the movement of absorbed gas within the amorphous phase. Additional factors, which have been noted as affecting the properties of semi-crystalline polymers, include orientation of the crystalline phase, chain stretching and free volume changes. It is also believed that these crystalline regions can promote nucleation by acting as heterogenous nucleating agents.

Adsorption and absorption of gaseous molecules is greatly influenced by the temperature of the polymer system in relation to its glass transition temperature. When $T>T_g$ the amorphous regions of the polymer or protein system become fluid although motion is still restricted by the crystalline phase (if present) if $T<T_m$. The solubility of the gaseous phase in the polymer matrix is similar to that of gas into a viscous fluid. When $T<T_g$ the polymer remains glassy with limited chain mobility. When gases are taken up they become trapped within polymer chains and physically disrupt the bonding between the polymer chains. In this case the

free volume of the polymer is increased and the absorbed gas has a temporary plasticising effect. During this process the solubility of these gases into the solid phase is governed by surface adsorption rates. High solubility of a gas within a polymer results in more blowing agent which benefits nucleation and cell growth.

The uptake of gases within a solid matrix is a controlling factor in batch foaming. During this process, plasticisation of the solid matrix can occur which provides the system with sufficient mobility to enable foaming. The resulting cellular structure is solidified by the loss of this plasticisation as the gaseous phase moves out of the polymer and into the bubble resulting in an increase in polymer viscosity.

In extrusion systems where a fluid melt is produced, the melt experiences additional plasticisation by the introduction of a gas phase from PBA or CBA. This decreases the viscosity of the polymer melt, reducing the melt pressure with respect to the internal bubble pressure, favouring faster bubble growth. The solidification of the foamed structure once again corresponds to a change in polymer viscosity. Once the melt has exited the extruder and depressurises, the gas migrates into the nucleated bubbles resulting in cell growth, and the material expands. The melt also cools which induces crystallisation and increases the viscosity slowing cell growth, and solidifies the foam structure.

Diffusivity of gas within a polymeric material is dictated by the polymer chain mobility, packing, crystallinity and degree of crosslinking, which are temperature dependent. The diffusion rate is dependent on the gas concentration gradient which decreases as the material approaches saturation. The presence of side chains in a polymer decreases packing resulting in a more amorphous structure, increasing diffusivity. An increase in the crosslinking within a polymer decreases diffusivity and solubility of the gas [54].

High diffusivity of gases within a polymer is ideal for nucleation but has a detrimental effect on bubble growth. High diffusivity results in greater nucleation as the gas leaves the polymer/BA phase quickly, giving a finer cellular structure, but during bubble growth, the gas can escape from the bubble and material easily, reducing bubble size. Diffusivity is particularly important in extrusion processes as the material has a short time before it cools. Gas diffusivity can be manipulated by controlling polymer viscosity and crystallinity by adjusting temperature, enabling bubble size and cell density to be controlled.

The solubility and diffusivity of gases within traditional polymers is well defined and gases with a variety of phases (subcritical, supercritical and gaseous) have been used. Gas solubility and diffusivity in protein-based thermoplastics is not widely reported, but will depend on the blowing agent, denaturants and

plasticisers used. For example proteins have been selected for film and coating applications due to their low oxygen permeabilities, but protein films have high water vapour permeabilities [55].

## Viscoelastic Behavior and Melt Rheology in Foaming

Polymers and proteins have defined thermal transitions where they change from a solid to a melt. The ability of polymers to foam is closely related to their temperature dependent viscoelastic behaviour which is a controlling factor in both batch and extrusion foaming systems. Foaming behaviour is greatly influenced by viscosity and is related to melt strength, extensional viscosity and the ability to display strain hardening. The mechanisms which control foaming are linked to the amorphous and semi-crystalline nature of these materials and the presence of side chains.

As previously described, bubble growth during foaming is directly linked to the viscosity of the polymer and the pressure difference between the bubble and the matrix. As such, polymer viscosity is a controlling factor for foaming and influences nucleation and stabilisation as well. Ideally viscosity of the polymer is low during the nucleation phase to enable high nucleation rates. It should then increase during bubble growth to restrain bubble growth.

This is commonly achieved through loss of the gaseous phase from the polymer melt or a decrease in temperature to produce high viscosities which stabilise the foam structure in amorphous polymers. If the viscosity of the polymer is too low and the melt strength is poor, the cells are prone to rupture and collapse. In materials with chain branching, *e.g.* polypropylene, strain hardening occurs which can be used to overcome low melt strength [56]. For semi-crystalline polymers the stabilisation effects are also related to crystallization of the material in addition to the factors listed above.

Many attempts have been made to describe the required rheological properties for foaming in relation to melt strength and extensional viscosity. Extensional viscosity is described as being the factor which allows two materials with the same shear viscosity to behave differently in extensional flow. Extensional flows are experienced by polymers in processes such as such as fiber spinning, film blowing and extrusion foaming [57]. The relationship between extensional viscosity and foaming ability is better defined by transient behaviour, as during foaming deformation occurs within a limited timeframe.

Extensional viscosity can be determined from Rheotens curves if there is optical monitoring of the extrudate size, however the results are qualitative. Therefore, the Rheotens method is more commonly used to determine melt strength [57]. The

melt strength is defined as the maximum tensile strength required to break the strand extruded through a capillary with a gradual increase in haul off speed. Sufficient melt strength is required for foaming in addition to extensional viscosity.

**Strain Hardening**

The correlation between melt strength, melt elasticity and strain hardening has been reviewed in depth for polyolefin materials, which are favoured in many applications due to their toughness, flexibility and chemical resistance. For foam extrusion, polyethylene (PE) has typically been favoured over polypropylene due to cost, thermal and chemical stability and processability (PE has a wide foaming window). Polypropylene foams demonstrate high stiffness and can be used static load bearing applications. However, their manufacture is limited as they demonstrate low melt strength and little elasticity. Consequently the cells within polypropylene foams rupture easily as the cell walls are not able to withstand the extensional forces which occur during foaming.

The melt strength of PP can be improved by introducing long-chain branches which restrict the movement of polymer chains under strain and introduce strain hardening effects, stabilising the bubbles during growth and reducing cell coalescence and rupture. An increase in the long chain branching (LCB) content of PP resulted in lower and broader DSC melting peaks, a reduction in crystallinity, and increased zero-shear and elongational viscosities. This resulted in lower foam densities with well-developed and uniform foam structures compared to unbranched PP [58]. Another study looking at blends of linear PP with LCB PP found that increasing LCB PP content past 50% had little effect on the degree of foaming because elongational viscosity of 100% LCB PP was similar to 50% linear PP:50% LCB PP blends [59].

The extensional viscosity of proteins and thermoplastics thereof have been linked to the secondary structure of the proteins for zein and kafirin under film blowing conditions. The film blowing process requires good melt deformability and elongational properties which is similar to the properties required for foaming. Two studies have been conducted to correlate the molecular structure, rheological behaviour and film blowing abilities of these proteins. Zein-based materials containing a high proportion of α-helical structures produced the best blown films, with the highest extensional viscosity, best strain hardening behaviour and haul of force. It was concluded that the change in extensional behaviour could be contributed to the relative content of α-helical to β-sheets [53].

Another study examined film formation from kafirin protein, where it was found that heat treatments promoted β-sheets formation which reduced film forming

ability. Freeze-dried material contained the highest proportion of α-helical structures. The higher strain and tensile strength films produced from freeze-dried kafirin is a result of not only the greater ratio of α-helical structures to β-sheets and other protein conformations but also their homogenous distribution and the ability of native-like structures to pack together more efficiently than denatured and aggregated proteins [55].

The correlation between secondary structure and foaming ability has been discussed for the foaming ability of zein proteins. Plasticised zein protein (75% zein: 25% PEG400) has been shown to depend heavily on the concentration of β-sheets within the original zein protein. During this study zein was obtained from the same producer and extracted using the same technique, however FTIR analysis detected differences in the secondary structure of the zein protein. This suggests that variability within protein supplies such as small changes in growth conditions, extraction or protein aging may influence foaming results. The foaming ability of these zein proteins was once again linked to the ratio of α-helical to β-sheet content. The governing conformation was linked to the β-sheet content which influenced how deformable the plasticised material was. Zein with a higher concentration of β-sheets resulted in a collapsed foam under batch foaming conditions which was contributed to the material being unable to withstand deformation during foaming. In comparison the zein a lower β-sheet content resulted in a far more deformable material and a fine cell low density foam [6].

## BATCH FOAMING

An effective method for producing cellular foams is the batch foaming technique, also known as the autoclave method. Batch foaming can produce microcellular foams, structures with cell sizes smaller than 10 μm and cell population density greater than $10^9$ cells.$cm^{-3}$ [60].

Microcellular foams are attractive because the material's bulk density is reduced while possessing high impact strength, toughness, stiffness-to-weight ratio, low thermal conductivity as well as low weight and cost [61].

There are two approaches to batch foaming. The first is the ***temperature soak*** method where the polymer at room or low temperature is placed in a high-pressure gas environment which forces the gas to diffuse into the polymer matrix. The vessel is depressurised and material transferred to a mould or water bath and heated past the glass transition temperature, resulting in the gas nucleating and forming micro-bubbles. Subsequently, the material is cooled resulting in a stable foam.

The second approach is the ***pressure quench*** method where the material is heated in an autoclave past its glass transition temperature and exposed to gas at high pressure, resulting in the gas diffusing into the material. The pressure is released resulting in the gas forming micro-bubbles in the polymer, and the temperature lowered resulting in a stable foam. Fig. **4-A** shows a typical set-up of a supercritical batch foaming system [62].

The setup consists of an autoclave which is temperature controlled by circulating oil heated/cooled by a cryo-thermostat. The $CO_2$ is supplied by a $CO_2$ cylinder connected to a gas booster. Pressure and temperature are monitored and computer controlled. For batch foaming, cell morphology, size and number can be manipulated by controlling pressure, temperature, gas type, saturation time, nucleating agents and depressurisation rate. Polymer crystallinity, viscosity, and melt strength also influences cell size, density and the resulting foam mechanical properties.

**Gas Absorption**

Gas absorption can be measured directly by change in weight of the material or indirectly by measuring foam density after the material has been foamed. Absorption will depend on gas pressure, absorption time, gas solubility, and diffusion rate.

Gas diffusion rate and solubility will be dependent on gas and material type, decrease with increasing polymer viscosity (which decreases with increasing temperature) and crystallinity (which is dependent on the melting temperature of the crystalline regions and whether or not absorption is carried out above the melting temperature of the crystalline regions).

Doourdiani, *et al.*, were able to manipulate the crystallinity of HDPE, PB, PP and PET by heating them above the melting temperature and cooling them at different rates following compression moulding into a film. Slow cooling rates induced high crystallinity while cold water quenching on the material gave the lowest crystallinity. $CO_2$ solubility was halved and diffusivity decreased by 5% for PP and up to 100 fold for PET when crystallinity was increased from 45% to 69% for PP and 36-58% for PET [65]. Increasing gas pressure will increase gas absorption and polymer swelling and decrease in foam cell size. PLA (grades 3001D, 8051D and 4060D) showed an increase in swelling ratio of 1.04 to 1.16-1.20 when $CO_2$ gas pressure was increased from 6 to 22 MPa (at 190°C), while gas solubility increased from 0.04 to 0.14 g/g [66].

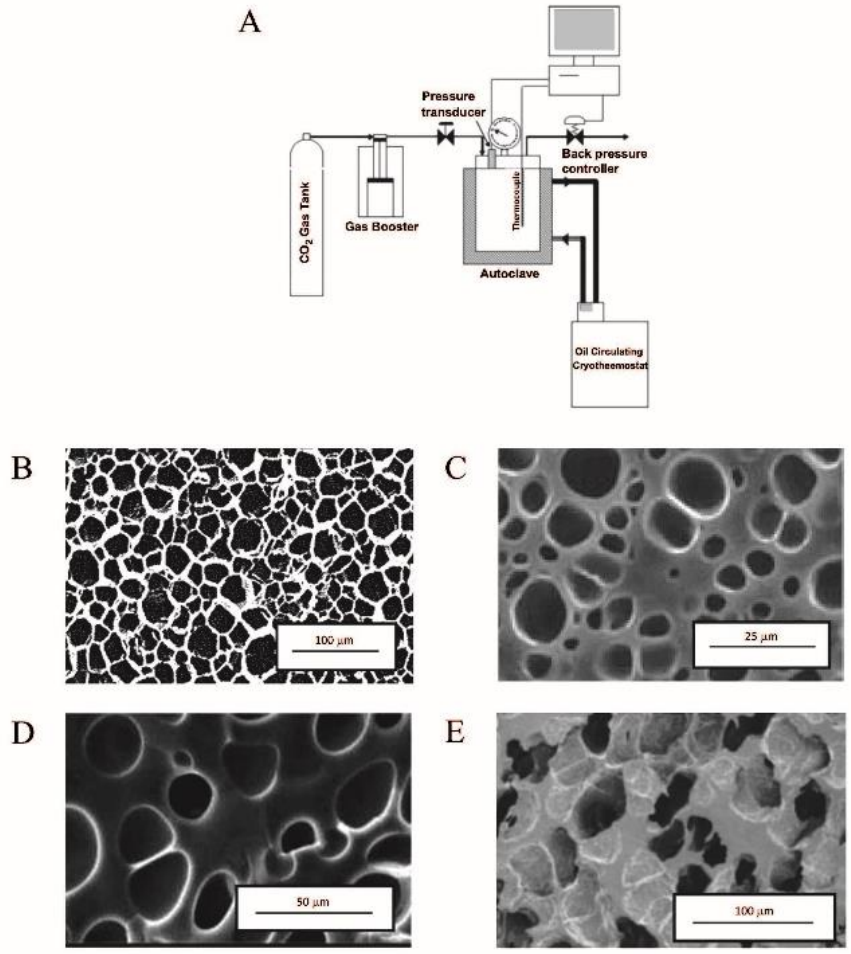


**Fig. (4). A:** Typical batch foaming system [62] **B:** SEM image of TPZ (Thermoplastic Zein) foamed with $N_2$-$CO_2$ 80-20 vol%, $P_{sat}$ = 180 bar, $T_f$ =79°C [20] **C:** SEM image of TPZ (Thermoplastic Zein) foamed with $N_2$-$CO_2$ 80-20 vol%, $P_{sat}$ = 170 bar, $T_f$ =55°C [63] **D:** SEM image of TPG (Thermoplastic Gluten) foamed with $CO_2$, $P_{sat}$ =85 bar, $T_f$ =100°C [19] **E:** SEM image of NTP/PLA blend foamed with supercritical $CO_2$, $P_{sat}$ = 200 bar, $T_f$ =55°C [64]. Images reproduced with permission, see note[2].

Aionicesei *et al.* showed similar results for poly(L-lactide), PLLA (42 kDa, semi-crystalline) and poly(D, L-lactide-co-glycolide) PLGA (72 kDa, 50:50 D and L-lactide, amorphous) where $CO_2$ solubility doubled or tripled when $CO_2$ pressure was increased from 10-30 MPa. PLLA had almost twice the $CO_2$ solubility of PLGA (0.75 g/g compared to 0.4 g/g for PLGA at 30 MPa), but both had similar diffusion coefficients, probably due PLLA being semi-crystalline and a lower molecular weight, while PLGA is amorphous, but a larger molecular weight [67]. Similarly, $CO_2$ solubility in polymethyl methacrylate (PMMA) increased from 0.08 g/g at 15 MPa to 0.24 g/g at 25 MPa [68]. LLDPE showed a foam density of

0.27 g/cm$^3$ when saturated with $N_2$ at 12 MPa compared to 0.17 g/cm$^3$ at 20 MPa [69]. Polystyrene showed a decrease in average cell size with increased $CO_2$ pressure from 440 μm at 7.5 MPa to 40 μm at 10 MPa when foamed at 80°C [56].

Increasing gas absorption time will increase the amount of gas adsorbed in the matrix up until it reaches saturation, which will decrease foam density. This behaviour is also linked to diffusion rate which is dependent on the polymer, gas and temperature. Higher temperatures will reduce polymer viscosity and increase diffusivity, reducing saturation time. For example, LDPE at 125°C saturated with $N_2$ took longer to reach saturation (8 min at 12 MPa) than LDPE at 135°C (5 min), while LLDPE at 119°C took 10 min and 8 min at 135°C [69].

## Foaming

Extent of foaming will depend on the amount of gas absorbed (see previous section), temperature and pressure at which the material is foamed, depressurisation rate, and polymer melt strength, viscosity and elasticity. These effects on foaming can be measured by foam density, cell density, cell size and cell size distribution.

Kwon and Bae showed higher $CO_2$ gas solubility (manipulated by ranging $CO_2$ pressure between 15-25 MPa) in PMMA will result in greater cell density and lower cell mean diameter when the material is foamed [68].

A higher foaming temperature will generally reduce foam density, but this will be polymer dependent. For example LLDPE foamed at 123°C had a foam density of 0.08 g/cm$^3$ compared to 0.17 g/cm$^3$ at 119°C, while LDPE showed little difference in foam density when foamed at 125°C and 135°C [69]. The foaming temperature window will depend on the melt strength of the polymer, which is dependent on polymer viscosity and temperature. Higher viscosities will slow bubble growth, while high foaming temperatures will reduce viscosity and increase gas diffusion and bubble growth [56, 70]. As the bubble grows, and the matrix stretches around it, the matrix will undergo strain hardening as previously described, which will slow bubble growth. If bubble growth is too fast for the polymer, it will result in collapsed bubbles. For example LLDPE foamed at temperatures greater than 123°C resulted in collapsed bubbles, whereas LDPE, which has a greater melt strength than LLDPE, had a broad foaming window of 105 to 160°C, and cell size and morphology was largely independent of temperature tested [69]. LLDPE foamed at lower temperatures and showed more irregular cell morphology due to the presence of crystalline regions in the polymer melt.

Polymer viscosity and melt strength can be increased by grafting long chain branches (LCB) onto the polymer back bone, or extending chain length. Grafting

LCB onto polystyrene resulted in a narrower cell size distribution and smaller average cell diameters, and higher cell densities (2 wt% LCB grafted PS gave a 100 fold increase in cell density compared to ungrafted PS foamed with $CO_2$ at 10 MPa and 110°C). Cell size and distribution increased with increasing foaming temperature (0-19 μm at 70°C to 70-230 μm at 110°C), while the effect of chain branching on cell density was more pronounced for the higher foaming temperatures (80-110°C) [56].

Increased depressurisation rate increases cell nucleation, resulting in higher cell densities and lower cell size [61]. Bimodal foams, *i.e.* foams with two discrete cell size distributions, can be generated by using two step depressurisation after the polymer has been saturated with gas. These have the advantage of having a low thermal conductivity and low weight from the larger average cell size while retaining the high mechanical strength imparted by the microcellular foam. Bimodal foams were produced from PS saturated with $CO_2$ at 20 MPa and 100°C and depressurised to 15 MPa, held for a period of time, and then depressurised to ambient pressure. Increasing holding time from 0 to 60 min increased the average cell diameter from 4 μm to 22 μm and reduced cell density from $8x10^8$ cells per $cm^3$ to ~ $1x10^6$ cells per cm3 [61].

Dorourdiani *et al.*, showed that HDPE, PB, PP and PET with increased crystallinities (see previous section) had quite different foam morphologies. Samples with lower crystallinities had a more regular cell structure and smaller cell size, while samples with the higher crystallinities were more difficult to foam only exhibiting foam structures in a few localised regions in the polymer. This was partly due to lower gas solubility and diffusivity at higher crystallinities, but Dorourdiani *et al.* also speculated that $CO_2$ acted to plasticise the polymer, resulting in easier foaming at lower crystallinities and higher $CO_2$ concentrations in the matrix [65]

Liao *et al.* manipulated the crystallinities of unbranched and branched PP by heating it to 180°C, exposing it to $CO_2$ at 14 MPa for 4 hours, cooling it to 130°C at holding at that temperature for different periods of time before depressurising. Longer holding times for unbranched and branched PP resulted in increased crystallinities (observed by measuring the spherulite size and density) and consequently smaller cell sizes and larger cell densities. Reducing holding time resulted in ellipsoid shaped cells, while the longer holding times gave more spherical cells [70]. Unfortunately their foaming windows for unbranched and branched PP were quite different so a direct comparison between using the same conditions for the two types was not possible.

LCB onto polystyrene resulted in a narrower cell size distribution and smaller average cell diameters, and higher cell densities (2 wt% LCB grafted PS gave a 100 fold increase in cell density compared to ungrafted PS foamed with $CO_2$ at 10 MPa and 110°C). Cell size and distribution increased with increasing foaming temperature (0-19 μm at 70°C to 70-230 μm at 110°C), while the effect of chain branching on cell density was more pronounced for the higher foaming temperatures (80-110°C) [56].

Increased depressurisation rate increases cell nucleation, resulting in higher cell densities and lower cell size [61]. Bimodal foams, *i.e.* foams with two discrete cell size distributions, can be generated by using two step depressurisation after the polymer has been saturated with gas. These have the advantage of having a low thermal conductivity and low weight from the larger average cell size while retaining the high mechanical strength imparted by the microcellular foam. Bimodal foams were produced from PS saturated with $CO_2$ at 20 MPa and 100°C and depressurised to 15 MPa, held for a period of time, and then depressurised to ambient pressure. Increasing holding time from 0 to 60 min increased the average cell diameter from 4 μm to 22 μm and reduced cell density from $8x10^8$ cells per $cm^3$ to ~ $1x10^6$ cells per cm3 [61].

Dorourdiani *et al.*, showed that HDPE, PB, PP and PET with increased crystallinities (see previous section) had quite different foam morphologies. Samples with lower crystallinities had a more regular cell structure and smaller cell size, while samples with the higher crystallinities were more difficult to foam only exhibiting foam structures in a few localised regions in the polymer. This was partly due to lower gas solubility and diffusivity at higher crystallinities, but Dorourdiani *et al.* also speculated that $CO_2$ acted to plasticise the polymer, resulting in easier foaming at lower crystallinities and higher $CO_2$ concentrations in the matrix [65]

Liao *et al.* manipulated the crystallinities of unbranched and branched PP by heating it to 180°C, exposing it to $CO_2$ at 14 MPa for 4 hours, cooling it to 130°C at holding at that temperature for different periods of time before depressurising. Longer holding times for unbranched and branched PP resulted in increased crystallinities (observed by measuring the spherulite size and density) and consequently smaller cell sizes and larger cell densities. Reducing holding time resulted in ellipsoid shaped cells, while the longer holding times gave more spherical cells [70]. Unfortunately their foaming windows for unbranched and branched PP were quite different so a direct comparison between using the same conditions for the two types was not possible.

## EXAMPLES OF BATCH FOAMED PROTEINS

There are only a few examples of successfully batch foamed proteins using the autoclave method. These used zein, gelatin and bloodmeal (which was blended with PLA).

Salerno *et al.* [20] foamed protein based discs cut from hot-pressed gelatin with 20 wt% glycerol and zein with 25 wt% PEG 400 (Fig. **4-B**). They explored varying the gas composition using a mixture of $N_2$ and $CO_2$, saturation pressures between 6-18 MPa at 70°C, foaming temperatures between 50-140°C, and pressure drop rates of 25 and 70 MPa/s. The best foams from zein were obtained using 80% $N_2$ and 20% $CO_2$ at 18 MPa at 70°C, with a foam density of 0.1 g/cm$^3$ and average cell size of 32 μm. At lower foaming temperatures (44°C), the cells were smaller (14 μm) with thicker walls with a foam density of 0.65 g/cm$^3$, due to the increased viscosity of the material, while higher temperatures (100°C) resulted in apparent cell shrinkage (15 mm) due to gas diffusion through the cell walls. Gelatin foam densities were between 0.5 to 0.7 g/cm$^3$ and cell sizes ranged between 3 to 25 mm when foamed at 44-120°C, but temperatures above this resulted in browning and loss of glycerol.

Olivierio *et al.* [63] found adding acid or alkali derived lignin to zein thermoplastics was detrimental to foaming (using similar conditions to Salerno *et al.*), and were only able to produce microcellular foams (Fig. **4-C**) with addition of lignin up to 1% by weight. Olivierio *et al.* [19] also foamed hot pressed gelatin (with 20% glycerol)/poly(butylene succinate) discs (Fig. **4-D**) using $CO_2$ at 6.5-8.5 MPa at 100 and 120°C and foaming temperatures between 75-100°C. Gelatin was immiscible in PBS and *vice versa*, but the presence of PBS reduced the cell size compared to plasticised gelatin foams which was between 15-40 μm.

Trujillo-de Santiago *et al.* [30] produced foams from zein (plasticised with PEG 400), starch (with urea and formaldehyde (UF) and sorbital and glycerol (SG), a blend of starch and zein (with UF and SG), and blue maize (SG)). The materials were saturated with $CO_2$ at 15 MPa and 70°C, and foamed at temperatures between 75 to 140°C. Foamed zein increased eight fold in volume, followed by starch (UF) which increased in volume by six times. Starch (SG), the zein/starch blend, and blue maize showed only a slight increase in volume and the morphology appeared to be fractures in the material rather than regular cells.

Walallavita *et al.* [64] blended Novatein® thermoplastic (NTP) (a bloodmeal protein based bioplastic) with PLA (Ingeo™ 4060D, fully amorphous) at NTP concentrations between 5-60 wt%. Extruded rods were saturated with $CO_2$ at 6 MPa, transferred to a hot water bath and heated to 70°C. Rods were also foamed

by saturating them with $CO_2$ at 20 MPa at 50°C, followed by depressurisation. Expansion ratio decreased with increased NTP content (Fig. **4-E**).

## FOAM EXTRUSION

Extrusion foaming is highly economical due to the continuous nature of this operation. Foam extrusion can be carried out in any of the common extruder configurations: twin screw extruders (TSE), single screw extruders (SSE) or tandem lines [71], but the equipment must produce a sufficient melt temperature to decompose the blowing agent, the pressure of the melt must be kept high to prevent gas dissolution and the back pressure in the hopper must be controllable to ensure consistent results [71]. Each of the extruder configurations has unique advantages and disadvantages and are typically optimised for a particular polymer/blowing agent system through a trial-and-error approach. Specialised extruders have been designed for foaming applications, although to do so the behaviour of the material and the subsequent interaction of the blowing agent with this material must be well defined. Typically, the extruder contains several zones along the barrel where temperature, pitch, element type can be varied to better control melt properties and pressure (Fig. **5-A**).

The polymeric material is melted and blended with any CBAs within the first zone, the material is then mixed and PBAs can be added. As a general rule of thumb the feed zone within a foaming system must be lower than the initial decomposition temperature of the CBA if it is added with the feed [71]. The material is extruded across the remaining zones, where changes in temperature further alter the rheology of the material to enable foaming such that when the material reaches the die nucleation and bubble growth can occur [72].

Until then the gaseous phase remains dissolved within the polymer melt due to pressure within the barrel. Within these systems foaming occurs under free expansion (atmospheric pressure) unlike foaming conducted *via* injection moulding were the limited volume of the mould dictates the pressure experienced by the expanding melt. Once the material has exited the die, the material must solidify quickly before the gaseous phase causes excessive cell rupture or collapse.

The operating parameters such as screw speed, extrusion temperature, die size and the configuration of the screw elements all influence the properties of the resulting foams such as cell size, cell density, expansion ratio and radial expansion ratio. There are a limited number of examples of extrusion foaming of thermoplastic proteins, as such parameter optimisation has yet to be presented for foaming thermoplastic proteins and these are expected to be highly protein dependent. Therefore, the influence that these parameters have are described in

relation to traditional polyolefin foaming and biopolymers such as starch and PLA.

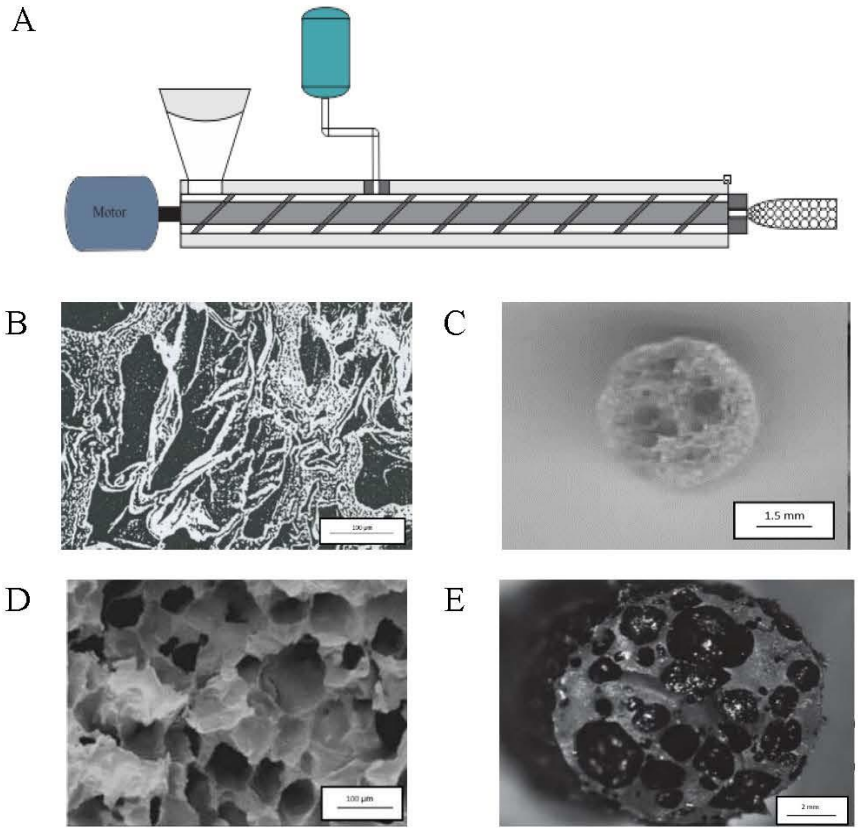


**Fig. (5).** **A**: diagram of a foam extruder with PBA capability, **B**: SEM image of Thermoplastic Soy foamed at 150-160°C [73], **C:** Image of 70% Zein 30% Pearl Millet Flour, Screw Speed 80 RPM, Die Size 2 mm [74], **D.** SEM image of PLA/SPC, 2 phr CBA, Screw Speed 60 RPM, Die Size 1 mm [23], **E.** Image of NTP/PE--MAH/LLDPE Foam, Steam Blown, Screw Speed 150 RPM, Die Size 10 mm [75]. Images reproduced with permission see note[3].

During extrusion foaming the behaviour of all thermoplastics are relatively similar therefore it is expected that thermoplastic protein foams will display similar responses to changes in extrusion speed, die size, CBA, PBA and nucleating agent content.

Foam extrusion behaviour of polyethylene and polypropylene is well defined and has been reviewed extensively [7, 51, 76, 77]. One review outlines the behaviour of polyolefins within extrusion foaming using linear low density polyethylene (LDPE) and polypropylene (PP) as examples. Sodium bicarbonate and citric acid

was used as a blowing agent. The material was extruded through a single screw extruder, 19 mm in diameter with a length/diameter (L/D) ratio of 25. The extruded foam was then submerged in a water bath to stabilise the foam structure [78]. This particular study discusses a comprehensive set of process variables including melt temperature, cooling water temperature, and blowing agent content on the resulting cell size and distribution. Material characteristics such as molecular weight, structure, melt viscosity and melt tension was also investigated.

The foaming ability of these materials was shown to be directly correlated with the molecular weight of the polymer. Higher molecular weights resulted in smaller cells and lower overall expansion due to the increase in polymer viscosity. The highest foaming ability was demonstrated for polypropylenes with a molecular weight of 231,000 (degree of foaming: 98%) and for LDPE with a similar molecular weight (degree of foaming: 65%). Melt tension was observed to be the governing factor which dictated the differences in foaming ability of the PP when compared to LDPE [78]. PP has a lower melt strength than PE hence lower degree of foaming was observed in PE systems, as an increase in melt tension restrains the bubble growth and results in smaller cells and a corresponding decrease in the foam expansion.

The effect of melt temperature on extrusion foaming was determined between 180-240°C for PP and LDPE. Foaming was observed to increase for both polyolefins with increasing melt temperature from 180-240°C due to a reduction in viscosity. Changes in blowing agent content (sodium bicarbonate/citric acid blend) in polypropylene systems resulted in a decrease in cell size as more gas was generated with greater nucleation rates. An addition of 5 wt% of these CBAs resulted in a degree of foaming of approximately 98%, while 2 wt% achieved 45%.

Stabilisation of the foam structure *via* cooling is also particularly important. In polypropylene systems, the degree of foaming observed was directly linked to the cooling temperature. Highest degrees of foaming were observed when the cooling temperature was lowered to 0-20°C in comparison to a melt temperature of 200°C. While a reduction in foaming degree was evident at higher cooling temperatures >30°C with the lowest foaming degree of 38% observed when the cooling temperature was only 65°C. This emphasizes the stabilising effect which higher cooling rates can have on foamed extrudates. Despite the greater solidification of the extrudate surface with lower temperature no change in cell size was observed.

Extrusion foaming has also been applied to amorphous PLA with azodicarbonamide (azo) as the blowing agent. A single screw extruder with an

L/D of 25 with five temperature zones of 138, 193, 232, 177, 149°C from feeder to die was used. Optimal CBA content for PLA was 0.8% which gave foam densities of 0.55 g/cm$^3$ compared to LDPE, which was 2% and a foam density of 0.45 g/cm$^3$. CBA content above and below this gave higher foam densities, which could be explained by phase separation occurring during extrusion resulting in lower amounts of gas within the polymer melt thereby decreasing expansion. A corresponding increase in rod diameter was observed with small quantities of CBA but degassing occurred at the die for blends with increased CBA content [79].

Extrusion foaming has also been used to produce starch based products for loose fill applications. Starch alone is high hydrophilic in nature which is detrimental to the physical and mechanical properties of the foam because it will readily absorb water in a humid environment. Therefore, starch is either modified before extrusion or blended with materials like polystyrene. The water which is incorporated with the starch typically acts as the blowing agent. For a 70% starch 30% polystyrene blend the optimum water content was 18% which gave a radial expansion ratio of 28-29 at processing temperatures of 140 and 160°C respectively, with large cells of up to 1 mm. Increasing water content further plasticised the material so its melt viscosity was too low to sustain foaming and the cell walls lacked the strength to contain the expanding bubbles [80]. Addition of talc, a nucleating agent and filler, reduced the radial expansion ratio and overall expansion ratio of these foams, but increased cell density from 24 cells/cm$^2$ to 342 cells/cm$^2$ at 3% talc to a blend with 20% moisture content (MC), narrowed cell size distribution, but increased bulk density from 14.6 to 17.7 kg/m$^3$ and made the foam more brittle. For foams containing talc, an optimal composition was found to be 18% MC, 1% talc and an extrusion temperature of 160°C [80].

## THERMOPLASTIC PROTEIN EXTRUSION FOAMING

Previous reviews of foam extrusion of proteins have typically discussed the necessity of blending proteins with carbohydrates, flours or PLA, and there are very few examples of foamed unblended thermoplastic proteins [1, 76]. In this section four examples of protein foam extrusion will be discussed. These studies have all been conducted with the final product intended for packaging applications. The first is a true thermoplastic protein foam produced from soy protein, the second and third studies examine the foaming ability of blends of zein protein with pearl millet flour and soy protein concentrate - PLA blends. The final study investigated blends of Novatein® Thermoplastic Protein, a thermoplastic derived from bloodmeal with linear low density polyethylene.

Thermoplastic SPI was prepared by extruding SPI, water, glycerol and salts

($CaCl_2$, sodium tripolyphosphate (STP), and $ZnSO_4$) in a co-rotating twin screw extruder and granulated. This was foamed using a CBA in a single screw extruder equipped with a six inch flat sheet die at 150-160°C. The resulting foams had a density of 0.4-0.6 g/cm$^3$ (Fig. **5-B**). Blends which were heavily plasticised had a lower Young's modulus while those with lower levels of glycerol addition produced a rigid foam structure [73]. Using STP resulted in a more processable and consolidated thermoplastic material, possibly due to disruption of ionic bonding between or within protein chains, but a higher foam density (0.62 g/cm$^3$). Adding $CaCl_2$, or $ZnSO_4$ increased Young's modulus, possibly due to $Ca^{2+}$ and $Zn^{2+}$ ions crosslinking negatively charged groups on the proteins. Adding $CaCl_2$ gave lower densities (0.53 g/cm$^3$), higher tensile strength (3.56 MPa) and elongation at break (24.1%) compared to adding $ZnSO_4$ (0.58 g/cm$^3$, 3.03 MPa and 21.19% respectively). All foams showed similar elongational to break despite the increase in tensile modulus which was due to a similar degree of crosslinking.

Zein protein (70-75%) can be combined with pearl millet flour (25-30%), derived from cereal crops, to produce foams [74]. The composition of pearl millet flour can vary significantly depending upon growing conditions, however, the material typically contains 8.5-19.5% protein, and 63.1-78.5% starch. The foamed blends contained 4.6 g water, 20 g polyethylene glycol (PEG-400) and 3.0 g ammonium bicarbonate per 100 g of zein/flour. Foaming was conducted using a compact extruder with a 1.5-2.0 mm die, screw speeds between 20 and 150 rpm with a temperature profile from hopper to die of 65, 105, 95, 80°C. A foam expansion ratio of 2-3.2 was achieved with a decrease in moisture content from 12% to 6.5%. Zein formed a continuous matrix while the pearl millet remained as discrete particles (Fig. **5-C**). The average cell size was 5 μm although the cell distribution observed was broad and foam density ranged from 0.35-0.5 g/cm$^3$. The elastic modulus of these foams under compression was 25-50 MPa.

Another study investigated the ability of polylactic acid (PLA) and soy protein concentrate (SPC) to foam (Fig. **5-D**) through twin screw extrusion using poly(2-ethyl-2-oxazoline) as a compatibiliser [23]. The material was foamed in a secondary extrusion step following compounding with a CBA (4-methylbenzen--1-sulfonohydrazide with 5% $CaCO_3$ for nucleation) and co-compatibliser of polymeric methylene diphenyl diiscocynate (pMDI). PLA/SPC blends were prepared using a co-rotating twin screw extruder with a screw diameter of 18 mm and an L/D of 40 with a screw speed of 150 RPM. The temperature profile was 90, 120, 140, 150, 160, 160, 155°C from hopper to die. The blends also contained a compatibiliser (PEOX, 3 phr), and citroflex A-4 (6 parts per hundred parts resin) and glycolube WP2200 (2 phr) as a plasticiser. Extrusion foaming was conducted using a screw speed of 60 RPM, die size of 1 mm and with a variable die temperature of 115-160°C. Cell rupture was a problem during extrusion and

SP/PLA blends displayed severe degradation at higher processing temperatures.

Gas from the CBA lowered melt viscosity enabling lower extrusion temperatures to be used. Adding pMDI as an interfacial modifier promoted cross linking between the hydroxyl groups of PLA and the amine groups of SPC which resulted in a higher viscosity. Cell densities in foams without pMDI decreased with increasing foaming temperature but increased by 1.7-1.8 times when pMDI was added. For foams without pMDI, the cell density increased with increasing CBA content up to 0.5-2 phr, after which cell density decreased. With pMDI, cell density was higher overall, possibly due to a decrease in nucleation activation energy through a heterogenous nucleation mechanism, but decreased with increasing CBA content. CBA content and extrusion temperature affected the pressure drop by altering viscosity. The material without pDMI had its lowest bulk density (0.53 g/cm$^3$) when extruded through a die at 140°C while blends wih pMDI displayed the lowest bulk densities (0.77 g/cm$^3$) at 150°C with 2 phr CBA.

In other research, expansion ratios of 1.85 and less were observed for an extrusion foamed blend of a thermoplastic bloodmeal (Novatein®) and linear low density polyethylene (LLDPE) in the presence of polyethylene grafted maleic anhydride (Fig. **5-E**) as a compatibiliser (PE-g-MAH) [75]. Foaming was conducted by adding Novatein® granules to LLDPE and PE-g-MAH in the hopper of a twin screw extruder. Sodium bicarbonate was used as the blowing agent and the material subjected to an extrusion profile of 70,100,100,110,120°C feeder to die. The die size was 10 mm.

As the proportion of NTP was increased the foaming ability reduced until consolidation of the extrudate was lost. A blend of 50% NTP, 10% PE-g-MAH and 40% LLDPE without additional blowing agent resulted in a bulk density of 0.58 g/cm$^3$. The addition of compatibliser at 6, 8 and 10% had no effect on the foam expansion ratio. Increasing the die temperature from 120 to 140°C resulted in a decrease in radial expansion ratio from 1.37 to 1 and the extrudate surface appeared to be more degraded. Addition of sodium bicarbonate as a blowing agent resulted in a very fine cellular structure while the bulk density remained constant, and the final material was more flexible than foams without the blowing agent.

Foam extrusion cooking is an analogous technique to extrusion foaming and is highly relevant to extrusion foaming processes involving proteins in particular. Extrusion foam cooking is common for starch/carbohydrate based snack foods and whey or soy protein are commonly added to improve the nutritional value of the snack food [81, 82]. Examples of research using foam extrusion cooking are listed in Table **1**, and two examples are discussed below.

**Table 1. Extrusion cooking of protein foams. Carb-carbohydrate SPC- soy protein concentrate, SWS- sweet whey solids, WPC- whey protein concentrate, WPI- whey protein isolate. TS- twin screw, SS- single screw. ER – expansion ratio, EI- expansion index.**

| Blend Properties | | | | | | | | Extrusion Conditions | | Foam Properties | | | |
|---|---|---|---|---|---|---|---|---|---|---|---|---|---|
| Protein | Protein Purity (%) | Protein Added (wt. %) | Max Protein (%) | Carb | Protein in Carb Phase (%) | Carb Added (wt. %) | Total Protein (%) | Screw Type | Screw Speed | ER | EI | Radial ER | Ref |
| Acid Casein | 88.5 | 50 | 44.25 | Potato Starch | 0.02 | 50 | 44.35 | SS | 80 | - | | 3.98-4.96 | [83] |
| Casein Casinate | 92 | 25 | 23 | Corn Meal | 9.0 | 75 | 29.75 | TS | 300 | - | 5.5 | - | [84] |
| Cow Pea | 27 | 100 | 27 | Sorghum Meal | 8.5 | 0 | 27 | TS | 200 | 2.0-5.4 | | - | [85] |
| Soy Bean Protein | 51.5 | 50 | 25.75 | Potato Starch | 0.02 | 50 | 25.85 | SS | 100 | - | | 1.93-2.70 | [83] |
| SPC | 71 | 50 | 35.5 | Corn starch | - | - | 35.5 | TS | 230-300 | 3.5-5.2 | | - | [86] |
| SPC | - | - | 30 | Corn Meal | - | - | - | TS | 250 | - | | - | [87] |
| SPC | 64.7 | 14.00 | 9.0 | Corn Meal | 6.5 | 64.15 | 13.16 | TS | 300 | - | | - | [88] |
| SPI | - | - | 30 | Corn Meal | - | - | - | TS | 250 | - | | - | [87] |
| SPI/SPC | 89.3/ 64.7 | 8.70/ 4.0 | 10.36 | Corn Meal | 6.5 | 66.25 | 14.66 | TS | 300 | - | | - | [88] |
| SWS | 12.9 | 50 | 6.45 | Potato Flour | 8 | 50 | 10.45 | TS | 300 | | 1.0-2.2 | - | [89] |
| SWS | 12.9 | 50 | 6.45 | Rice Flour | 5.7 | 50 | 9.3 | TS | 300 | | 0.7-2.8 | - | [89] |
| SWS | 12.9 | 50 | 6.45 | Corn | 5.6 | 50 | 9.25 | TS | 300 | | 0.6-2.3 | - | [89] |
| WPC | 58.3 | 25 | 14.58 | Potato Starch | 0.02 | 75 | 14.59 | SS | 80 | - | | 3.05-3.45 | [83] |
| WPC | 80 | - | 40 | Corn Starch | - | - | 40 | TS | 200 | 4-26 | | - | [90] |
| WPC | 80-86 | 30 | 25.80 | Corn Starch | - | - | 25.80 | TS | 140 | - | | 5.43-10.9 | [91] |
| WPC | 34.9 | 50 | 17.45 | Potato Flour | 8 | 50 | 21.45 | TS | 300 | | 1.2-2.2 | - | [89] |
| WPC | 34.9 | 50 | 17.45 | Rice Flour | 5.7 | 50 | 20.3 | TS | 300 | | 0.8-2.8 | - | [89] |
| WPC | 34.9 | 50 | 17.45 | Corn | 5.6 | 50 | 20.25 | TS | 300 | | 0.5-2.3 | - | [89] |
| WPC | 80 | 25 | 20 | Corn meal | - | - | 20 | TS | 300 | - | | - | [92] |
| WPC | 78.7 | 25 | 19.68 | Corn Meal | 9.0 | 75 | 26.43 | TS | 300 | - | 5.2 | - | [84] |

*(Table 1) contd.....*

| Blend Properties | | | | | | | | Extrusion Conditions | | Foam Properties | | | |
|---|---|---|---|---|---|---|---|---|---|---|---|---|---|
| Protein | Protein Purity (%) | Protein Added (wt. %) | Max Protein (%) | Carb | Protein in Carb Phase (%) | Carb Added (wt. %) | Total Protein (%) | Screw Type | Screw Speed | ER | EI | Radial ER | Ref |
| WPC | 70.2 | 7.5 | 5.27 | Pearl Millet Flour | 10.50 | 92.50 | 14.98 | TS | 350 | - | 4.34 | - | [82] |
| WPC | 34 | 15 | 5.1 | Corn starch | - | - | 5.1 | - | - | - | | - | [93] |
| WPI | 93.3 | 35 | 32.66 | Corn Meal | 7.2 | 65 | 37.34 | TS | 800 | 4.5-9 | | - | [94] |
| WPI | 93.6 | 25 | 23.4 | Corn Meal | 9.0 | 75 | 30.15 | TS | 300 | - | 4.5 | - | [84] |
| WPI | 92 | 18 | 16.56 | Corn starch | - | - | 16.56 | TS | 300 | - | | - | [81] |

Typical production conditions for expanded products for protein carbohydrate blends use a twin screw extruder operating around 300 RPM. Die sizes are typically limited to 3-3.2 mm in size and typical processing temperatures are between 70-150°C with lower feed zone temperatures of 30°C occurring in some systems (Table **1**). Moisture content, protein type, protein purity and the composition of the carbohydrate phase all affect the mechanical and physical properties of the resulting foams.

When foaming WPI and corn starch blends, an increase in the water content, which acts as a plasticiser and blowing agent, reduced the required specific mechanical energy from 315-359 kJ/kg at 23% moisture content to 274-314 kJ/kg for 27% moisture [81].

At the higher moisture content (27%) expansion ratio and radial expansion ratio was reduced as the melt no longer had the required melt strength to sustain the foamed structure. Increased water content in the blend was observed to reduce cell size from 1.06-2.94 mm at 23% MC to 1.00-2.05 mm at 27% MC. Foam hardness decreased with increasing whey protein up to 12% whey, due to the gelling properties of whey [81].

In another study, addition of soy protein concentrate to starch with high amylose content increased foam mechanical strength. Crushing force measured by a texture analyser increased from 10 N at 0% SPC to 42 N at 20% SPC. Increasing SPC further resulted in a lower crush strength than the control foam, probably due to protein agglomeration due to heat and shear, as well as reducing water available to starch to gelatinise during extrusion [86].

## CONCLUSION

Protein based foams present a new and exciting area for research. They provide a means to reduce dependence on fossil fuels, and decrease the environmental impact of non-biodegradable foams. Proteins can be sourced from a wide variety of plant or animal products or wastes, reducing the impact on food supply.

Foaming is a trade-off between manipulating polymer properties for increasing gas solubility to reduce foam density and increase cell nucleation, diffusivity which needs to be high initially for nucleation and low later on to reduce bubble coalescence and prevent gas loss while the polymer is cooling. Solubility will depend on polymer properties such as crystallinity and gas type and gas pressure, while diffusivity is dependent on polymer viscosity which is dependent on crystallinity, polymer type and chain branching, and melt temperature. Bubble formation is also dependent on melt strength, *i.e.* the ability of the material to contain the bubble, which is dependent on the same properties as for polymer viscosity.

The main challenges to be overcome with protein based foams are:

1. Controlling protein-protein interactions so that they can extruded or batch foamed at temperatures lower than the protein degradation temperature using combination of denaturants, reducing agents and plasticisers to reduce hydrophobic interactions, hydrogen bonding, and cysteine-cysteine bonds, as well as increasing free volume between chains to increase chain mobility. Protein-protein interactions are dictated by the amino-acid sequence of the proteins, the secondary structures that they form, and environment they are in, so a potential area of future research is manipulating protein amino acid sequence to produce plastics with desired properties.
2. Dried denatured proteins are rich in β-sheets, and will form more β-sheets when exposed to heat, which results in a highly crystalline, brittle material with low melt strength and extremely high extensional viscosity which is detrimental to producing foams. Furthermore, protein based thermoplastics need mechanical shear as well as heat to form a melt, which provides a challenge for batch foaming, while for extrusion foaming, mechanical shear is provided by the extruder. Proteins such as zein with a high α-helical content have been successfully used to produce foams and films.
3. Proteins have poor gas solubility and high gas diffusion properties, which results in low foam cell densities and high bulk densities compared to conventional foams. A combination of $CO_2$ and $N_2$ gas as a blowing agent has been successfully used for zein and gelatin in batch foams, while water or chemical blowing agents serve for extruded zein, soy and bloodmeal protein

foams. Blending proteins with starch or other polymeric materials such as PLA is another way of improving gas solubility and diffusion properties.

The main proteins to be successfully foamed are zein, gelatin, soy and bloodmeal. Whey has been used as an additive in food foams where the main material is starch. As research progresses and new proteins tried, we expect to see more successful protein based foams in the future.

## NOTES

[1] Reproduced from J.A.Kiernan 'Formaldehyde, formalin, paraformaldehyde and glutaraldehyde: What they are and what they do', Microscopy Today, v.1: 8-12, Fig. **2**, 2000, copyright Cambridge University Press, with permission.

[2] **A.** Reprinted from The Journal of Supercritical Fluids, 58/1, Y.-M Corre, A. Maazouz, J. Duchet, and J. Reignier, "Batch foaming of chain extended PLA with supercritical $CO_2$: Influence of the rheological properties and the process parameters on the cellular structure,", Page No. 177-188, Copyright (2011), with permission from Elsevier. **B.** Reproduced with permission from the journal International Polymer Processing, IPP, Vol.22, 2007, pp 480-488, by A. Salerno, M. Oliviero, E. Di Maio and S. Iannace, © Carl Hanser Verlag GmbH & Co.KG, Muenchen. **C.** Reproduced with permission M. Oliviero, L. Verdolotti, I. Nedi, F. Docimo, E. Di Maio, and S. Iannace, "Effect of two kinds of lignins, alkaline lignin and sodium lignosulfonate, on the foamability of thermoplastic zein–based bionanocomposites", 48 (6), pp. 516-525, copyright © 2012 by the authors. Reprinted by permission of SAGE Publications, Ltd. **D.** Reproduced with permission, from B. Liu, L. Jian, and J. Zhang, "Extrusion foaming of Poly (lactic acid)/Soy protein concentrate blends", Macromolecular Materials and Engineering, Wiley. Copyright ©2011 WILEY-VCH Verlag GmbH & Co. KGaA, Weinheim. **E.** Reproduced from A. Walallavita, C. J. R. Verbeek, and M. C. Lay, "Blending Novatein Thermoplastic Protein with PLA for carbon dioxide assisted batch foaming," In: Proceedings of PPS-31: The 31st International Conference of the Polymer Processing Society–Conference Papers, Jeju Island, South Korea, 2015., with the permission of AIP Publishing (http://dx.doi.org/10.1063/1.4942311)

[3] **B.** Image reproduced with permission from the authors: P. Mungara, J. W. Zhang, and J. Jane. **C.** Image reproduced from "Development and characterization of extruded biodegradable foams based on zein and pearl millet flour" with permission from the authors. **D.** Reproduced with permission from Wiley, from M. Olivero, L. Sorrentino, L. Cafiero, B. Galzerano, A. Sorrentino, and S.

Iannace, "Foaming behaviour of bio based blends based on thermoplastic gelatin and poly(butylene succinate)", Journal of Applied Polymer Science, Wiley. © Wiley periodicals, Inc. J. Appl. Polym. Sci. 2015, 132, 42704. **E.** Reproduced from C. Gavin, M. C. Lay, and C. J. R. Verbeek, "Extrusion foaming of protein-based thermoplastic and polyethylene blends," In: Proceedings of PPS-31: The 31st International Conference of the Polymer Processing Society–Conference Papers, Jeju Island, South Korea, 2015., with the permission of AIP Publishing (http://dx.doi.org/10.1063/1.4942308)

## CONFLICT OF INTEREST

The author (editor) declares no conflict of interest, financial or otherwise.

## ACKNOWLEDGEMENTS

Declared none.

## REFERENCES

[1] G. Mensitieri, E. Di Maio, G.G. Buonocore, I. Nedi, M. Oliviero, L. Sansone, and S. Iannace, "Processing and shelf life issues of selected food packaging materials and structures from renewable resources", *Trends Food Sci. Technol.*, vol. 22, no. 2–3, pp. 72-80, March 2011. [http://dx.doi.org/10.1016/j.tifs.2010.10.001]

[2] Smithers Rapra, *Polymer Foams Market Expected to Consume 25.3 Million Tonnes by 2019,* 2014. Available at: http://www.smithersrapra.com/news/ 2014/may/polymer-foam-market-to-consume-25-3-million-tonnes Accessed: 2nd Aug. 2015

[3] Freedonia Group Inc, *US Natural Polymer Demand (2002-2012),* 2008. Available at: http://www.plasticsnews.com/article/20081208/FYI/312089989/us-natural-polymer-demand-2002-12 Accessed: 2nd Aug. 2015

[4] MarketsandMarkets.com, *Bioplastics & Biopolymers Market by Type (Bio PET, Bio PE, PLA, PHA, Bio PBS, Starch Blends, and Regenerated Cellulose), by Application (Packaging, Bottles, Fibers, Agriculture, Automotive, and Others) & by Geography – Trends & Forecasts to 2018,* 2014. Available at: http://www.marketsandmarkets.com/Market-Reports/biopolymers-bioplastics-market-88795240.html Accessed: 2nd Aug. 2015

[5] *The Biopolymers Market is Expected to Generate Global Revenue of 3.67 Billion US Dollars By 2018,* 2014. Available at: http://milksci.unizar.es/bioquimica/temas/azucares/disacaridos.html

[6] C. Marrazzo, E. Di Maio, and S. Iannace, "Foaming of synthetic and natural biodegradable polymers", *J. Cell. Plast.*, vol. 43, no. 2, pp. 123-133, 2007. [http://dx.doi.org/10.1177/0021955X06073214]

[7] S.T. Lee, C.B. Park, and N.S. Ramesh, "Introduction to polymeric foams", In: *Polymeric Foams: Science and Technology.* , S.T. Lee, C.B. Park, N.S. Ramesh, Eds., 1st ed CRC Press: Boca Raton, FL, 2007.

[8] S.T. Lee, "History and trends of polymeric foams: From process/product to performance/regulation", In: *Polymeric Foams: Technology and Developments in Regulation, Process and Products.* , S.T. Lee, D. Scholz, Eds., 1st ed CRC Press: Boca Raton, FL, 2009, pp. 1-40.

[9] S. Park, D. Bae, and K. Rhee, "Soy protein biopolymers cross-linked with glutaraldehyde," ", *J. Am. Oil Chem. Soc.*, vol. 77, no. 8, pp. 879-884, 2000. [http://dx.doi.org/10.1007/s11746-000-0140-3]

[10] J.M. Raquez, M. Deléglise, M.F. Lacrampe, and P. Krawczak, "Thermosetting (bio)materials derived from renewable resources: A critical review", *Prog. Polym. Sci.,* vol. 35, no. 4, pp. 487-509, 2010. [http://dx.doi.org/10.1016/j.progpolymsci.2010.01.001]

[11] J.A. Kiernan, "Formaldehyde, formalin, paraformaldehyde and glutaraldehyde: what they are and what they do", *Micros. Today,* vol. 1, no. 5, pp. 8-12, 2000.

[12] C.J. Verbeek, and L.E. van den Berg, "Extrusion processing and properties of protein-based thermoplastics", *Macromol. Mater. Eng.,* vol. 295, no. 1, pp. 10-21, 2010. [http://dx.doi.org/10.1002/mame.200900167]

[13] C.J. Verbeek, and J.M. Bier, "Synthesis and characterization of thermoplastic agro-polymers", In: *A Handbook of Applied Biopolymer Technology: Synthesis, Degradation and Applications.* , S.K. Sharma, A. Mudhoo, Eds., 1st ed Royal Society of Chemistry, 2011. [http://dx.doi.org/10.1039/9781849733458-00197]

[14] J.M. Bier, *"The Eco-Profile of Thermoplastic Protein Derived from Bloodmeal"*, Masters Thesis, University of Waikato, New Zealand, 2010.

[15] J.M. Bier, C.J. Verbeek, and M.C. Lay, "Thermal transitions and structural relaxations in protein-based thermoplastics", *Macromol. Mater. Eng.,* vol. 299, no. 5, pp. 524-539, 2014. [http://dx.doi.org/10.1002/mame.201300248]

[16] J.M. Bier, C.J. Verbeek, and M.C. Lay, "Thermal and mechanical properties of bloodmeal-based thermoplastics plasticized with tri(ethylene glycol)", *Macromol. Mater. Eng.,* vol. 299, no. 1, pp. 85-95, 2013. [http://dx.doi.org/10.1002/mame.201200460]

[17] J.M. Bier, C.J. Verbeek, and M.C. Lay, "Using synchrotron FTIR spectroscopy to determine secondary structure changes and distribution in thermoplastic protein", *J. Appl. Polym. Sci.,* vol. 130, no. 1, pp. 359-369, 2013. [http://dx.doi.org/10.1002/app.39134]

[18] J.M. Bier, C.J. Verbeek, and M.C. Lay, "Thermally resolved synchrotron FT-IR microscopy of structural changes in bloodmeal-based thermoplastics", *J. Therm. Anal. Calorim.,* vol. 115, no. 1, pp. 433-441, 2014. [http://dx.doi.org/10.1007/s10973-013-3340-8]

[19] M. Oliviero, L. Sorrentino, L. Cafiero, B. Galzerano, A. Sorrentino, and S. Iannace, "Foaming behavior of biobased blends based on thermoplastic gelatin and poly(butylene succinate)", *J. Appl. Polym. Sci.,* vol. 132, no. 48, pp. 1-9, 2015. [http://dx.doi.org/10.1002/app.42704] [PMID: 25866416]

[20] A. Salerno, M. Oliviero, E. Di Maio, and S. Iannace, "Thermoplastic foams from zein and gelatin", *Int. Polym. Process.,* vol. 22, no. 5, pp. 480-488, 2007. [http://dx.doi.org/10.3139/217.2065]

[21] J.R. Barone, W.F. Schmidt, and N. Gregoire, "Extrusion of feather keratin", *J. Appl. Polym. Sci.,* vol. 100, no. 2, pp. 1432-1442, 2006. [http://dx.doi.org/10.1002/app.23501]

[22] J.R. Barone, W.F. Schmidt, and C.F. Liebner, "Thermally processed keratin films", *J. Appl. Polym. Sci.,* vol. 97, no. 4, pp. 1644-1651, 2005. [http://dx.doi.org/10.1002/app.21901]

[23] B. Liu, L. Jiang, and J. Zhang, "Extrusion foaming of poly (lactic acid)/soy protein concentrate blends", *Macromol. Mater. Eng.,* vol. 296, no. 9, pp. 835-842, 2011. [http://dx.doi.org/10.1002/mame.201000449]

[24] P. Guerrero, and K. de la Caba, "Thermal and mechanical properties of soy protein films processed at different pH by compression", *J. Food Eng.,* vol. 100, no. 2, pp. 261-269, 2010. [http://dx.doi.org/10.1016/j.jfoodeng.2010.04.008]

[25] J.L. Jane, and S. Wang, Soy protein-based thermoplastic composition for preparing molded articles, 1996.U.S. Patent 5523293

[26] J. Zhang, P. Mungara, and J. Jane, "Mechanical and thermal properties of extruded soy protein sheets", *Polymer (Guildf.),* vol. 42, no. 6, pp. 2569-2578, 2001.
[http://dx.doi.org/10.1016/S0032-3861(00)00624-8]

[27] E. Di Maio, R. Mali, and S. Iannace, "Investigation of thermoplasticity of zein and kafirin proteins: Mixing process and mechanical properties", *J. Polym. Environ.,* vol. 18, no. 4, pp. 626-633, 2010.
[http://dx.doi.org/10.1007/s10924-010-0224-x]

[28] D.J. Sessa, G.W. Selling, J.L. Willett, and D.E. Palmquist, "Viscosity control of zein processing with sodium dodecyl sulfate", *Ind. Crops Prod.,* vol. 23, no. 1, pp. 15-22, 2006.
[http://dx.doi.org/10.1016/j.indcrop.2005.02.001]

[29] L. Verdolotti, M. Oliviero, M. Lavorgna, V. Iozzino, D. Larobina, and S. Iannace, "Bio-hybrid foams by silsesquioxanes cross-linked thermoplastic zein films", *J. Cell. Plast.,* vol. 51, no. 1, pp. 75-87, 2015.
[http://dx.doi.org/10.1177/0021955X14529138]

[30] G. Trujillo-de Santiago, C. Rojas-de Gante, S. García-Lara, L. Verdolotti, E. Di Maio, and S. Iannace, "Thermoplastic processing of blue maize and white sorghum flours to produce bioplastics", *J. Polym. Environ.,* vol. 23, no. 1, pp. 72-82, 2015.
[http://dx.doi.org/10.1007/s10924-014-0708-1]

[31] S.H. Richert, "Physical-chemical properties of whey protein foams", *J. Agric. Food Chem.,* vol. 27, no. 4, pp. 665-668, 1979.
[http://dx.doi.org/10.1021/jf60224a036]

[32] K.G. Marinova, E.S. Basheva, B. Nenova, M. Temelska, A.Y. Mirarefi, B. Campbell, and I.B. Ivanov, "Physico-chemical factors controlling the foamability and foam stability of milk proteins: Sodium caseinate and whey protein concentrates", *Food Hydrocoll.,* vol. 23, no. 7, pp. 1864-1876, 2009.
[http://dx.doi.org/10.1016/j.foodhyd.2009.03.003]

[33] D. Gammariello, J. Laverse, V. Lampignano, A.L. Incoronato, and M.A. Del Nobile, "Effect of compositional formulation on texture and microstructural of whey protein foam", *Food Res. Int.,* vol. 53, no. 1, pp. 496-501, 2013.
[http://dx.doi.org/10.1016/j.foodres.2013.05.023]

[34] J. Leman, T. Dołgań, M. Smoczyński, and Z. Dziuba, "Fractal characteristics of microstructure of beta-lactoglobulin preparations and their emulsifying properties", *Food Sci. Technol. (Campinas.),* vol. 8, no. 3, p. 29, 2005.

[35] H-B. Chen, Y-Z. Wang, and D.A. Schiraldi, "Foam-like materials based on whey protein isolate", *Eur. Polym. J.,* vol. 49, no. 10, pp. 3387-3391, 2013.
[http://dx.doi.org/10.1016/j.eurpolymj.2013.07.019]

[36] N. Kaisangsri, O. Kerdchoechuen, and N. Laohakunjit, "Characterization of cassava starch based foam blended with plant proteins, kraft fiber, and palm oil", *Carbohydr. Polym.,* vol. 110, no. 1, pp. 70-77, 2014.
[http://dx.doi.org/10.1016/j.carbpol.2014.03.067] [PMID: 24906730]

[37] P.R. Salgado, V.C. Schmidt, S.E. Ortiz, A.N. Mauri, and J.B. Laurindo, "Biodegradable foams based on cassava starch, sunflower proteins and cellulose fibers obtained by a baking process", *J. Food Eng.,* vol. 85, no. 3, pp. 435-443, 2008.
[http://dx.doi.org/10.1016/j.jfoodeng.2007.08.005]

[38] X. Li, A. Pizzi, M. Cangemi, P. Navarrete, C. Segovia, V. Fierro, and A. Celzard, "Insulation rigid and elastic foams based on albumin", *Ind. Crops Prod.,* vol. 37, no. 1, pp. 149-154, 2012.
[http://dx.doi.org/10.1016/j.indcrop.2011.11.030]

[39] X. Li, A. Pizzi, M. Cangemi, V. Fierro, and A. Celzard, "Flexible natural tannin-based and protein-

based biosourced foams", *Ind. Crops Prod.,* vol. 37, no. 1, pp. 389-393, 2012. [http://dx.doi.org/10.1016/j.indcrop.2011.12.037]

[40] Y. Lin, and F. Hsieh, "Water-blown flexible polyurethane foam extended with biomass materials", *J. Appl. Polym. Sci.,* vol. 65, no. 4, pp. 695-703, 1997. [http://dx.doi.org/10.1002/(SICI)1097-4628(19970725)65:4<695::AID-APP8>3.0.CO;2-F]

[41] S.K. Park, and N. Hettiarachchy, "Physical and mechanical properties of soy protein-based plastic foams", *J. Am. Oil Chem. Soc.,* vol. 76, no. 10, pp. 1201-1205, 1999. [http://dx.doi.org/10.1007/s11746-999-0094-3]

[42] L.C. Chang, Y. Xue, and F.H. Hsieh, "Comparative study of physical properties of water-blown rigid polyurethane foams extended with commercial soy flours", *J. Appl. Polym. Sci.,* vol. 80, no. 1, pp. 10-19, 2001. [http://dx.doi.org/10.1002/1097-4628(20010404)80:1<10::AID-APP1068>3.0.CO;2-Y]

[43] Y. Mu, X. Wan, Z. Han, Y. Peng, and S. Zhong, "Rigid polyurethane foams based on activated soybean meal", *J. Appl. Polym. Sci.,* vol. 124, no. 5, pp. 4331-4338, 2012. [http://dx.doi.org/10.1002/app.35612]

[44] S. Kumar, E. Hablot, J.L. Moscoso, W. Obeid, P.G. Hatcher, B.M. DuQuette, D. Graiver, R. Narayan, and V. Balan, "Polyurethanes preparation using proteins obtained from microalgae," ", *J. Mater. Sci.,* vol. 49, no. 22, pp. 7824-7833, 2014. [http://dx.doi.org/10.1007/s10853-014-8493-8]

[45] Y-Q. Zhang, "Applications of natural silk protein sericin in biomaterials", *Biotechnol. Adv.,* vol. 20, no. 2, pp. 91-100, 2002. [http://dx.doi.org/10.1016/S0734-9750(02)00003-4] [PMID: 14538058]

[46] R. Elshereef, J. Vlachopoulos, and A. Elkamel, "Comparison and analysis of bubble growth and foam formation models", *Eng. Comput.,* vol. 27, no. 3, pp. 387-408, 2010. [http://dx.doi.org/10.1108/02644401011029943]

[47] N.S. Ramesh, "Fundamentals of bubble nucleation and growth in polymers", In: *Polymeric Materials: Mechanisms and Materials.* , S.T. Lee, N.S. Ramesh, Eds., 1st ed CRC Press Boca Raton: FL, 2004. [http://dx.doi.org/10.1201/9780203506141.ch3]

[48] J. Wang, *"Rheology of Foaming Polymers and its influence on Microcellular Processing"*, PhD Thesis, University of Toronto, Canada, 2009.

[49] V. Kumar, *"Process Synthesis for Manufacturing Microcellular Thermoplastic Parts: A Case Study in Axiomatic Design"*, PhD Thesis, Massachusetts Institute of Technology, US, 1988.

[50] D.R. Uhlmann, and B. Chalmers, "The energetic of nucleation", *Ind. Eng. Chem. Res.,* vol. 57, no. 9, pp. 19-31, 1965. [http://dx.doi.org/10.1021/ie50669a006]

[51] S.T. Lee, C.B. Park, and N.S. Ramesh, "Foaming fundamentals", In: *Polymeric Foams: Science and Technology.* 1st ed CRC Press: Boca Raton, FL, 2007.

[52] N.G. McCrum, C. Buckley, and C.B. Bucknall, *Principles of Polymer Engineering.* Oxford University Press, 1997.

[53] M. Oliviero, E. Di Maio, and S. Iannace, "Effect of molecular structure on film blowing ability of thermoplastic zein," ", *J. Appl. Polym. Sci.,* vol. 115, no. 1, pp. 277-287, 2010. [http://dx.doi.org/10.1002/app.31116]

[54] A.V. Nawaby, and Z. Zhang, "Solubility and diffusivity", In: *Thermoplastic Foam Processing: Principles and Development.* , S.T. Lee, Ed., 1st ed CRC Press: Boca Raton, 2004.

[55] C. Gao, J. Taylor, N. Wellner, Y.B. Byaruhanga, M.L. Parker, E.N. Mills, and P.S. Belton, "Effect of preparation conditions on protein secondary structure and biofilm formation of kafirin", *J. Agric. Food Chem.,* vol. 53, no. 2, pp. 306-312, 2005.

[http://dx.doi.org/10.1021/jf0492666] [PMID: 15656666]

[56] R. Liao, W. Yu, and C. Zhou, "Rheological control in foaming polymeric materials: I. Amorphous polymers", *Polymer (Guildf.),* vol. 51, no. 2, pp. 568-580, 2010.
[http://dx.doi.org/10.1016/j.polymer.2009.11.063]

[57] R. Gendron, "Rheological behavior relevant to extrusion foaming", In: *Thermoplastic Foam Processing: Principles and Development.* , S.T. Lee, Ed., 1st ed CRC Press: Boca Raton, 2005.

[58] G. Nam, J. Yoo, and J. Lee, "Effect of long-chain branches of polypropylene on rheological properties and foam-extrusion performances", *J. Appl. Polym. Sci.,* vol. 96, no. 5, pp. 1793-1800, 2005.
[http://dx.doi.org/10.1002/app.21619]

[59] H. Münstedt, and F.R. Schwarzl, *Deformation and Flow of Polymeric Materials.* Springer: Berlin, 2014. [Germany]

[60] D.F. Baldwin, C.B. Park, and N.P. Suh, "A microcellular processing study of poly(ethylene terephthalate) in the amorphous and semicrystalline states. Part I: Microcellular nucleation", *Polym. Eng. Sci.,* vol. 36, no. 11, pp. 1437-1445, 1996.
[http://dx.doi.org/10.1002/pen.10538]

[61] J-B. Bao, T. Liu, L. Zhao, and G-H. Hu, "A two-step depressurization batch process for the formation of bi-modal cell structure polystyrene foams using $scCO_2$", *J. Supercrit. Fluids,* vol. 55, no. 3, pp. 1104-1114, 2011.
[http://dx.doi.org/10.1016/j.supflu.2010.09.032]

[62] Y-M. Corre, A. Maazouz, J. Duchet, and J. Reignier, "Batch foaming of chain extended PLA with supercritical $CO_2$: Influence of the rheological properties and the process parameters on the cellular structure", *J. Supercrit. Fluids,* vol. 58, no. 1, pp. 177-188, 2011.
[http://dx.doi.org/10.1016/j.supflu.2011.03.006]

[63] M. Oliviero, L. Verdolotti, I. Nedi, F. Docimo, E. Di Maio, and S. Iannace, "Effect of two kinds of lignins, alkaline lignin and sodium lignosulfonate, on the foamability of thermoplastic zein-based bionanocomposites", *J. Cell Plast.,* vol. 48, no. 6, pp. 516-525, 2012.
[http://dx.doi.org/10.1177/0021955X12460043]

[64] A. Walallavita, C.J. Verbeek, and M.C. Lay, "Blending novatein thermoplastic protein with pla for carbon dioxide assisted batch foaming", *Proceedings of PPS-31: The 31st International Conference of the Polymer Processing Society–Conference Papers,* 2015 Jeju Island, South Korea

[65] S. Doroudiani, C.B. Park, and M.T. Kortschot, "Effect of the crystallinity and morphology on the microcellular foam structure of semicrystalline polymers", *Polym. Eng. Sci.,* vol. 36, no. 21, pp. 2645-2662, 1996.
[http://dx.doi.org/10.1002/pen.10664]

[66] S.H. Mahmood, M. Keshtkar, and C.B. Park, "Determination of carbon dioxide solubility in polylactide acid with accurate PVT properties", *J. Chem. Thermodyn.,* vol. 70, pp. 13-23, 2014.
[http://dx.doi.org/10.1016/j.jct.2013.10.019]

[67] E. Aionicesei, M. Škerget, and Ž. Knez, "Measurement of $CO_2$ solubility and diffusivity in poly(l-lactide) and poly(d,l-lactide-co-glycolide) by magnetic suspension balance", *J. Supercrit. Fluids,* vol. 47, no. 2, pp. 296-301, 2008.
[http://dx.doi.org/10.1016/j.supflu.2008.07.011]

[68] Y-K. Kwon, and H-K. Bae, "Production of microcellular foam plastics by supercritical carbon dioxide", *Korean J. Chem. Eng.,* vol. 24, no. 1, pp. 127-132, 2007.
[http://dx.doi.org/10.1007/s11814-007-5022-3]

[69] C. Yu, Y. Wang, B. Wu, and W. Li, "A direct method for evaluating polymer foamability", *Polym. Test.,* vol. 30, pp. 118-123, 2011.
[http://dx.doi.org/10.1016/j.polymertesting.2010.11.001]

[70] R. Liao, W. Yu, and C. Zhou, "Rheological control in foaming polymeric materials: II. Semi-

crystalline polymers", *Polymer (Guildf.),* vol. 51, pp. 6334-6345, 2010. [http://dx.doi.org/10.1016/j.polymer.2010.11.001]

[71] D. Scholz, "Development of endothermic chemical foaming/nucleation agents and it processes", In: *Polymeric Foams: Technology and Developments in Regulation, Process, and Products.* , S.T. Lee, D. Scholz, Eds., 1st ed CRC Press USA, 2009, pp. 42-65.

[72] W. Ernst, J.r. Oblotzki, and H. Potente, "Description of the foaming process during the extrusion of foams based on renewable resources", *J. Cell. Plast.,* vol. 42, no. 3, pp. 241-253, 2006. [http://dx.doi.org/10.1177/0021955X06063513]

[73] P. Mungara, J.W. Zhang, and J. Jane, "Extrusion processing of soy protein-based foam", *Polymer Prepr.,* vol. 39, no. 2, pp. 148-149, 1998.

[74] M. Filli, M. Sjoqvist, C. Ohgren, M. Stading, and M. Rigdahl, "Development and characterization of extruded biodegradable foams based on zein and pearl millet flour", *Annu. Trans. NRS,* vol. 19, 2011.

[75] C. Gavin, M.C. Lay, and C.J. Verbeek, "Extrusion foaming of protein-based thermoplastic and polyethylene blends", *Proceedings of PPS-31: The 31st International Conference of the Polymer Processing Society–Conference Papers,* 2015 Jeju Island, South Korea

[76] S.T. Lee, and C.B. Park, *Foam Extrusion: Principles and Practice.* 2nd ed Taylor & Francis: Boca Raton, 2014. [http://dx.doi.org/10.1201/b16784]

[77] S.T. Lee, C.B. Park, and N.S. Ramesh, "General foam process technologies", In: *Polymeric Foams: Science and Technology.* , S.T. Lee, C.B. Park, N.S. Ramesh, Eds., 1st ed CRC Press: Boca Raton, FL, 2007.

[78] C.H. Lee, K-J. Lee, H.G. Jeong, and S.W. Kim, "Growth of gas bubbles in the foam extrusion process", *Adv. Polym. Technol.,* vol. 19, no. 2, pp. 97-112, 2000. [http://dx.doi.org/10.1002/(SICI)1098-2329(200022)19:2<97::AID-ADV3>3.0.CO;2-B]

[79] S. Lee, L. Kareko, and J. Jun, "Study of thermoplastic PLA foam extrusion", *J. Cell. Plast.,* vol. 44, no. 4, pp. 293-305, 2008. [http://dx.doi.org/10.1177/0021955X08088859]

[80] H.A. Pushpadass, G.S. Babu, R.W. Weber, and M.A. Hanna, "Extrusion of starch-based loose-fill packaging foams: effects of temperature, moisture and talc on physical properties", *Packag. Technol. Sci.,* vol. 21, no. 3, pp. 171-183, 2008. [http://dx.doi.org/10.1002/pts.809]

[81] E. Cheng, S. Alavi, T. Pearson, and R. Agbisit, "Mechanical–acoustic and sensory evaluations of cornstarch–whey protein isolate extrudates", *J. Texture Stud.,* vol. 38, no. 4, pp. 473-498, 2007. [http://dx.doi.org/10.1111/j.1745-4603.2007.00109.x]

[82] D.N. Yadav, T. Anand, Navnidhi, and A.K. Singh, "Co-extrusion of pearl millet-whey protein concentrate for expanded snacks", *Int. J. Food Sci. Technol.,* vol. 49, no. 3, pp. 840-846, 2014. [http://dx.doi.org/10.1111/ijfs.12373]

[83] M. Włodarczyk-Stasiak, and J. Jamroz, "Analysis of sorption properties of starch–protein extrudates with the use of water vapour", *J. Food Eng.,* vol. 85, no. 4, pp. 580-589, 2008. [http://dx.doi.org/10.1016/j.jfoodeng.2007.08.019]

[84] C. Onwulata, R. Konstance, P. Smith, and V. Holsinger, "Co-extrusion of dietary fiber and milk proteins in expanded corn products", *LWT-Food Sci. Technol. (Campinas.),* vol. 34, no. 7, pp. 424-429, 2001.

[85] L.A. Pelembe, C. Erasmus, and J.R. Taylor, "Development of a protein-rich composite sorghum–cowpea instant porridge by extrusion cooking process", *LWT - Food Sci. Technol. (Campinas.),* vol. 35, no. 2, pp. 120-127, 2002.

[86] L-J. Zhu, R. Shukri, N.J. de Mesa-Stonestreet, S. Alavi, H. Dogan, and Y-C. Shi, "Mechanical and

microstructural properties of soy protein–high amylose corn starch extrudates in relation to physiochemical changes of starch during extrusion", *J. Food Eng.,* vol. 100, no. 2, pp. 232-238, 2010. [http://dx.doi.org/10.1016/j.jfoodeng.2010.04.004]

[87] J. Faller, B. Klein, and J. Faller, "Acceptability of extruded corn snacks as affected by inclusion of soy protein", *J. Food Sci.,* vol. 64, no. 1, pp. 185-188, 1999. [http://dx.doi.org/10.1111/j.1365-2621.1999.tb09888.x]

[88] R.P. Konstance, C.I. Onwulata, P.W. Smith, D. Lu, M.H. Tunick, E.D. Strange, and V.H. Holsinger, "Nutrient-based corn and soy products by twin-screw extrusion", *J. Food Sci.,* vol. 63, no. 5, pp. 864-868, 1998. [http://dx.doi.org/10.1111/j.1365-2621.1998.tb17915.x]

[89] C.I. Onwulata, P.W. Smith, R.P. Konstance, and V.H. Holsinger, "Incorporation of whey products in extruded corn, potato or rice snacks", *Food Res. Int.,* vol. 34, no. 8, pp. 679-687, 2001. [http://dx.doi.org/10.1016/S0963-9969(01)00088-6]

[90] K.E. Allen, C.E. Carpenter, and M.K. Walsh, "Influence of protein level and starch type on an extrusion-expanded whey product", *Int. J. Food Sci. Technol.,* vol. 42, no. 8, pp. 953-960, 2007. [http://dx.doi.org/10.1111/j.1365-2621.2006.01316.x]

[91] F.P. Matthey, and M.A. Hanna, "Physical and functional properties of twin-screw extruded whey protein concentrate–corn starch blends", *LWT - Food Sci. Technol. (Campinas.),* vol. 30, no. 4, pp. 359-366, 1997.

[92] C.I. Onwulata, and R.P. Konstance, "Extruded corn meal and whey protein concentrate: Effect of particle size", *J. Food Process. Preserv.,* vol. 30, no. 4, pp. 475-487, 2006. [http://dx.doi.org/10.1111/j.1745-4549.2005.00082.x]

[93] A.M. Trater, S. Alavi, and S.S. Rizvi, "Use of non-invasive X-ray microtomography for characterizing microstructure of extruded biopolymer foams", *Food Res. Int.,* vol. 38, no. 6, pp. 709-719, 2005. [http://dx.doi.org/10.1016/j.foodres.2005.01.006]

[94] C.I. Onwulata, R.P. Konstance, J.G. Phillips, and P.M. Tomasula, "Temperature profiling: Solution to problems of co-extrusion with whey proteins", *J. Food Process. Preserv.,* vol. 27, no. 5, pp. 337-350, 2003. [http://dx.doi.org/10.1111/j.1745-4549.2003.tb00521.x]

# Blending Novatein Thermoplastic Protein with PLA for Carbon Dioxide Assisted Batch Foaming

A full conference paper

By

A. S. Walallavita[1], C. J. R. Verbeek, & M. C. Lay

Published in

***AIP Conference Proceedings***

[1]As first author, I prepared the initial draft manuscript, which was refined and edited in consultation with my supervisors, who have been credited as co-authors.

# Blending Novatein® Thermoplastic Protein with PLA for Carbon Dioxide Assisted Batch Foaming

Anuradha Walallavita, Casparus J.R. Verbeek, Mark Lay

*University of Waikato, Hamilton 3240, New Zealand*

*asw15@students.waikato.ac.nz, jverbeek@waikato.ac.nz, mclay@waikato.ac.nz*

**Abstract.** The convenience of polymeric foams has led to their widespread utilisation in everyday life. However, disposal of synthetic petroleum-derived foams has had a detrimental effect on the environment which needs to be addressed. This study uses a clean and sustainable approach to investigate the foaming capability of a blend of two biodegradable polymers, polylactic acid (PLA) and Novatein® Thermoplastic Protein (NTP). PLA, derived from corn starch, can successfully be foamed using a batch technique developed by the Biopolymer Network Ltd. NTP is a patented formulation of bloodmeal and chemical additives which can be extruded and injection moulded similar to other thermoplastics. However, foaming NTP is a new area of study and its interaction with blowing agents in the batch process is entirely unknown. Subcritical and supercritical carbon dioxide have been examined individually in two uniquely designed pressure vessels to foam various compositions of NTP-PLA blends. Foamed material were characterised in terms of expansion ratio, cell size, and cellular morphology in order to study how the composition of NTP-PLA affects foaming with carbon dioxide. It was found that blends with 5 wt. % NTP foamed using subcritical $CO_2$ expanded up to 11 times due to heterogeneous nucleation. Morphology analysis using scanning electron microscopy showed that foams blown with supercritical $CO_2$ had a finer cell structure with consistent cell size, whereas, foams blown with subcritical $CO_2$ ranged in cell size and showed cell wall rupture. Ultimately, this research would contribute to the production of a biodegradable foam material to be used in packaging applications, thereby adding to the application potential of NTP.

**Keywords:** Novatein® Thermoplastic Protein, biodegradable polymers, blends, polylactic acid, carbon dioxide
**PACS:** 81.05.Rm, 61.25.hk

## INTRODUCTION

The polymer industry has grown to incorporate polymeric foams, which is presently influencing almost every aspect of daily life. Foams possess beneficial characteristics such as low density and good sound absorption properties. They are used extensively in protective packaging, seat cushioning, and thermal insulation. However, the synthetic polymer industry is under environmental scrutiny because of their limited resistance to degradation and consumption of fossil fuels – which will eventually be depleted. These issues can be addressed by replacing synthetic foams (i.e. polystyrene, polypropylene and polyvinylchloride) with bio-based alternatives.

Bloodmeal, a highly denatured protein, is a readily available by-product of the meat processing industry. Bloodmeal and water alone is incapable of forming an extrudable melt and therefore, require additives such as sodium sulfite (SS), sodium dodecyl sulfite (SDS), urea, and triethylene glycol (TEG) as plasticizer. The combination of these additives allows bloodmeal to be extruded and injection moulded into various commercial products, including plant pots, weasand clips, and weed mat clips. This formulation is patented by Aduro Biopolymers and is known as Novatein® Thermoplastic Protein (NTP) [1].

Polylactic acid (PLA) is a linear aliphatic polyester prepared by either catalytic ring opening polymerization of lactide, or condensation polymerization of the free acid. PLA has valuable physical properties such as processability, thermoplasticity, and high strength. Further benefits include biodegradability, biocompatibility, and low production cost ($1-2/kg) [2, 3]. Furthermore, PLA can be foamed using a batch process with carbon dioxide ($CO_2$) as a "green" blowing agent [4].

$CO_2$, as an environmentally friendly blowing agent, is a popular choice for foam applications. $CO_2$ has desirably low critical temperature (31.1 °C) and pressure (74 Bar), in combination with its high solubility in polylactic acid and plasticizing ability, foaming with supercritical $CO_2$ can be performed at relatively low temperatures [5, 6]. $CO_2$

is relatively benign compared to other organic solvents, and residual $CO_2$ in the cellular structure does not harm its intended application.

The aim of this research was to improve the batch foaming capability of NTP by blending with PLA. $CO_2$ in the subcritical and supercritical state was investigated as the physical blowing agent. Resultant foams were analysed in terms of foam density, cell size, and morphology. This is done as an initial investigation towards producing a biodegradable foam material with desirable characteristics, which can improve market penetration for NTP.

## MATERIALS AND METHODS

### Preparation of Novatein Thermoplastic Protein (NTP)

Bloodmeal was supplied by Wallace Corporation, New Zealand, and is mainly bovine with some chicken blood. Bloodmeal was sieved to an average particle size of 700 μm before mixing with additives. Analytical grade SS and technical grade SDS were purchased from BDH Lab Supplies and Biolab NZ, respectively. Triethylene glycol (TEG) was used as plasticizer and was obtained from Merck. NTP samples were prepared by dissolving the required additives in distilled water on a hot plate until the temperature reached 50-60 ºC. This solution was added to bloodmeal powder and mixed in a high speed mixer for 5 min. Plasticizer was added to the mixture and blended for a further 3 to 4 minutes. The mixture was stored in sealed bags for at least 24 hours at <4 ºC prior to extrusion.

### Preparation of NTP-PLA Blends via Extrusion

A fully amorphous grade of PLA (Ingeo™ 4060D) was obtained from NatureWorks LLC. NTP-PLA blends at 6 different compositions were compounded using a LabTech Twin Screw extruder with L/D ratio of 44:1. Screws were co-rotating and were maintained at a constant rotation speed of 150 rpm for all experiments. Prior to extrusion, PLA pellets were dried in an oven at 45 ºC for 4 hours to a moisture content of 250 ppm. This was deemed essential by the suppliers in order to minimize hydrolysis during melt processing.

The extruder temperature profiles were chosen such that as the NTP composition increased in the blend, the extruder temperature profile decreased. The formulation of NTP used degrades at temperatures above 180 ºC, hindering melt strength. Neat PLA was extruded at a maximum temperature of 200 ºC in the compression section of the extruder, whereas blends with 60 % NTP had a compression section temperature of 130 ºC. The extrudates were cooled in cold water immediately after exiting the die. Extruded strands had a diameter of approximately 3 mm, and were cut to a length of 120 mm. The extruded blends were stored at 23 ± 2 ºC and 50 ± 10 % relative humidity for at least 24 hours prior to foaming. All samples, including neat PLA, were prepared in the same way using extrusion for comparability reasons.

### Foaming

Commercial purity (>99%) $CO_2$ obtained from BOC New Zealand, was used in the subcritical and supercritical state, therefore, two different experimental apparatuses were constructed on site for research purposes.

Subcritical $CO_2$ impregnation was carried out in a 2 L pressure vessel at a pressure of 60 bar. The processing parameters were chosen based on a processing window determined from previous studies on PLA foams blown with $CO_2$ [4]. After the saturation time had been reached, the vessel was depressurized rapidly. Samples were removed and quickly weighed to monitor $CO_2$ sorption between different NTP-PLA compositions. Immediately following this, samples were submerged for 15 s in a hot water bath at 70 ºC. The polymer was held at temperatures above its $T_g$ which causes the polymer to soften and leads to cell nucleation and growth within the polymer matrix. The final step involved quenching the foams in cold water to prevent further changes and freeze the cell morphology. Quenched samples were carefully dried to remove moisture in order to prevent premature hydrolytic degradation.

Supercritical $CO_2$ impregnation was carried out in a 100 mL stainless steel pressure vessel at a pressure of 200 bar. This pressure was obtained using a Dionex SFE-703 supercritical fluid pumping unit. The vessel containing the samples was heated to a temperature of 50 ºC using an autoclave, a thermocouple was connected to the inside of the pressure vessel in order to monitor temperature accurately throughout the process. After the saturation time had been reached, pressure was reduced to atmospheric causing the system to reach a supersaturated state. Foaming occurred via nucleation and growth of pores inside the polymeric matrix. Samples were removed from the vessel and subsequently submerged in a hot water bath at 70 ºC to check for any further expansion.

## Characterization

The resulting foams produced using subcritical and supercritical $CO_2$ were characterized by measuring foam density following ASTM Standard D1622. Specimens were conditioned at 23 ± 2 °C and 50 ± 10 % relative humidity prior to testing. The expansion ratio was calculated using Equation 1 and the values reported were the average of at least 3 samples.

$$Expansion\ Ratio = \frac{Density\ of\ unfoamed\ sample}{Density\ of\ foamed\ sample} \quad (1)$$

The cellular structures of the foams were characterized using images obtained from a Hitachi S-4700 scanning electron microscope (SEM). Samples were frozen in liquid nitrogen and sliced with a blade in order to maintain a clean cross-section of the cellular structure. Specimens were coated with platinum in a Hitachi E-1030 Ion Sputter before viewing under the SEM at 3 kV. A low accelerating voltage was chosen in order to minimize charging effects. Micrographs were subsequently analyzed using Image J software to determine the average cell diameter at each foaming condition.

## RESULTS AND DISCUSSION

The effect of NTP-PLA composition on $CO_2$ sorption at the subcritical $CO_2$ conditions are presented in Figure 1(a). $CO_2$ sorption at supercritical conditions was not measured since foams were produced before removal from the vessel. Samples containing 5 – 20 wt. % NTP had a $CO_2$ uptake of ~20 wt. % which decreased as the NTP content in the blend increased. $CO_2$ sorption affected the degree of foaming and less expansion was observed as the $CO_2$ content in the polymer blend decreased, Figure 1(b).

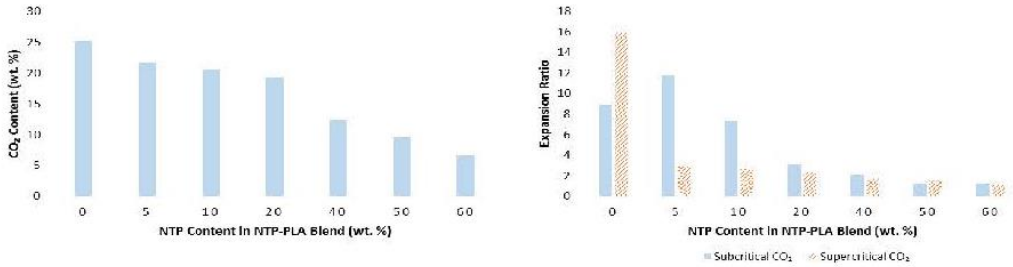


**FIGURE 1.** Effect of NTP-PLA composition on (a) $CO_2$ content using subcritical $CO_2$ and (b) expansion ratio.

Interestingly, in this study it was found that a greater expansion ratio was observed in foams containing 5 wt. % NTP when subcritical $CO_2$ was used, and the expansion ratio of 10 wt. % NTP was only slightly below the neat PLA control. This phenomenon can be explained using classical nucleation theory, which states that the interfaces in multi-phase systems serve as heterogeneous nucleation sites, lowering the surface free energy [7-9]. For an immiscible blend system, the activation energy barrier for bubble nucleation is reduced upon addition of a second-phase component because of the large amount of interfacial volume in blends. Furthermore, $CO_2$ concentration at the phase interface is higher than that in the polymer matrix due to the low energy barrier. A study carried out by Liao et al. [7] applied the same theory when they foamed PLA-polystyrene (PS) blends with supercritical $CO_2$. Compared to PS bulk, the PLA-PS interface had a lower activation energy barrier and higher $CO_2$ concentration which resulted in bubble nucleation preferentially occurring at the interface upon depressurizing.

When supercritical $CO_2$ was used to foam NTP-PLA blends, the expansion ratio did not rise above 3 times expansion and decreased in small increments as the NTP content in the blend increased. Specimens expanded inside the vessel when pressure was reduced to atmospheric, and no further expansion was seen when NTP-PLA were submerged in a hot water bath at 70 °C.

Foam morphologies of all samples were analyzed using SEM and average cell sizes are presented in Table 1. In this work it was found that most blends had a large variance between cell sizes, especially the blends foamed with subcritical $CO_2$. Whereas foams blown with supercritical $CO_2$ at 0, 5, and 10 % NTP showed a consistent cell size throughout the sample (Figure 2(a)). Cell sizes of foams with NTP content of 40 % and above were not measured

due to inconsistent cellular morphology and unfoamed regions (Figure 2(b)). Although the ratio of PLA to NTP did not have a strong influence on cell size, however, using either subcritical or supercritical $CO_2$ had a distinct effect on size. Foams produced with subcritical $CO_2$ showed inconsistent cell size (Figure 2(c)), and cell walls seemed to have burst during the foam growth process (Figure 2(d)). This may be due to rapid expansion during the temperature soak method used for subcritical $CO_2$ foaming in comparison to the pressure drop method used for supercritical $CO_2$. When samples impregnated with subcritical $CO_2$ were submerged in a hot water bath at 70 ºC, a loud popping noise could be heard as the blowing agent rapidly escaped from the material, rupturing cell walls.

**TABLE (1).** Cell sizes (μm) at different NTP-PLA ratios.

| | Cell Size (μm) | |
|---|---|---|
| **Ratio of NTP : PLA in blend** | **Subcritical $CO_2$** | **Supercritical $CO_2$** |
| 0:100 (Neat PLA) | 52 – 430 | 248 |
| 5:95 | 39 – 239 | 27 |
| 10:90 | 160 – 361 | 40 |
| 20:80 | 141 – 465 | 16 – 328 |

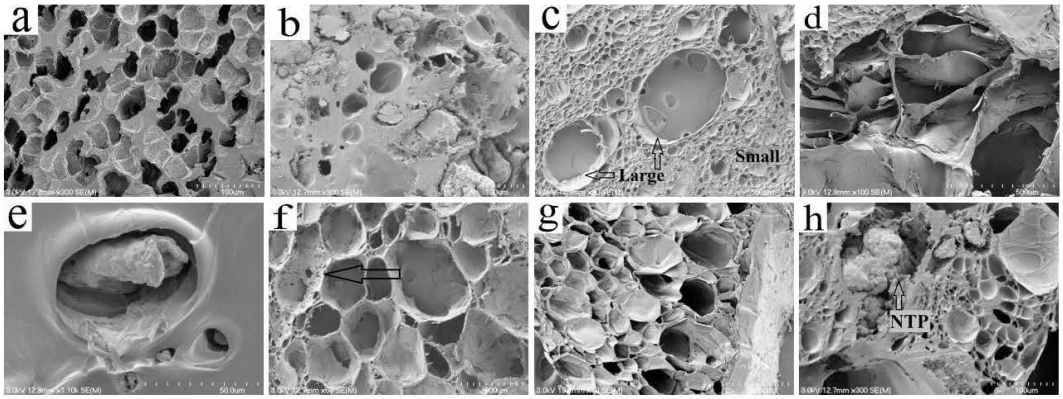


**FIGURE 2.** (a) 10 % NTP, supercritical $CO_2$ x300 (b) 60 % NTP, subcritical $CO_2$ x300 (c) Neat PLA, subcritical $CO_2$ x60 (d) 5 % NTP, subcritical $CO_2$ x100 (e) 5 % NTP, subcritical $CO_2$ x1.1k (f) Pore coalescence observed in neat PLA, subcritical $CO_2$ x60 (g) Neat PLA, supercritical $CO_2$ x60 (h) 40 % NTP, subcritical $CO_2$ x300.

Figure 2(e) is a classic example of heterogeneous nucleation. The foam was blown with subcritical $CO_2$ and had a NTP content of 5 %. Phase interfaces in multi-phase systems impact gas diffusivity, bubble nucleation and growth, as well as the final foam morphology [10-12]. According to classical nucleation theory, the interfaces of a multi-phase system has a lower activation energy than that in the polymer matrix. As a result, bubble nucleation initiates preferentially at sites with a lower energy barrier (heterogeneous system) while occurring synchronously in a homogeneous system [7]. Foam morphology is also affected by phase size and structure in the blend.

There was an obvious phenomenon of pore coalescence occurring in most of the blends, including neat PLA (arrow in Figure 2(f)). Pore coalescence occurs due to an uneven energy distribution in the system during pore growth. Smaller pores merge into larger pores to decrease the total surface area of the gas bubble, which in turn decreases the surface energy. Pore coalescence is a natural tendency during pore growth in order for the system to obtain a low energy state, and also explains the difference in cell sizes presented in Table 1.

Figure 2(g) shows the formation of a non-porous skin on neat PLA foamed at supercritical $CO_2$ conditions. This is commonly known for occurring in single-phase systems and is a result of gas molecules near the surface diffusing out of the sample faster than they can join nuclei [8]. It was found that NTP-PLA behaves as a typical immiscible system, with three primary phase morphologies which include the co-continuous phase, the continuous phase of NTP and continuous phase of PLA. This is especially evident at higher compositions of NTP; Figure 2(h) shows a grain of NTP embedded in a foamed PLA domain. Liao et al. [7] reached similar conclusions with their foam blends of PLA-PS blown with supercritical $CO_2$. They found that at a certain experimental condition, $CO_2$ induced crystallization caused the semi-crystalline PLA to exhibit a non-porous structure, while microcellular foam morphologies were generated in the PS domain.

## CONCLUSIONS AND RECOMMENDATIONS

For the first time, the batch foaming capability of NTP was assessed by blending with PLA and foamed using subcritical and supercritical carbon dioxide in two separate experimental set-ups. It was found that expansion ratio decreased as the composition of NTP in the blend increased. However, the presence of small amounts of NTP foamed at subcritical conditions allowed for heterogeneous nucleation to occur, expanding foams with 5 and 10 % NTP composition up to 11 times. Smaller expansion was seen when blends were foamed with supercritical $CO_2$, although SEM analysis showed a finer cellular structure with consistent cell size. Whereas, SEM micrographs of blends blown with subcritical $CO_2$ had ruptured cell walls and ranged in cell size.

The authors would like to convey recommendations for future studies. It is recommended that a compatibilizer be used for blending NTP and PLA in order to improve miscibility. Research has been undertaken on grafting itaconic anhydride onto PLA using reactive extrusion with dicumyl peroxide as the initiator. The results were successful although the research is yet to be published. Secondly, differential scanning calorimetry (DSC) should be carried out on NTP-PLA blends in order to determine degree of crystallinity, glass transition and melting temperature. Lastly, an optimum foaming window can be established by changing foaming conditions (temperature, pressure and time) and analyzing the resulting impact on foam density and cellular morphology.

## ACKNOWLEDGMENTS

The authors would like to thank Aduro Biopolymers for supplying Novatein® Thermoplastic Protein for foaming experiments. Thank you to the Biopolymer Network Ltd. team at Scion, Rotorua, for allowing experiments to be conducted onsite and sharing expertise on foaming PLA with $CO_2$. Thank you to the University of Waikato laboratory technicians and research supervisors, without whom this research would not have been possible. Thank you to the New Zealand Ministry of Business, Innovation and Employment for research funding (BPLY1302 contract).

## REFERENCES

1. K. L. Pickering, C. J. R. Verbeek, C. Viljoen and L. E. Van Den Berg, U.S. Patent No. 0234,515 (16 September 2010).
2. W. Zhang, B. Chen, H. Zhao, P. Yu, D. Fu, J. Wen and X. Peng, *Appl. Polym. Sci.,* **130**, 3066-3073 (2013).
3. E. Richards, R. Rizvi, A. Chow and H. Naguib, *Polym Environ.* **16**, 258-266 (2008).
4. M. R. J. Witt and S. Shah, U.S. Patent No. 8,283,389 (9 October 2012).
5. A. Salerno and C. D. Pascual, *RSC Adv.,* **3**, 17355-17363 (2013).
6. E. Aionicesei, M. Škerget and Ž. Knez, *J. Supercrit. Fluids*, **47**, 296-301 (2008).
7. X. Liao, H. Zhang, Y. Wang, L. Wu and G. Li, *RSC Adv.*, **4**, 45109-45117 (2014).
8. S. K. Goel and E. J. Beckman, *Polym. Eng. Sci.,* **34**, 1148-1156 (1994).
9. J. S. Colton and N. P. Suh, *Polym. Eng. Sci.,* **27**, 485-492 (1987).
10. H. Ruckdäschel, P. Gutmann, V. Altstädt, H. Schmalz and A. H. E. Müller, *Adv. Polym. Sci.*, **227**, 199 (2010).
11. W. Zhai, H. Wang, J. Yu, J. Dong and J. He, *J. Polym. Sci., Part B: Polym. Phys.*, **46**, 1641-1651 (2008).
12. X. Han, J. Shen, H. Huang, D. L. Tomasko and L. J. Lee, *Polym. Eng. Sci.,* **47**, 103-111 (2007).

# Properties of Blends between Poly(lactic acid) and Novatein Thermoplastic Protein

Extended Abstract

By

A.S. Walallavita*, C.J.R. Verbeek, M.C. Lay

Poster Presentation

***Bioprocessing Network Conference***

**Properties of Blends between Poly(lactic acid) and Novatein Thermoplastic Protein**

Anuradha Walallavita*, Casparus J.R. Verbeek, Mark C. Lay

*School of Engineering, Faculty of Science and Engineering,*
*University of Waikato, Hamilton 3240, New Zealand.*

*asw15@students.waikato.ac.nz*, jverbeek@waikato.ac.nz, mclay@waikato.ac.nz*

Novatein® (NTP) is a protein-based thermoplastic that can be extruded and injection moulded, however it has low tensile strength. Poly(lactic acid) (PLA) is a sustainably derived and industrially compostable polymer which could be blended into NTP to improve this limitation. In this study reactive extrusion was used to produce a blend of NTP and PLA for new applications where cheap and degradable materials are required. Various compositions of NTP/PLA were prepared with and without a compatibilizer, PLA grafted with itaconic anhydride (PLA-g-IA). Results showed that the addition of 50 wt. % PLA increased the tensile strength of neat NTP by 66 %, while the addition of compatibilizer had a 58 % higher tensile strength than the blend without compatibilizer. Scanning electron microscopy revealed that the addition of compatibilizer reduced the presence of cracks and voids in fracture surfaces, resulting in a more homogenous microstructure. Differential scanning calorimetry and X-ray diffraction scans showed that the PLA was fully amorphous after processing.

# Compatibilizing Effects of Itaconic Anhydride on Blends between Poly(lactic acid) and Novatein Thermoplastic Protein

Extended Abstract

By

A.S. Walallavita*, C.J.R. Verbeek, M.C. Lay

Oral Presentation

***32nd International Conference of the Polymer Processing Society***

# Compatibilizing Effects of Itaconic Anhydride on Blends between Poly(lactic acid) and Novatein Thermoplastic Protein

Anuradha Walallavita, Casparus J.R. Verbeek, Mark Lay

*University of Waikato, Hamilton 3240, New Zealand*

*asw15@students.waikato.ac.nz, jverbeek@waikato.ac.nz, mclay@waikato.ac.nz*

**Abstract.** Novatein®, a protein-based thermoplastic, was blended with poly(lactic acid) (PLA) using reactive extrusion to produce a cheap and degradable material with improved mechanical properties over neat Novatein. Various compositions of Novatein/PLA were prepared with and without a compatibilizer, PLA grafted with itaconic anhydride (PLA-g-IA).

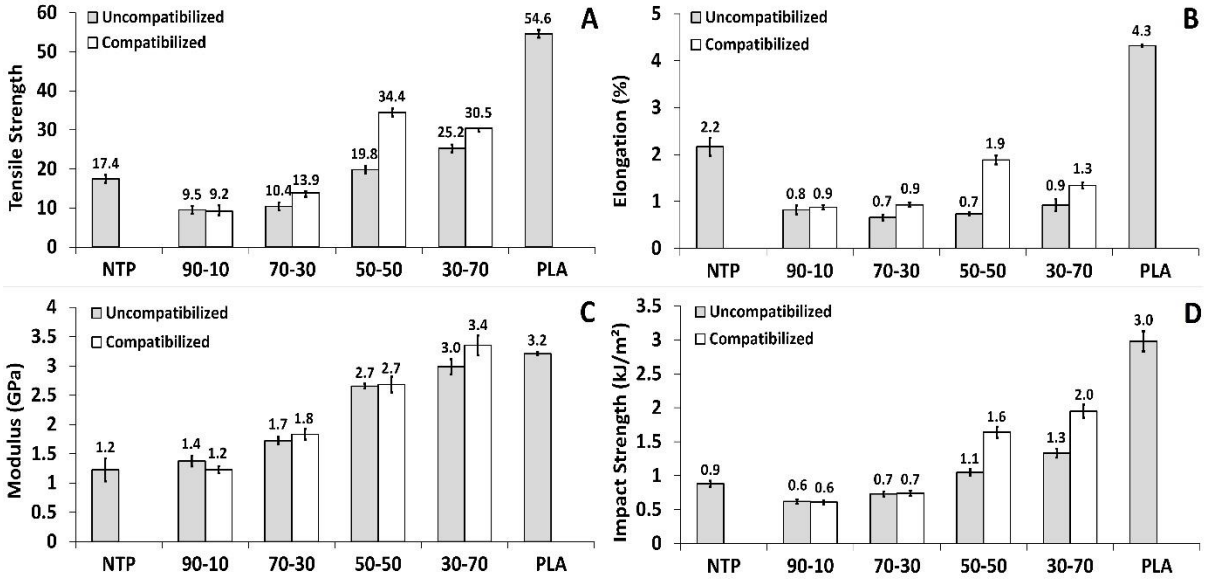


**FIGURE 1.** Tensile strength (A), percent elongation (B), secant modulus (C) and impact strength (D) of Novatein/PLA blends with and without compatibilizer.

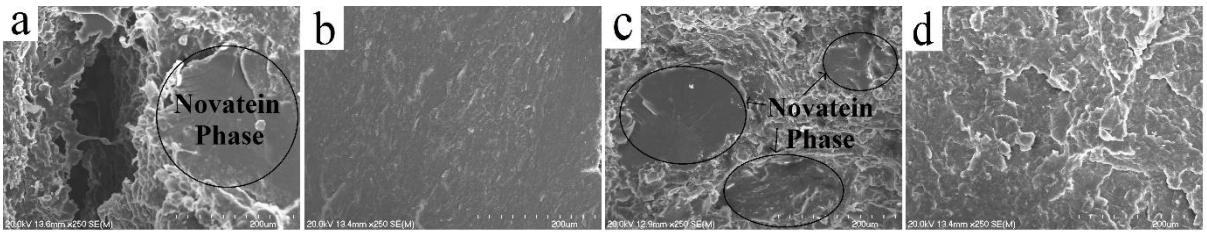


**FIGURE 2.** SEM images of tensile tested fracture surfaces at magnification x 250 a) 90-10 b) 90-10 IA/DCP c) 50-50 d) 50-50 IA/DCP.

Novatein had a tensile strength of 17.4 MPa while a blend of Novatein with PLA-g-IA at 50 wt. % loading increased the tensile strength to 34.4 MPa (Figure 1.A). All Novatein and PLA-g-IA blends showed an improvement in elongation at break i.e. from 0.74 to 1.88 at 50-50 composition (Figure 1.B). Impact strength of 50-50 IA/DCP was higher than 30-70 blend without compatibilizer (Figure 1.D). Scanning electron microscopy revealed that adding compatibilizer reduced the presence of cracks and voids in fracture surfaces, resulting in a more homogenous microstructure (Figure 2.a and b). In the 50/50 blend, the Novatein phase became finer and more evenly dispersed within the PLA matrix (Figure 2.c and d). Blending Novatein with PLA can widen its use in many agricultural and packaging applications, but require itaconic anhydride as compatibilizer.

**Keywords:** Novatein® Thermoplastic Protein, biodegradable polymers, blends, polylactic acid, itaconic anhydride.

# Biopolymer Foam Blends of Poly(lactic acid) and Novatein Thermoplastic Protein

Extended Abstract

By

A.S. Walallavita*, C.J.R. Verbeek, M.C. Lay

Keynote Presentation

***Europe/Africa Conference of the Polymer Processing Society***

# Biopolymer Foam Blends of Poly(lactic acid) and Novatein Thermoplastic Protein

Anuradha S. Walallavita*, Casparus J.R. Verbeek, Mark C. Lay

*School of Engineering, Faculty of Science and Engineering,*

*University of Waikato, Hamilton 3240, New Zealand.*

*asw15@students.waikato.ac.nz*, jverbeek@waikato.ac.nz, mclay@waikato.ac.nz*

A batch processing method was used to fabricate foams comprising of a blend of poly(lactic acid) (PLA) and Novatein, a protein-based thermoplastic. Various compositions of Novatein/PLA were prepared with and without a compatibilizer, PLA grafted with itaconic anhydride (PLA-g-IA). These were foamed at varying temperatures above the material's $T_g$ (80 – 160 °C). This batch foaming technique has successfully been implemented to foam both semi-crystalline and amorphous PLA using an environmentally benign blowing agent, subcritical $CO_2$, however, batch foaming semi-crystalline Novatein is more difficult due to the constraining effects of the nature of the material.

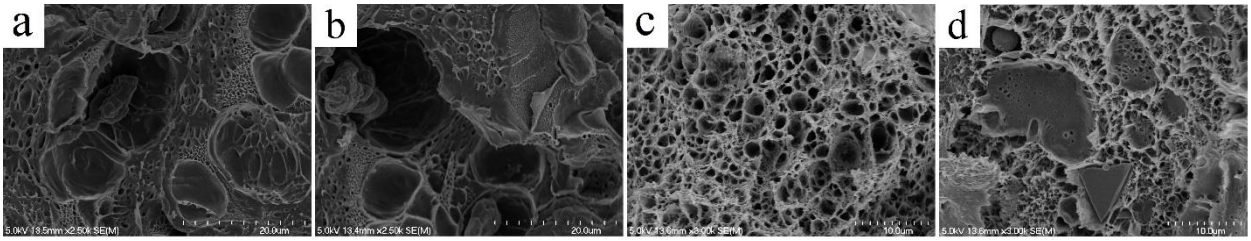


**FIGURE 1: a) and b) $NTP_{50}$-$PLA_{50}$ foamed at 80°C with magnification x2.5k, c) and d) $NTP_{30}$-$PLA_{70}$ foamed at 140°C with magnification x3.0k.**

**TABLE 1: Cell properties of blends foamed at 80 °C with and without IA/DCP as compatibilizer.**

| Blend Composition (wt.%) | Cell Size (μm) | | Cell Density (cells/cm$^3$) | |
|---|---|---|---|---|
| | Uncompatibilized | Compatibilized | Uncompatibilized | Compatibilized |
| $NTP_{50}$-$PLA_{50}$ | 3.36 | 1.04 | $8.44 \times 10^{21}$ | $1.04 \times 10^{24}$ |
| $NTP_{30}$-$PLA_{70}$ | 22.5 | 6.11 | $1.22 \times 10^{18}$ | $1.32 \times 10^{22}$ |
| $NTP_{10}$-$PLA_{90}$ | 42.7 | 9.69 | $1.88 \times 10^{15}$ | $2.71 \times 10^{18}$ |
| PLA | 55.4 | - | $5.18 \times 10^{14}$ | - |

Pure Novatein cannot form a cellular structure at a foaming temperature of 80 °C, however in a blend with 50 wt. % of PLA (Figure 1.a and b), microcells formed with smaller cell sizes (3.36 μm) and higher cell density ($8.44 \times 10^{21}$ cells/cm$^3$) compared to pure PLA and blends with higher amounts of PLA (Table 1). The incorporation of 50 wt. % Novatein in PLA increased the crystallinity of the blend and the matrix stiffness of Novatein was high enough to restrain cell coalescence and cell collapse. Furthermore, the introduction of a crystalline phase from Novatein has created additional interfacial area for nucleation (interface between crystalline and amorphous phases). At a foaming temperature of 140 °C (Figure 1.c and d), $NTP_{30}$-$PLA_{70}$ showed a unique interconnected porous morphology with a pore size of 3.29 μm and cell density of $6.72 \times 10^{22}$ which can be attributed to the $CO_2$-induced plasticization effect. Foaming of multi-phase systems offers a great opportunity to enhance the properties of porous materials, however, controlling the foaming process can be challenging. The outcome of this study can lead to a wider understanding about the foaming process and resulting morphologies of semi-crystalline and amorphous polymer blends.

# Co-Authorship Forms

THE UNIVERSITY OF WAIKATO
Te Whare Wānanga o Waikato

# Co-Authorship Form

Postgraduate Studies Office
Student and Academic Services Division
*Wahanga Ratonga Matauranga Akonga*
The University of Waikato
Private Bag 3105
Hamilton 3240, New Zealand
Phone +64 7 858 5096
Website: http://www.waikato.ac.nz/sasd/postgraduate/

This form is to accompany the submission of any PhD that contains research reported in published or unpublished co-authored work. **Please include one copy of this form for each co-authored work.** Completed forms should be included in your appendices for all the copies of your thesis submitted for examination and library deposit (including digital deposit).

Please indicate the chapter/section/pages of this thesis that are extracted from a co-authored work and give the title and publication details or details of submission of the co-authored work.

Chapter 3 - Morphology and Mechanical Properties of Itaconic Anhydride Grafted Poly(lactic acid) and Thermoplastic Protein Blends. Pages 59 - 89. Currently in press with International Polymer Processing. DOI 10.3139/217.3343.

| | |
|---|---|
| Nature of contribution by PhD candidate | As first author of this paper, the candidate conducted all experimental work under the guidance of the supervisor, and prepared the initial draft manuscript, which was refined and edited with consultation with the supervisor, who has been credited as co-author. |
| Extent of contribution by PhD candidate (%) | 90 |

## CO-AUTHORS

| Name | Nature of Contribution |
|---|---|
| Johan Verbeek | Guidance with experimental work and editing of manuscript |
| Mark Lay | Guidance with experimental work |
| | |
| | |
| | |
| | |

## Certification by Co-Authors

The undersigned hereby certify that:

- the above statement correctly reflects the nature and extent of the PhD candidate's contribution to this work, and the nature of the contribution of each of the co-authors; and
- in cases where the PhD candidate was the lead author of the work that the candidate wrote the text.

| Name | Signature | Date |
|---|---|---|
| Johan Verbeek |  | 27/03/18 |
| Mark Lay | 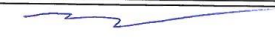 | 27/03/18 |
| | | |
| | | |
| | | |
| | | |

THE UNIVERSITY OF WAIKATO
Te Whare Wānanga o Waikato

# Co-Authorship Form

**Postgraduate Studies Office**
Student and Academic Services Division
*Wahanga Ratonga Matauranga Akonga*
The University of Waikato
Private Bag 3105
Hamilton 3240, New Zealand
Phone +64 7 858 5096
Website: http://www.waikato.ac.nz/sasd/postgraduate/

This form is to accompany the submission of any PhD that contains research reported in published or unpublished co-authored work. **Please include one copy of this form for each co-authored work.** Completed forms should be included in your appendices for all the copies of your thesis submitted for examination and library deposit (including digital deposit).

Please indicate the chapter/section/pages of this thesis that are extracted from a co-authored work and give the title and publication details or details of submission of the co-authored work.

Chapter 4 - Biopolymer Foams from Novatein Thermoplastic Protein and Poly(lactic acid). Pages 92 - 102. Published in Applied Polymer Science. DOI 10.1002/APP.45561.

| | |
|---|---|
| Nature of contribution by PhD candidate | As first author of this paper, the candidate conducted all experimental work under the guidance of the supervisor, and prepared the initial draft manuscript, which was refined and edited with consultation with the supervisor, who has been credited as co-author. |
| Extent of contribution by PhD candidate (%) | 90 |

## CO-AUTHORS

| Name | Nature of Contribution |
|---|---|
| Johan Verbeek | Guidance with experimental work and editing of manuscript |
| Mark Lay | Guidance with experimental work |
| | |
| | |
| | |
| | |

## Certification by Co-Authors

The undersigned hereby certify that:

- the above statement correctly reflects the nature and extent of the PhD candidate's contribution to this work, and the nature of the contribution of each of the co-authors; and
- in cases where the PhD candidate was the lead author of the work that the candidate wrote the text.

| Name | Signature | Date |
|---|---|---|
| Johan Verbeek |  | 27/03/18 |
| Mark Lay |  | 27/03/18 |
| | | |
| | | |
| | | |
| | | |

THE UNIVERSITY OF WAIKATO
Te Whare Wānanga o Waikato

# Co-Authorship Form

**Postgraduate Studies Office**
Student and Academic Services Division
*Wahanga Ratonga Matauranga Akonga*
The University of Waikato
Private Bag 3105
Hamilton 3240, New Zealand
Phone +64 7 858 5096
Website: http://www.waikato.ac.nz/sasd/postgraduate/

This form is to accompany the submission of any PhD that contains research reported in published or unpublished co-authored work. **Please include one copy of this form for each co-authored work.** Completed forms should be included in your appendices for all the copies of your thesis submitted for examination and library deposit (including digital deposit).

Please indicate the chapter/section/pages of this thesis that are extracted from a co-authored work and give the title and publication details or details of submission of the co-authored work.

Appendices - Protein Plastic Foams. Pages 110 - 150. Published in Advances in Physicochemical Properties of Biopolymers.

| | |
|---|---|
| Nature of contribution by PhD candidate | As co-author, I prepared the first draft of the sections on batch foaming, and together with the other authors, revised and edited the entire manuscript into the form accepted for publication. |
| Extent of contribution by PhD candidate (%) | 25 |

## CO-AUTHORS

| Name | Nature of Contribution |
|---|---|
| Johan Verbeek | Guidance with editing of manuscript |
| Mark Lay | Guidance with editing of manuscript |
| Chanelle Gavin | Prepared first draft and editing of manuscript |
| | |
| | |
| | |

## Certification by Co-Authors

The undersigned hereby certify that:

- the above statement correctly reflects the nature and extent of the PhD candidate's contribution to this work, and the nature of the contribution of each of the co-authors; and
- in cases where the PhD candidate was the lead author of the work that the candidate wrote the text.

| Name | Signature | Date |
|---|---|---|
| Johan Verbeek | 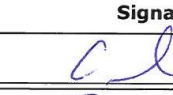 | 27/03/18 |
| Mark Lay |  | 27/03/18 |
| Chanelle Gavin | 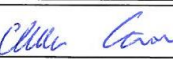 | 27/03/18 |
| | | |
| | | |
| | | |

THE UNIVERSITY OF WAIKATO
Te Whare Wānanga o Waikato

# Co-Authorship Form

Postgraduate Studies Office
Student and Academic Services Division
*Wahanga Ratonga Matauranga Akonga*
The University of Waikato
Private Bag 3105
Hamilton 3240, New Zealand
Phone +64 7 858 5096
Website: http://www.waikato.ac.nz/sasd/postgraduate/

This form is to accompany the submission of any PhD that contains research reported in published or unpublished co-authored work. **Please include one copy of this form for each co-authored work.** Completed forms should be included in your appendices for all the copies of your thesis submitted for examination and library deposit (including digital deposit).

Please indicate the chapter/section/pages of this thesis that are extracted from a co-authored work and give the title and publication details or details of submission of the co-authored work.

Appendices - Blending Novatein Thermoplastic Protein with PLA for Carbon Dioxide Assisted Batch Foaming. Pages 152 - 156. Published in AIP Conference Proceedings. DOI 10.1063/1.4942311.

| | |
|---|---|
| Nature of contribution by PhD candidate | As first author of this paper, the candidate conducted all experimental work under the guidance of the supervisor, and prepared the initial draft manuscript, which was refined and edited with consultation with the supervisor, who has been credited as co-author. |
| Extent of contribution by PhD candidate (%) | 90 |

## CO-AUTHORS

| Name | Nature of Contribution |
|---|---|
| Johan Verbeek | Guidance with experimental work and editing of manuscript |
| Mark Lay | Guidance with experimental work and editing of manuscript |
| | |
| | |
| | |
| | |

## Certification by Co-Authors

The undersigned hereby certify that:

- the above statement correctly reflects the nature and extent of the PhD candidate's contribution to this work, and the nature of the contribution of each of the co-authors; and
- in cases where the PhD candidate was the lead author of the work that the candidate wrote the text.

| Name | Signature | Date |
|---|---|---|
| Johan Verbeek |  | 27/03/18 |
| Mark Lay |  | 27/03/18 |
| | | |
| | | |
| | | |
| | | |